The Mcm2-7 Replicative Helicase is Essential to Coordinate DNA replication, Checkpoint Regulation and Sister Chromatid Cohesion

by

Feng-Ling Tsai

Bachelor of Science, University of San Francisco 2005

Submitted to the Graduate Faculty of

the Kenneth P. Dietrich School of Arts and Sciences

in partial fulfillment

of the requirements for the degree of

Doctor of Philosophy

University of Pittsburgh

2012

UNIVERSITY OF PITTSBURGH

Dietrich School of Arts and Sciences

This dissertation was presented

by

Feng-Ling Tsai

It was defended on

March 15, 2012

and approved by

Karen Arndt, PhD, Professor, Biological Sciences

Roger Hendrix, PhD, Distinguished Professor, Biological Sciences

Andrew VanDemark, PhD, Assistant Professor, Biological Sciences

John Woolford, Jr. PhD., Professor, Biological Sciences, Carnegie Mellon University

Dissertation advisor: Anthony Schwacha, PhD, Associate Professor, Biological Sciences

The Mcm2-7 Replicative Helicase is Essential to Coordinate DNA replication, Checkpoint Regulation and Sister Chromatid Cohesion

Feng-Ling Tsai, PhD

University of Pittsburgh, 2012

DNA replication is a complex and highly regulated cellular process that ensures faithful duplication of the entire genome. To prevent genomic instability, several additional processes are coordinated with DNA replication. Eukaryotic cells employ a conserved surveillance mechanism called the S-phase checkpoint to activate a phosphorylation cascade while encountering DNA damage during DNA replication. In addition, DNA replication must also coordinate with sister chromatid cohesion, so that sister DNAs that emerge from the forks are physically connected until chromosomal segregation takes place. Mcm2-7, the eukaryotic replicative helicase that unwinds dsDNA and is positioned at the vanguard of the replication fork, is likely the commonality among these cellular processes. In my thesis work, I find that ATP hydrolysis in one specific active site (Mcm6/2) is required to mediate the DNA replication checkpoint response, sister chromatid cohesion, and DNA replication initiation. Further examination reveals that a subcircuit of a checkpoint pathway that includes *MEC1* and *MRC1* and ending with Mcm2-7 is required to mediate sister chromatid cohesion. Finally, misregulation of these processes causes genomic instability and likely missegregation of chromosomes. My findings lead to a model where the regulation of ATP hydrolysis at the Mcm6/2 active site by Mrc1 modulates Mcm2/5 gate opening and gate closure during initiation, DNA damage and sister chromatid cohesion.

TABLE OF CONTENTS

LIST OF TABLES

LIST OF FIGURES

PREFACE

I would like to thank all of the people listed below from the bottom of my heart. They have helped and supported me throughout my graduate career. This thesis would not have been possible without them.

First, I would like to thank my thesis advisor Dr. Tony Schwacha. He has given me his full support during my entire time in his lab. I appreciate his guidance and mentorship in shaping me into an independent scientist. When we first started out the *2DENQ* project, I encountered many technical difficulties, and there were times that we were not sure which direction this project should go. However, Tony has always been very patient and encouraging, which helped me overcome the challenges. I thank him for all his guidance over these years.

I would also like to thank my thesis committee, past and present— Dr. Susan Gilbert, Dr. Karen Arndt, Dr. Roger Hendrix, Dr. Andy VanDemark and Dr. John Woolford. They have been guiding me through my graduate research and giving me valuable comments and suggestions.

I also need to thank the past and present members of the Schwacha lab, especially Dr. Matt Bochman, Nick Simon, Sriram Vijayraghavan, Rebecca Theophanous, Whitney White and Rania Elbakri. During my thesis writing, Nick and Sriram have given me helpful comments on my thesis draft. Thank you for your friendship, it's been a pleasure to work with all of you.

I appreciate all the help I've got from my collaborators Dr. David MacAlpine, Heather MacAlpine and Joseph Prinz. They have helped me generously from library preparation to genomic analysis. Without them, the genomic project would not be possible. I am very grateful to have such wonderful collaborators like them.

I would like to thank the entire Biological Sciences department for being a supportive working environment. I would like to thank Cathy Barr, Crystal Petrone and Pat Dean particularly for their help, encouragement and conversations throughout my graduate school years. I want to acknowledge the Arndt lab for the use of microscope and reagents. Specifically, I want to thank Peggy Shirra who has taught me everything I know about yeast genetics.

I would also like to thank Michael Weinreich, John Diffley, Stephen P. Bell, Peter Sorger, Katsuhigo Shirahige, Carol Newlon, Douglas Koshland, Stephen Elledge, Anja-Katrin Bielinsky, William Bonner and Richard Kolodner for kind gifts of strains and plasmids, Jeffrey Lawrence for helpful discussion of the statistical analysis of cytological plasmid segregation data, Cherie Poth and Rania El-bakeri for technical assistance, and Sriram Vijayraghavan for PYMOL modeling of the Mcm2-7 complex.

Lastly, and most importantly, I definitely need to thank my loving parents for their full support. They have always given me words of encouragement, and have confidence in me. I also appreciate my parents for offering their love and their willingness to help in the thesis writing process during the few weeks I was writing at home…even though they don't know about Mcms. Their spiritual help has made my doctoral research possible and I want to thank them for being such wonderful parents.

CO-AUTHORSHIP STATEMENT

Feng-Ling Tsai carried out all the experiments presented in this thesis with the following exceptions. Dr. Anthony Schwacha helped with the revision of the thesis draft. Heather MacAlpine prepared the library DNA required for the ChIP-seq experiments. Joseph Prinz performed all the genomic analysis presented in **Chapter 3**. Dr. David MacAlpine supervised the conduct of genomic experiments and analyses.

1.0 INTRODUCTION

DNA replication is a cellular process that must be highly regulated to preserve genome integrity (Branzei and Foiani, 2010; Remus and Diffley, 2009). During DNA replication, replication forks may encounter damage. In such incidences, DNA replication is downregulated by the DNA replication checkpoint (DRC), a surveillance system that causes both cell cycle arrest and stabilization of the replication fork (Branzei and Foiani, 2009). Furthermore, DNA replication must also coordinate with sister chromatid cohesion (SCC), in which the ring-shaped cohesin complex physically connects the sister DNAs to ensure faithful chromosomal segregation (Nasmyth and Haering, 2009). Although protein factors involved in DNA replication are often found to play overlapping roles in DRC and SCC, the common target of regulation in all three cellular processes remains unclear. A potential candidate is the Mcm2-7 replicative helicase, the eukaryotic molecular motor that unwinds double-stranded DNA (dsDNA) at the replication fork. This introduction reviews eukaryotic DNA replication initiation and elongation, the biochemical and structural aspects of Mcm2-7 and related helicases, the regulation of DNA replication by the DRC and the coordination of DNA replication with the SCC.

1.1 EUKARYOTIC DNA REPLICATION

In all organisms, the entire genome must be faithfully duplicated and transmitted from the mother cell to daughter cells during each cell cycle. To achieve this fidelity, DNA replication is highly regulated and coordinated with cell cycle progression. During the G1 phase of the cell cycle, pre-replicative complexes (pre-RC) consisting of ORC, Cdc6, Cdt1 and Mcm2-7 are formed on DNA (reviewed in (Bell and Dutta, 2002)). DNA replication initiation is triggered by two conserved kinases, cyclin dependent kinases (CDK) and Dbf4-dependent kinases (DDK) (reviewed in (Labib, 2010)). CDK phosphorylates initiator proteins Sld2 and Sld3 (Tanaka et al., 2007; Zegerman and Diffley, 2007), and DDK targets the Mcm2-7 complex (Randell et al., 2010; Sheu and Stillman, 2006, 2010). Upon phosphorylation, Sld2 and Sld3 promote the binding of replication factors GINS and Cdc45 to Mcm2-7, resulting in helicase activation (Bruck and Kaplan, 2011). During S phase, double-stranded DNA (dsDNA) is unwound by the replicative helicase, to provide the necessary templates for DNA polymerases. Both DNA replication initiation and elongation are carefully monitored by the replication checkpoint to achieve precise duplication. Despite the importance of the replication checkpoint, the mechanistic details of how it regulates DNA replication are largely unknown. An understanding of the complex regulation of DNA replication is essential for elucidating its coordination with the replication checkpoint and SCC discussed in **Chapters 3** and **4**.

1.1.1 DNA replication initiation

In prokaryotes, genome sizes are relatively small; a circular *E. coli* genome is only 4.6 million base pairs (Lodish, 2000). Initiation of DNA replication was initially described as the binding of

an initiator protein to a single specific sequence on DNA called replicator (origin of replication), and followed by recruitment of proteins involved in DNA unwinding (Jacob et al., 1963). In eukaryotes, while this basic model can be applied, the initiation process is much more complicated. Due to the large eukaryotic genome sizes (human genome is ~1000 times bigger than *E. coli* genome), DNA replication is initiated at multiple origins (reviewed in (Masai et al., 2011)). Moreover, the number of proteins involved in eukaryotic DNA replication is much larger than for prokaryotic DNA replication (Remus and Diffley, 2009). In eukaryotes, most of the key proteins are evolutionarily conserved, suggesting that the mechanism of DNA replication is likely the same among eukaryotes (Araki, 2011).

DNA replication initiation in eukaryotes is regulated by a two-step mechanism (reviewed in (Remus and Diffley, 2009)). The first step is the loading of the eukaryotic replicative helicase during G1, Mcm2-7 in an inactive form. This is achieved by the binding of the initiator complex (origin recognition complexes (ORC)) to specific regions of DNA, called replication origins. This is followed by the recruitment of the loading factor Cdc6. Subsequently, the Cdt1-Mcm2-7 heptamer is then recruited to the DNA bound ORC-Cdc6, resulting in a head-to-head double hexamer that has been shown to encircle dsDNA in EM studies (Evrin et al., 2009; Remus et al., 2009) (Figure 1). Recent *in vitro* studies have shown that multiple Cdt1 proteins are recruited to a single ORC to promote the replication competence of Mcm2-7 double hexamers by facilitating the recruitment of accessory factors GINS and Cdc45 (Takara and Bell, 2011). In this process, ATP hydrolysis by Cdc6 is required for the loading of Mcm2-7 onto DNA and the release of Cdt1 (Randell et al., 2006). The pre-replicative complex (pre-RC) formed remains inactive at this stage.

The second step of DNA replication initiation results in the cell cycle dependent activation of the Mcm2-7 helicase. Upon entering S phase, two conserved kinases Dbf4-dependent Cdc7 kinase (DDK) and S-phase cyclin-dependent kinase (S-CDK) are required for DNA replication (reviewed in (Labib, 2010)). DDK phosphorylates several Mcm subunits including Mcm2, Mcm4 and Mcm6 (Lei et al., 1997; Randell et al., 2010; Sheu and Stillman, 2006, 2010). Although Mcm5 is not a substrate of DDK, work in budding yeast shows that a recessive mutation, *mcm5-bob1*, bypasses the deletion of the essential gene *CDC7*, suggesting that DDK phosphorylation of Mcm2-7 is its main target (Hardy et al., 1997). Later structural work of an archaeal Mcm complex containing an analogous mutation suggests that this bypass could result from a subtle domain shift in Mcm5 (Fletcher et al., 2003). Therefore, Cdc7 may activate Mcm2-7 by causing a subtle conformational change. In addition, some evidence suggests that DDK phosphorylation may also be required to promote Cdc45 association with Mcm2-7 (Sheu and Stillman, 2010).

In contrast, CDK phosphorylation results in Mcm2-7 activation through the recruitment of accessory proteins. CDK phosphorylates initiator proteins Sld2 and Sld3 (RecQ4 and Treslin in humans) and promotes their binding to a third initiator protein Dpb11 (TopBP1 in human) (Boos et al., 2011; Kumagai et al., 2011; Tanaka et al., 2007; Zegerman and Diffley, 2007). In addition to Dpb11, recent studies in budding yeast have shown that CDK-dependent phosphorylation of Sld2 also promotes the association of DNA polymerase ε and the replication factor GINS (Sld5, Psf1, Psf2, Psf3) complex (Muramatsu et al., 2010). Upon initiation, Mcm2-7 forms the CMG (Cdc45, Mcm2-7 and GINS) complex with its activating factors Cdc45 and GINS complex (Ilves et al., 2010; Moyer et al., 2006) (Figure 1).

Mcm2-7 loading during G1 and its activation during S phase are mutually exclusive events that limit replication to a single round. Once entering S-phase, the elevated CDK levels prevent further Mcm2-7 loading through multiple mechanisms. ORC2 and ORC6 are phosphorylated by CDK (Nguyen et al., 2001), blocking the interaction between ORC and Cdt1 (Chen and Bell, 2011; Wilmes et al., 2004). Cdc6 is also a target of CDK; phosphorylated Cdc6 undergoes ubiquitin-mediated proteolysis (Perkins et al., 2001) . In yeast, CDK phosphorylation of Mcm2-7 promotes its export out of the nucleus during S, G1 and G2 (Liku et al., 2005; Nguyen et al., 2000; Tanaka and Diffley, 2002). Together, these overlapping mechanisms ensure that origin firing occurs once and only once during each cell cycle.

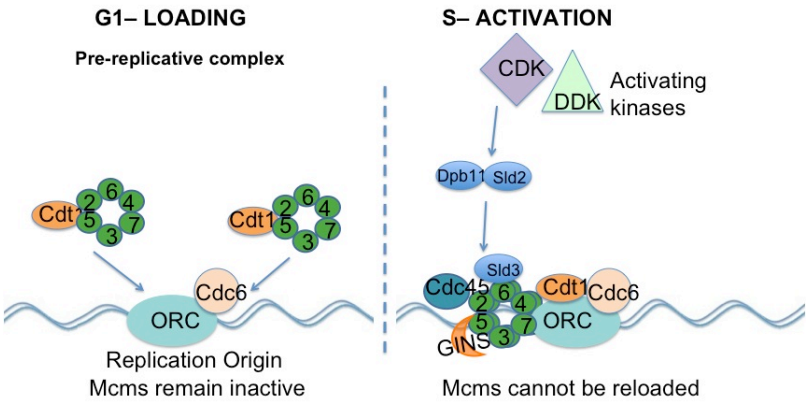

Figure 1. DNA replication initiation

The loading and activation steps of replicative helicase during DNA replication initiation. G1 loading of Mcm2-7 is facilitated by Orc, Cdc6 and Cdt1. Upon entering S phase, CDK and DDK phosphorylation of Sld2, Sld3, and Mcm2-7 promotes the association of GINS and Cdc45 with Mcm2-7, resulting in helicase activation. In addition,

CDK phosphorylation of multiple targets prevents any additional loading of Mcm2-7 and prevents re-replication (See text for details.)

1.1.2 DNA replication elongation

The key molecular motor required for replication fork progression during elongation is the eukaryotic replicative helicase, the CMG complex. With its ATPase activity, the Mcm2-7 complex constitutes the catalytic core, whereas Cdc45 and the GINS complex are activating factors (Bochman and Schwacha, 2008; Ilves et al., 2010).

Many experiments highlight the involvement of Mcm2-7 in DNA unwinding. Like the replicative helicase in *E. coli*, Mcm2-7 is required for both initiation and elongation (Mott and Berger, 2007). Genome-wide association of pre-RC components ORC and MCMs with replication origins was shown in chromatin-immunoprecipitation (ChIP) microarray studies (Wyrick et al., 2001). Using ChIP experiments, it was also shown that Mcm2-7 migrates away from origin regions to non-origin regions with similar kinetics as DNA polymerase ε and Cdc45 (Aparicio et al., 1997). Inactivation of at least five out of six Mcm subunits using conditional degron alleles inhibits replication fork progression irreversibly, indicating that Mcm2-7 is essential for DNA replication elongation (Labib et al., 2000). The involvement of Mcm2-7 in replication elongation was also shown in vertebrates (Pacek and Walter, 2004). Later works in budding yeast and *Drosophila* show that both Cdc45 and GINS are keys to fork progression (Gambus et al., 2006; Moyer et al., 2006). Consistent with their roles as the replicative helicase,

both Mcm2-7 alone and the CMG complex display helicase activity *in vitro* (Bochman and Schwacha, 2008; Ilves et al., 2010).

In addition to the CMG complex, the replisome is composed of additional core replication factors (i.e. DNA polymerases, replication clamps, and clamp loaders) and numerous other factors that lack functional parallels in *E. coli*. A replisome progression complex purified from budding yeast arrested in S phase contains the following proteins: DNA polymerase α, subunits within the CMG complex, Mcm10, Top1, histone chaperone Spt16, replication checkpoint mediators Mrc1, Csm3 and Tof1, and sister chromatid cohesion protein Ctf4 (Gambus et al., 2006; Gambus et al., 2009). Furthermore, Ctf18 has been found to physically interact with Mcm2-7 as shown by co-immunoprecipitation (Ma et al., 2010). Some of these proteins play roles in other processes as well as replication. For example, Mrc1 physically couples DNA polymerase ε and Mcm2-7 helicase, and is required for normal fork progression, yet is also needed for the replication checkpoint (Alcasabas et al., 2001; Lou et al., 2008; Szyjka et al., 2005). Similarly, Ctf4 physically couples Mcm2-7 and DNA polymerase α, and is involved in sister chromatid cohesion (Gambus et al., 2009; Hanna et al., 2001). This large assembly of proteins suggests that DNA replication coordinates with other nuclear processes.

In summary, the loading and activation of the replicative helicase, Mcm2-7, is central to the regulation of DNA replication. In **Chapter 1.2**, the biochemical properties of this enzymatic motor will be discussed. The relationships of DRC and SCC with DNA replication are discussed in **Chapter 1.3** and **Chapter 1.4**.

1.1.3 Temporal program of origin firing

As mentioned, eukaryotic genomes are 2-1000 fold larger than prokaryotic genomes (Lodish, 2000), therefore, DNA replication is initiated at multiple origins in order to complete DNA replication in a timely manner. In budding yeast, replication origins are well-defined, and consist of autonomous replication sequence (ARS) consensus sequences (Newlon and Theis, 1993), in the company of more poorly defined B elements (Marahrens and Stillman, 1992). Replication origins fire with a pre-determined temporal program, such that some origins fire early in S-phase, while some fire late (Raghuraman and Brewer, 2010). Such a temporal program is especially advantageous under replicative stress condition, which can be caused by nucleotide depletion. Under replication stress, replication fork stalls, and cells activate a surveillance mechanism called S-phase checkpoint that monitors DNA replication to inhibit late origin firing and prevent replication of damaged DNA (Branzei and Foiani, 2009). Work in budding yeast shows that the repression of late origin firing is lost in checkpoint mutants *mec1* and *rad53* during hydroxyurea (HU) exposure, a chemical that depletes nucleotide precursors (Feng et al., 2006; Santocanale and Diffley, 1998). In addition to the replication checkpoint response, the temporal program also correlates with transcriptional activity. Regions that have a high transcriptional activity, i.e. the euchromatic region with less densely packed DNA, are usually replicated early (Zink, 2006). In contrast, the heterochromatin regions are replicated late (Zink, 2006). Histone modification is also important in the repression of late origin firing (reviewed in (Raghuraman and Brewer, 2010)). Experiments in budding yeast and *Drosophila* both show that deletion of the *RPD3* gene encoding for a histone deacetylase, results in early replication of late origins (Aggarwal and Calvi, 2004; Knott et al., 2009; Vogelauer et al., 2002). Replication origins are rather inefficient in eukaryotes. In *S. pombe*, most replication origins fire

roughly 30% of the time (Patel et al., 2006). Similarly, replication origins in *S. cerevisiae* only fire in a fraction of cells (Friedman et al., 1997; Yamashita et al., 1997). Higher eukaryotes contain excess number of dormant origins that only fire under replication stress condition (Ge et al., 2007; Ibarra et al., 2008).

Although budding yeast has a well-defined temporal program with sequence specific origins, this is not always the case for other species. Replication initiation in *Xenopus* and *Drosophila* embryos occurs at random sites before mid-bastula transition (Hyrien et al., 1995; Mahbubani et al., 1992; Shinomiya and Ina, 1991), resulting in a different replication pattern in each cell. These observations force one to reexamine the temporal program. One model that was proposed to reconcile these problems suggests that perhaps the order of origin firing is a mix between strictly deterministic (i.e. with a pre-determined temporal order) and strictly stochastic (Raghuraman and Brewer, 2010). The regulation of origin firing order takes place at broad regions of the genome, but stochastic origin firing also occurs at a local level. In this model, some origins have higher probability of firing early in the S-phase, while others fire more efficiently late in the S-phase. This model predicts that the overlaps between the origin distribution in early and late S-phase would account for the cell-to-cell differences.

1.1.4 Misregulation of DNA replication and genomic instability

Cancer arises through genomic instability, a syndrome characterized by extra chromosomes, chromosomal rearrangements, and increased mutations (reviewed in (Blow and Gillespie, 2008)). To prevent genomic instability, chromosome segregation must coordinate with high-fidelity DNA replication and proper S-phase checkpoint controls. Misregulation of DNA replication leads to unstable replication forks and aberrant DNA structures (reviewed in (Branzei

and Foiani, 2009; Branzei and Foiani, 2010; Kastan and Bartek, 2004)); abnormal chromosomal segregation results in aneuploidy (Shen, 2011). The consequence of misregulation of DNA replication is different from that of chromosomal segregation, where the former would result in the loss of chromosomes (1:0 segregation) and the later would result in extra chromosomes (0:2 segregation).

Defects in Mcm2-7 can lead to cancer. One example of a well-characterized replication mutant is the cancer-prone mutant allele of *MCM4*, *mcm4chaos3*. This allele was originally identified from a forward genetic screen in mice (Shima et al., 2007). Female mice homozygous for this mutation are prone to mammary tumors (Shima et al., 2007). In mouse embryonic fibroblasts, *mcm4chaos3* causes double-stranded break formation detected as γ-H2AX foci (Kawabata et al., 2011). Furthermore, the *Drosophila* Mcm2-7 complex containing the *mcm4chaos3* mutation is structurally unstable (Kawabata et al., 2011), suggesting that *in vivo*, this mutation may cause the replisome to disassemble. In yeast, the corresponding allele causes a classical plasmid loss phenotype and chromosomal translocation, suggesting a defect in DNA replication and consistent with the genomic instability observed in cancer (Li et al., 2009; Shima et al., 2007).

The expression levels of replication factors must also be appropriately regulated. Upregulated Mcm expression is observed in many human malignancies (Blow and Gillespie, 2008). Overexpression of Mcm proteins can be potentially used as an early diagnostic marker for cancer (Padmanabhan et al., 2004); however, it was not clear whether overexpression of *MCM* genes causes cancer or is simply a consequence of tumorigenesis. Recently, overexpression of Mcm7 has been observed in lung cancer tissues and RNAi knockdown of Mcm7 suppresses cell growth. (Toyokawa et al., 2011). This result suggests that Mcm

overexpression may cause tumor formation. Regulation of DNA replication is therefore crucial to preserve genome integrity.

In order to preserve genomic stability, eukaryotic cells evolved conserved S-phase checkpoint during DNA replication (Branzei and Foiani, 2010) and the spindle assembly checkpoint (SAC) during mitosis (Kops et al., 2005). The S-phase checkpoint serves to ensure high fidelity of DNA replication (Branzei and Foiani, 2010). The SAC is required to monitor proper chromosomal attachment to the microtubules prior to anaphase entry (Kops et al., 2005). Defective SAC can often lead to aneuploidy, which is a common characteristic of tumorigenesis (Silva et al., 2011). Misregulation of Mcm2-7 is only one of the many factors that can lead to genomic instability.

1.2 THE EUKARYOTIC REPLICATIVE HELICASE MCM2-7

1.2.1 Initial discovery and characterization of Mcm2-7

Genes encoding the Mcm2-7 subunits were identified almost 30 years ago in several independent genetic screens in budding yeast and fission yeast. In the 1980s, Bik Tye's lab conducted a yeast genetic screen to isolate mutants defective in plasmid segregation (Maine et al., 1984). Forty mutants constituting sixteen complementation groups were isolated from this screen. These mutants were divided into two groups: mutants that are defective in maintaining plasmids with specific ARSs and mutants that are defective in the segregation of a wide variety of different plasmids. It was proposed that genes identified by the first group were required for DNA replication initiation, and genes identified by the second group were required for chromosomal

segregation. Replication initiation mutants isolated in this screen correspond to genes encoding Mcm2, Mcm3 and Mcm5. Furthermore, mutations in *MCM1* and *MCM10* were also isolated in this genetic screen; *MCM1* encodes a transcription factor needed for Mcm2-7 expression (Passmore et al., 1989), and *MCM10* encodes a DNA replication initiation factor (Merchant et al., 1997). *MCM1* and *MCM10* do not share sequence homology with Mcm2-7 and are not part of the Mcm2-7 helicase. In a separate screen, David Botstein's group isolated cold sensitive cell division cycle mutants (Moir et al., 1982). The mutans for *CDC54* (*MCM4*) and *CDC45*, part of the CMG complex, were isolated and found to arrest with a large bud and single nucleus at restrictive temperature (Moir et al., 1982). Several suppressors of this allele were also isolated, corresponding to mutations in *CDC46* (*MCM5*), *CDC47* (*MCM7*) (Moir et al., 1982). *MCM6* was discovered in a genetic screen in *S. pombe* as a missegregation *mis5* mutant (Takahashi et al., 1994); the corresponding gene was later identified by bioinformatics in *S. cerevisiae* (Goffeau et al., 1996). As evidence accumulated indicating that they work together, these genes were later renamed to be Mcm2 through Mcm7 (Chong et al., 1996).

The Mcm protein family is evolutionarily conserved in eukaryotes and archaea. The eukaryotic Mcm family contains six independent subfamilies (Mcm2-7), and most archaea, with a few exceptions, only have one Mcm homolog (reviewed in (Bochman and Schwacha, 2009; Forsburg, 2004)). While Mcm homologs are not normally found in prokaryotes, a Mcm-like helicase was identified in a bacteriophage genome (Samuels et al., 2009). Sequence alignment analysis revealed that all the subfamilies of Mcm2-7 share sequence similarity with each other, especially within a region encoding the ATPase domain (reviewed in (Bochman and Schwacha, 2009; Forsburg, 2004)). The six *MCM* genes form a family conserved among all sequenced eukaryotes (reviewed in (Forsburg, 2004)).

Initial characterization indicated a role for Mcm2-7 in DNA replication initiation. Using flow cytometry to study cell cycle progression, *mcm* mutants were shown to arrest with 1C DNA content at restrictive temperature (Hennessy et al., 1991). Later work in *Xenopus* showed that the Mcms are the "replication licensing factors" that limit DNA replication to once per cell cycle (Chong et al., 1995; Madine et al., 1995b). It was shown that purified *Xenopus* Mcm3 associates with chromatin during G1 to confer replication competency (Chong et al., 1995; Madine et al., 1995b).

1.2.2 The subunit composition and architecture of Mcm2-7.

Early biochemical investigation suggested that the Mcm complex formed a variety of oligomeric states. These subcomplexes include Mcm4/6/7, Mcm2/4/6/7, Mcm3/5, as well as Mcm2/3/4/5/6/7 (Davey et al., 2003; Ishimi, 1997; Kanter et al., 2008; Lee and Hurwitz, 2000). Today, it is clear that the functional state of the complex contains all six (Mcm2 through 7) subunits (reviewed in (Bochman and Schwacha, 2009; Forsburg, 2004)). Like many other replicative helicases, Mcm2-7 forms a ring-shaped structure as revealed by EM studies (Adachi et al., 1997; Bochman and Schwacha, 2007; Costa et al., 2011; Evrin et al., 2009; Remus et al., 2009). Gel filtration analyses demonstrated that Mcm2-7 forms a heterohexameric complex of ~615kDa with a stoichiometry of 1:1:1:1:1:1 in solution (Davey et al., 2003; Schwacha and Bell, 2001). More recently, it has been shown that Mcm2-7 can be loaded as a double hexamer on dsDNA (Evrin et al., 2009; Remus et al., 2009). Mcm2-7 is the true eukaryotic replicative helicase, as all the subunits are essential for DNA replication, and helicase activity has been demonstrated *in vitro* (Bochman and Schwacha, 2008; Labib et al., 2000).

The subunit organization order within the ring-shaped heterohexamer was deduced by dimer association studies (Figure 2). Five dimer pairs have been purified from human or yeast Mcms: Mcm6/2, Mcm5/3, Mcm3/7, Mcm7/4 and Mcm4/6, either by glycerol gradient or coimmunoprecipitation (Bochman et al., 2008; Davey et al., 2003; Yu et al., 2004). These studies predict an oligomerization order of Mcm2-Mcm6-Mcm4-Mcm7-Mcm3-Mcm5 (Figure 2). Dimer association between between Mcm2 and Mcm5 were only detected using crosslinking conditions (Yu et al., 2004), suggesting that the interface between Mcm2 and Mcm5 may form a gap in the toroidal complex. Indeed, this structural discontinuity between Mcm2 and Mcm5 and the predicted subunit organization order have recently been confirmed with EM using MBP tagged Mcms (Costa et al., 2011) (See **Chapter 1.2.5** for further discussions).

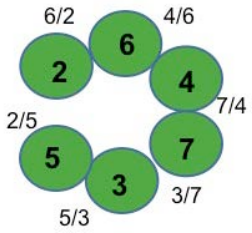

Figure 2. Mcm2-7 complex architecture

Mcm2-7 complex oligomerizes into a heterohexameric ring with a structural discontinuity between Mcm2 and Mcm5 (Costa et al., 2011).

1.2.3 ATP hydrolysis in Mcm2-7 complex

All six Mcm subunits belong to the AAA+ ATPase family (ATPases associated with a variety of cellular activities) (Hanson and Whiteheart, 2005; Koonin, 1993), in which ATPase active sites are formed *in trans* with one subunit providing the conserved Walker A and B motifs, and the other subunit providing the arginine finger motif (Figure 3). In the consensus sequence of Walker A motif, the conserved lysine (K) residue is required for nucleotide binding. In the Walker B and arginine finger motifs, conserved aspartate and glutamate (DE) and argnine (R) residues are crucial for nucleotide hydrolysis, respectively (Hanson and Whiteheart, 2005). To study the function of these conserved motifs, K→A, DE→NQ, and R→A mutations are commonly generated (Hanson and Whiteheart, 2005). ATP hydrolysis has been studied in the following dimer pairs Mcm3/5, Mcm4/6, Mcm3/7, Mcm2/6 and Mcm7/4 (Bochman et al., 2008; Davey et al., 2003; Stead et al., 2009). Mcm3/5 and Mcm4/6 have little or no detectable ATP hydrolysis, while Mcm3/7 has the highest ATPase activity, followed by Mcm2/6 and Mcm7/4, suggesting unequal contribution of ATP hydrolysis among these active sites (Bochman et al., 2008). Mutational analysis has been performed for Mcm3/7, Mcm2/6 and Mcm7/4 active sites to study ATPase active site formation within the dimer interface (Bochman et al., 2008; Davey et al., 2003; Stead et al., 2009). For example, the RA mutation in the arginine finger motif of Mcm3 subunit abolishes ATP hydrolysis of the Mcm3/7 dimer. The losses of Walker A and B motifs in Mcm7, by introducing KA and DENQ substitutions respectively, similarly abolishes ATP hydrolysis at this site. Therefore, the ATPase active site is formed combinatorially between the dimer interface of Mcm7 and Mcm3, with Mcm3 providing the arginine finger and Mcm7 providing the Walker A and Walker B motifs (Figure 3).

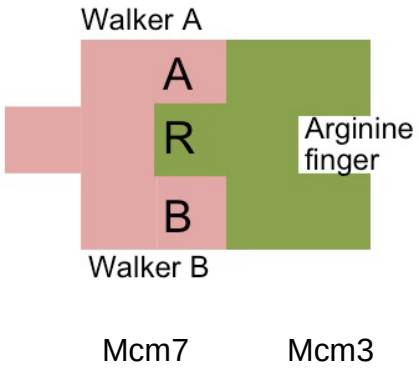

Figure 3. Combinatorial ATPase active sites

Formation of a combinatorial ATPase active site between Mcm3 and Mcm7 is shown as an example. Mcm7 provides Walker A and Walker B motifs *in cis*, while Mcm3 provides arginine finger motif *in trans*.

To understand the allosteric coordination among individual ATPase active sites, the ATPase activity of purified budding yeast Mcm2-7 was thoroughly studied (Schwacha and Bell, 2001). Mcm2-7 has three distinct kinetic modes of ATP hydrolysis—high, medium, and low. The preferred substrate for Mcm2-7 is adenosine triphosphates, and the β-phosphate is required for substrate binding. Mutational analysis shows that KA substitutions in the conserved Walker A motifs of any individual subunit abolish the ATPase activity of the entire complex, suggesting the coordinate involvements among all six ATPase active sites (Schwacha and Bell, 2001).

Biochemical analysis of double mutant combinations allows the ATPase active sites to be grouped into two different classes (Schwacha and Bell, 2001). Double mutants containing the KA mutations formed from any of Mcm4, 6, or 7 subunits are severely defective in ATP hydrolysis, whereas corresponding Mcm2, 3, or 5 mutant complexes hydrolyze ATP to nearly wild-type levels. Could Mcm2, 3, 5 serve regulatory roles? Indeed, it has been shown that ATP

hydrolysis at the Mcm6/2 active site is required to inhibit the helicase activity of a subcomplex of Mcm2-7, Mcm4/6/7 (Stead et al., 2009). These extensive characterizations of ATPase activity in Mcm2-7 established that Mcm4/6/7 is the catalytic core essential for ATP hydrolysis, and Mcm2/3/5 serve cryptic roles that are less related to robust catalysis. This is consistent with the observed helicase activity of the Mcm4/6/7 subcomplex (Ishimi, 1997; Kaplan et al., 2003; Lee and Hurwitz, 2000; You et al., 2002), as well as that of the Mcm4/7 dimer (Kanter et al., 2008). More recent results underscore the importance of Mcm2 and Mcm5 in the formation of the Mcm2/5 regulatory gate (Bochman and Schwacha, 2008; Costa et al., 2011).

Although ablating a single Walker A motif yields defective ATP hydrolysis in the Mcm2-7 complex, mutational analysis of Walker B and arginine finger motifs indicated that the contribution of each active site towards ATP hydrolysis of the entire complex is not interdependent (Bochman et al., 2008). In contrast to the Walker A mutations, most single Walker B or arginine finger mutants do not cause a large reduction of ATP hydrolysis. Exceptions to this include complexes containing Mcm4DENQ, Mcm7DENQ and Mcm3RA, suggesting that Mcm7/4 and Mcm3/7 active sites contribute significantly towards ATP hydrolysis. Furthermore, distinct dimer pairs also display differential contributions towards ATP hydrolysis. Among the five stable dimer pairs assayed, Mcm3/7 has the highest ATPase activity, followed by Mcm7/4 and Mcm6/2. Mcm4/6 and Mcm3/5 contribute very little to the ATP turnover. Thus, unlike homohexameric helicases, where all the ATPase active sites contribute equally, individual active sites in Mcm2-7 are functionally distinct.

1.2.4 *In vivo* roles of ATPase active sites in Mcm2-7

All six Mcm ATPase active sites are essential for viability (Schwacha and Bell, 2001). Mutations of the conserved residues have been generated in Walker A (K→A), Walker B (DE→NQ) and arginine finger (R→A) motifs for all the Mcm subunits. Complementation tests in budding yeast showed that most of the mutations are lethal, except for two Walker B mutants, *mcm2DENQ* and *mcm6DENQ*, and one arginine finger mutant, *mcm4RA* (Bochman et al., 2008; Schwacha and Bell, 2001). Consistent with the role of Mcm2-7 in dsDNA unwinding during S phase, overexpression of some Walker A mutants resulted in dominant lethality and blocked the cells in G1/S transition (Schwacha and Bell, 2001). Among the viable mutants, *mcm4RA* and *mcm6DENQ* grow similar to the wild type, and *mcm2DENQ* displays a slight growth defect (A. Schwacha, R, Elbakri, and S. Vijayraghavan, unpublished observations; **Chapter 3**), suggesting that perhaps only ATP binding but not ATP hydrolysis is essential *in vivo*. The growth defects of the Walker B and arginine finger motif mutants roughly correspond to their ATP hydrolysis defects *in vitro* (Bochman et al., 2008).

1.2.5 ssDNA binding of Mcm2-7

Mcm2-7 binds single-stranded DNA (ssDNA) in an ATP-dependent manner but this activity does not require ATP hydrolysis, as ssDNA is bound with the nonhydrolyzable ATP analogue, ATPγS (Bochman and Schwacha, 2007). Similar to the differential contribution of ATPase active sites towards ATP hydrolysis, each active site contributes differently to ssDNA binding. Mutational analysis shows that the Mcm3/7 and Mcm7/4 active sites are important for ssDNA binding (Bochman and Schwacha, 2007). Further, Mcm2/3/5 appears to regulate ssDNA binding

of Mcm4/6/7, as Mcm2-7 has a slower ssDNA association rate relative to Mcm4/6/7 subcomplex (Bochman and Schwacha, 2007).

1.2.6 Mcm2-7 helicase activity and involvement of the Mcm2/5 gate

Since Mcm2-7 is essential for DNA replication initiation and elongation (Aparicio et al., 1997; Labib et al., 2000), it is the potential candidate for the eukaryotic replicative helicase. However, biochemical evidence for the helicase activity of Mcm2-7 has only recently been shown (Bochman and Schwacha, 2008; Ilves et al., 2010). Studies using *S. cerevisiae* Mcm2-7 demonstrate that the reconstitution of helicase activity requires a specific reaction condition containing glutamate anion (Bochman and Schwacha, 2008). In *Drosophila*, DNA unwinding activity of Mcm2-7 can be reconstituted by inclusion of the known replication factors Cdc45 and GINS (Ilves et al., 2010). These two approaches both appear to activate the Mcm2-7 helicase by promoting the correct conformational changes in Mcm2-7.

EM studies show that both Mcm2-7 and Mcm4/6/7 form closed rings (Bochman and Schwacha, 2007; Costa et al., 2011), and DNA binding occurs in the central channel of the ring. Differences in circular ssDNA binding were observed for Mcm2-7 and Mcm4/6/7 (Bochman and Schwacha, 2008), suggesting that this ring-shaped complex must open to allow DNA binding. The ability of these complexes to bind circular ssDNA was tested in two different reaction conditions: by ATP preincubation with the Mcm proteins prior to DNA addition, or by mixing circular ssDNA with the Mcm proteins first prior to ATP addition. When these conditions were used to assay linear ssDNA binding, no differences between Mcm2-7 and Mcm4/6/7 were noticed (Bochman and Schwacha, 2008). However, the binding affinity of Mcm4/6/7 towards circular ssDNA is roughly 20 times lower than Mcm2-7 regardless of the order of addition

(Bochman and Schwacha, 2008). In contrast, Mcm2-7 binds ssDNA well when it is preincubated with circular ssDNA, but poorly when pre-incubated with ATP (Bochman and Schwacha, 2008). This suggests that although both complexes are toroidal (Bochman and Schwacha, 2007), Mcm2-7 likely contains an ATP-regulated discontinuity or "gate" in the ring that facilitates circular ssDNA binding. With many helicase (e.g. SV 40 T-antigen (Tag)), ATP is needed for oligomerization, where ATP at the dimer interfaces holds protein together (Gai et al., 2004). The Mcm2/5 interface may work the same. To determine whether this putative gate resides within the Mcm2/5 active site, the effects of Mcm5KA and Mcm2RA on circular ssDNA binding were tested (Bochman and Schwacha, 2008). Although ATP preincubation did not affect circular ssDNA binding of either complex, these two substitutions had opposite effects: Mcm2-7 containing Mcm5KA bound circular ssDNA well under both conditions (suggesting an "open" complex); however, complexes containing Mcm2RA bound circular ssDNA poorly under both conditions (suggesting a "closed" complex) (Bochman and Schwacha, 2008). These results suggest that the gap is formed at the Mcm2/5 interface.

Activation of Mcm2-7 helicase activity appears to require closure of the Mcm2/5 gate (Bochman and Schwacha, 2008). Paradoxically, ATP seems to have both positive and negative roles on ssDNA binding (reviewed in (Bochman and Schwacha, 2009)). It was then hypothesized that an unknown inhibitor may be present at the Mcm2/5 active site, and ATP serves to displace the inhibitor. It was found that the chloride ion may be lodged at the Mcm2/5 active site and inhibit the *in vitro* helicase activity, as reaction buffer condition that replaces chloride ion with glutamate anion reconstitutes *in vitro* helicase activity. The basis of this stimulation of helicase activity appears to be inversely related to the circular ssDNA binding activity. Preincubation of Mcm2-7 with 100 mM glutamate anion prior to addition of circular

ssDNA results in an effect similar to ATP preincubation, which reduces circular ssDNA binding (Bochman and Schwacha, 2008). Overall, this suggests that this large anion may displace an unknown inhibitor (perhaps chloride ion) in the Mcm2/5 gate and promote gate closure of the Mcm complex for helicase activity. Helicase activity is then inversely related to gate conformation: gate opening blocks helicase activity, and gate closure stimulates helicase activity.

In addition to circular ssDNA binding, linear ssDNA binding activity of Mcm2-7 and Mcm4/6/7 were also compared (Bochman and Schwacha, 2007). As previously mentioned, Mcm2-7 has a slower ssDNA association rate than Mcm4/6/7 (Bochman and Schwacha, 2007). Upon preincubation of Mcm2-7 with ATP, the ssDNA association rate of Mcm2-7 can be dramatically increased to levels similar to Mcm4/6/7 (Bochman and Schwacha, 2007). This suggests that the difference in ssDNA binding between these two complexes likely results from Mcm2/3/5. Consistent with this idea, Mcm2-7 containing the Mcm5KA or the Mcm2RA substitutions within the Mcm2/5 interface display enhanced ssDNA association rate without ATP preincubation (Bochman and Schwacha, 2007). This result suggests that Mcm2/5 active site may normally be bound to an unknown inhibitor, and either ATP preincubation or inclusion of an active site mutation displaces the inhibitor to facilitate linear ssDNA binding. It is also possible that glutamate anion may cause a conformational change in the Mcm complex to promote the Mcm2/5 gate closure.

On the other hand, *in vitro* helicase activity of *Drosophila* Mcm2-7 was reconstituted by addition of cofactors Cdc45 and GINS complex (Ilves et al., 2010), which forms the CMG complex. Cdc45 and GINS complex are not ATPases themselves, but they increase both the ATP hydrolysis and DNA binding affinity of the Mcm2-7 complex (Ilves et al., 2010). They

may promote allosteric remodeling in the Mcm2-7 complex to activate its helicase activity. Furthermore, Mcm2-7, Cdc45 and GINS interact with each other pairwise (Ilves et al., 2010).

Structural work indicates that Cdc45 and GINS activates Mcm2-7 by promoting closure of the Mcm2/5 gate (Costa et al., 2011). Single particle EM has shown that Mcm2-7 exists in either a planar form or a lock-washer form in equilibrium (Costa et al., 2011). In EM studies, the structural discontinuity within the ring was mapped to the Mcm2/5 active site using MBP tagged on specific Mcm subunits (Costa et al., 2011). Within the CMG complex, Cdc45 was mapped to the exterior of Mcm 2 region, and the GINS complex was mapped to the Mcm5 edge (Costa et al., 2011). This is consistent with the Mcm2/5 gate proposed from the biochemical work mentioned above. Although it is not directly involved in robust ATP hydrolysis or contributing towards the helicase activity, the regulation of the Mcm2/5 gate is coupled to the helicase activity (reviewed in (Bochman and Schwacha, 2009), (Bochman and Schwacha, 2008)). In the presence of a non-hydrolyzable nucleotide analog, ADP-BeF_3, the Mcm2/5 gate closes and the central channel within the CMG complex constricts (Costa et al., 2011). This study provides a mechanistic model for Mcm2-7 helicase activation, where Cdc45 and GINS binding to the Mcm2-7 complex promotes closure of the Mcm2/5 gate and activation of helicase activity (Figure 4).

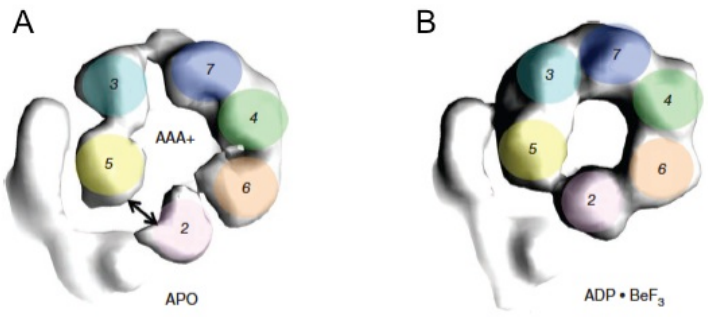

Figure 4. Cdc45 and GINS promote gate closure of Mcm2-7 upon nucleotide binding

A) Cdc45 and GINS are depicted in white. Mcm2-7 is viewed from the AAA+ domain in an Apo state. B) The Mcm2-7 ring closure in nucleotide bound state. These figures are adapted from (Costa et al., 2011), and reprinted with permission from Nature Publishing Group.

1.2.7 *In vivo* implications of the Mcm2/5 gate

The properties of the Mcm2/5 gate suggest several porential *in vivo* functions: 1) as DNA needs to be loaded into the central channel, this gate may be required to load Mcm2-7 onto replication origins prior to DNA replication begins, and 2) as gate closure is required for helicase activation, this gate may be used for regulation of helicase activation. There are two likely instances where helicase regulation may occur. The helicase activity may be blocked during G1 phase of the cell cycle, and gate closure only takes place during S phase, as suggested by the structural work of Botchan's group. In addition, the helicase activity may be downregulated during S-phase checkpoint activation (i.e. encountering DNA damage), to facilitate DNA repair.

1.2.8 DNA unwinding mechanism of the Mcm2-7 helicase

As there is no high resolution structure available for Mcm2-7, much of our understanding of Mcm2-7 is based upon the crystal structure of the archaeal Mcm mono-hexamer (Bae et al., 2009; Brewster et al., 2008; Fletcher et al., 2003; Liu et al., 2008). Archaeal Mcm complexes are usually homohexamers, with six identical Mcm subunits, each carries out the same function (Patel and Picha, 2000). In contrast, eukaryotic Mcm2-7 contains six distinct subunits and ATPase active sites, each contributes differentially towards ATP hydrolysis and helicase activity (reviewed in (Bochman and Schwacha, 2009)). This property allows one to conduct mutational analysis on specific subunits and study the mechanistic aspects of DNA unwinding. Yet, this is also a complicated and difficult system to study. To help understand the unwinding mechanism of Mcm2-7 recently proposed, models derived from the homohexameric helicases will be discussed first.

Structural work with the bovine papillomavirus E1 helicase demonstrates that this ring-shaped helicase wraps around ssDNA in its central channel (Enemark and Joshua-Tor, 2006). It was shown that sequential ATP hydrolysis among the six active sites is coupled to DNA translocation, where β hairpins (two anti-parallel β-strands that project into the central channel and interact with ssDNA via positive charged residues) from all six subunits form a spiral "staircase" that track along the DNA (Enemark and Joshua-Tor, 2006). This study provides an excellent example for the steric exclusion model which describes the classical view of DNA unwinding mechanism utilized by the hexameric helicases (Patel and Picha, 2000). This model requires the ssDNA to be encircled by the central channel, while the other strand is displaced (Figure 5). Early studies of a subcomplex of Mcm2-7, the Mcm4/6/7 trimer dimer, suggested that it unwinds dsDNA by steric exclusion (Kaplan et al., 2003). While most studies

have focused on the location and the nature (i.e. dsDNA or ssDNA) of the encircled strands, one recent study of the *Sulfolobus* Mcm has addressed the importance of the displaced strand. It was demonstrated that the excluded DNA strand wraps around the Mcm complex and is important for the DNA unwinding activities (Graham et al., 2011).

In the RecBCD helicase, dsDNA is separated and pulled by the RecB and RecD subunits, and then split across a pin protruding from the RecC subunit (Singleton et al., 2004). This study shows a variation of the steric exclusion model— the ploughshare model. This model was originally proposed to solve the problem arising from using the dsDNA pump model (see below), which would impede the cohesion establishment between sister chromatids and passage of the fork through the cohesin rings (Takahashi et al., 2005). This model proposes that the Mcm2-7 helicase loads onto dsDNA and drags a proteinaceous wedge to separate the strands after initial melting (Takahashi et al., 2005) (Figure 5). In the case of Mcm2-7, the proteinaceous wedge/pin may be the accessory factors GINS and Cdc45.

In addition to the above models, there is also a model that was proposed to account for several paradoxes observed in eukaryotic cells. In bacteria, DNA unwinding is achieved by the loading of two helicases to establish bi-directional forks (Mott and Berger, 2007). However, the Mcm2-7 complexes in both animal cells and yeast appear to exist in excess amount, with 10-100 Mcm2-7 loaded per replication (Edwards, 2002; Lei M, 1996). Another problem appears to be the lack of reconciliation between spatial localization and function of Mcm2-7. Although yeast chromatin immunoprecipitation (ChIP) experiments suggest the close proximity between the Mcm proteins and the fork (Aparicio et al., 1997), immunofluorescence studies in animal cells show that the Mcm proteins preferentially localize to non-replicating regions rather than the replicating regions (Dimitrova et al., 1999; Krude et al., 1996; Madine et al., 1995a). To account

for these discrepancies, the rotary pump model was proposed (Laskey and Madine, 2003). In this model, the dsDNA is unwound by coupling the rotational action and translocation of the Mcm complex that wraps around dsDNA and positions at a distance from the fork (Figure 5).

Finally, a dsDNA pump model was proposed to explain the SV40 Tag helicase (Gai et al., 2004; Li et al., 2003; Takahashi et al., 2005). Based on the crystal structure of SV40 Tag and the fact that it can be loaded onto dsDNA (Dean et al., 1992), it was proposed that melting of dsDNA takes place within the central channel to generate ssDNA, which is then extruded through the side channels (on the side wall of the hexamer) (Figure 5).

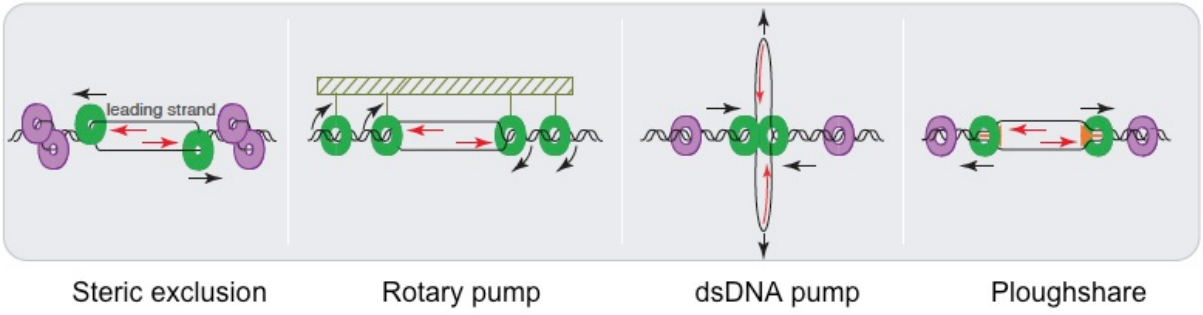

Figure 5. Proposed models for the DNA unwinding mechanism of Mcm2-7

This figure is adapted from (Takahashi et al., 2005), and reprinted with permission from Elsevier.

The Mcm2-7 unwinding mechanism was elucidated from studies of its loading and translocation. However, studies have uncovered unexpected complications not anticipated by any model. EM studies have shown that Mcm2-7 can be loaded onto dsDNA in an ORC- and Cdc6-dependent manner as a head to head double hexamer (Evrin et al., 2009; Remus et al.,

2009). These data suggest that Mcm2-7 may behave like the SV40 Tag or the E1 helicase, which also assembles as a double hexamer (Dean et al., 1992; Fouts et al., 1999). If Mcm2-7 indeed unwinds dsDNA as a dsDNA pump, then a stretched DNA immobilized at both ends should not be replicated. This has been specifically tested. Studies examining DNA replication in *Xenopus* egg extracts show that origin DNA can be replicated efficiently under constraint conditions with a single pair of replisomes, indicating that coupling between sister replisomes is not required (Yardimci et al., 2010). This study therefore strongly suggests that the Mcm2-7 helicase does not utilize a dsDNA pump model.

Furthermore, single molecule experiments using a completely reconstituted replication system demonstrate that the CMG complex translocates along the leading strand by encircling ssDNA (Fu et al., 2011), consistent with prior biochemical experiments shown that Mcm2-7 functions as a 3' to 5' replicative helicase (Bochman and Schwacha, 2008; Ilves et al., 2010; Ishimi, 1997; Lee and Hurwitz, 2000; Moyer et al., 2006). This experiment thus disproves the dsDNA pump model. The distinction between translocation along either ssDNA or dsDNA was first made using interstrand crosslinked plasmid DNA (to prevent interference of fork from the opposite direction) tagged with a biotin-SA ("roadblock") labeled on one strand of DNA or both strands (Fu et al., 2011) (Figure 6A). A ssDNA translocase should only be impeded by biotin-SA labeled on one strand of DNA, where a dsDNA translocase should be impeded when either strand is blocked. It was shown that the CMG complex is arrested more efficiently by a leading strand labeled with biotin-SA than the lagging strand (Fu et al., 2011), suggesting the CMG complex translocates on ssDNA.

An independent approach was taken to test whether the CMG complex translocates along the leading strand or lagging strand, or along dsDNA. DNA replication is allowed to initiate on

λ DNA immobilized in a microfluidic flow cell, with either the leading strand or lagging strand attached with “QDot” (Fu et al., 2011) (Figure 6B). DNA synthesis is visualized by SYTOX orange. If Mcm translocation occurs on the leading strand, it would be arrested with “Qdot” attached to a leading strand but not lagging strand. Indeed, the CMG complex collides with the QDot labeled on the leading strand more frequently than on the lagging strand (Fu et al., 2011). This study indicates that Mcm2-7 translocates on ssDNA within its central channel during DNA unwinding. These data together with previous studies (Yardimci et al., 2010) are consistent with the unwinding of dsDNA using the steric exclusion model by traveling along one strand and displacing the other strand.

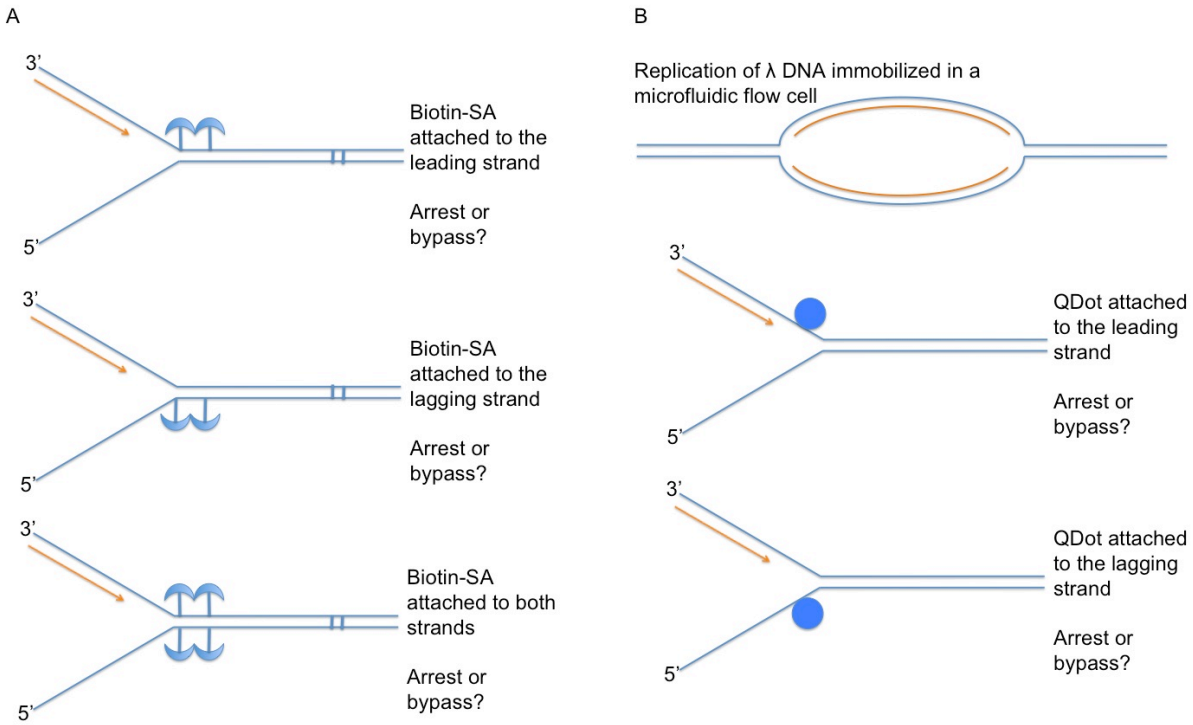

Figure 6. Evidence for the steric exclusion model

A. An interstrand crosslinked plasmid DNA is labeled with biotin-SA on the leading strand, lagging strand, or both strands. To assay whether the CMG complex arrests or bypasses the roadblock, the replication intermediates of the leading strands separated on a DNA sequencing gel were mapped. The replication of the leading strands allows one to determine the footprint of the CMG complex (Fu et al., 2011). B. QDot is attached to either a leading strand or a lagging; a rightward fork is shown as an example. In this assay, total DNA is labeled with SYTOX orange and dig-dUTP (fluorescein-labeled anti-dig antibody); either the leading strand or lagging strand was labeled with QDot. The arrest or bypass of DNA replication can be directly visualized (Fu et al., 2011).

Taken at face value, these results present a paradox: Mcms load onto dsDNA in the pre-RC yet encircle ssDNA during elongation. These results imply that Mcm2-7 subunit organization must be remodeled in some manner, possibly through the Mcm2/5 gate and perhaps the cofactors Cdc45 and GINS to facilitate initial melting. Recent EM studies have shown that Cdc45 and GINS binding to Mcm2-7 constricts the Mcm2/5 gate, and generates a external channel on the outer surface (Costa et al., 2011), perhaps this pore partitions the separated strands. Recent biochemical studies demonstrate that the activating factor GINS and the initiator protein Sld3 may compete with each other for Mcm2-7 binding, which may provide a mechanism for the initial DNA unwinding upon the formation of the CMG complex (Bruck and Kaplan, 2011). Future work is needed to determine how Mcm2-7 remodels from a dsDNA state to a ssDNA state.

1.3 THE S-PHASE CHECKPOINT

When dsDNA is unwound during DNA replication, ssDNA is generated and exposed to various environmental stresses. The S-phase checkpoint provides a surveillance system to ensure genome integrity. In response to DNA damage or replication stress, this checkpoint is activated to stop the cell cycle progression, and additionally regulates several aspects of DNA replication such as replication initiation (i.e. repressing late origin firing) and maintaining replication fork stability to prevent the dissociation of the replisomes from the replication forks (Branzei and Foiani, 2009; Zegerman and Diffley, 2009). It is possible that the S-phase checkpoint may target Mcm2-7, the molecular motor that drives fork progression through the regulation of its ATP hydrolysis. Indeed, it has been shown that Mcm2-7 undergoes checkpoint kinase-dependent phosphorylation (Cortez et al., 2004). Furthermore, it has been reported that the physical interaction between Mcm2-7 and checkpoint proteins is required for checkpoint activation during DNA damage (Komata et al., 2009). However, the mechanism involved is not clear. In this section, I will discuss the S-phase checkpoint cascade, the regulation of DNA replication by this cascade, and the evidenc supporting Mcm2-7 as a target of the S-phase checkpoint.

1.3.1 Discovery of the S-phase checkpoint

Over 20 years ago, Weinert and Hartwell first formulated the concept of a “checkpoint” (Weinert and Hartwell, 1988). In the presence of DNA damage, *RAD9* is required to delay cell cycle progression in G2 to prevent entry into mitosis in budding yeast. In a microcolony assay in the presence of DNA damage, *rad9* mutants but not wild type cells continued to divide, resulting in a high rate of lethality. It was proposed that all eukaryotes should have a similar control

mechanism that precents cell cycle progression until DNA damage is repaired. Later work revealed that *RAD17*, *RAD24*, *MEC3*, *MEC1* and *RAD53* were additionally required for cell cycle arrest (Weinert and Hartwell, 1993; Weinert et al., 1994). These checkpoint genes are present in higher eukaryotes and have similar functions (reviewed in (Branzei and Foiani, 2009)).

These checkpoint genes also function in the context of DNA replication. *MEC1* and *RAD53* are needed to delay the cell cycle in response to DNA damage by regulating DNA replication. The *rad53* and *mec1* mutants progress through S phase rapidly in the presence of DNA damage as opposed to the wild type (Paulovich and Hartwell, 1995). Around the same time, it was discovered that *MEC1* has a human homolog *ATM*, and a mutation in the *ATM* gene was responsible for the AT disorder (Savitsky et al., 1995). These results together show that *MEC1* (*ATM*) and *RAD53* (*CHK2* in human) regulate DNA synthesis during DNA damage, and these checkpoint pathways are conserved between yeast and human. The lack of arrest was also observed in mammalian cells carrying mutations in checkpoint genes. For example, cells from ataxia telangiectasia (AT) patients are defective for inhibiting DNA synthesis upon x-irradiation, although this was not interpreted as a checkpoint defect at that time (Busse et al., 1978; Painter and Young, 1980). The gene products of *RAD53* and *MEC1* were identified as protein kinases (Allen et al., 1994), indicating that the S-phase checkpoint is a signal transduction pathway involving a phosphorylation cascade.

1.3.2 Signals that trigger S-phase checkpoint activation

The S-phase checkpoint has been most thoroughly studied in budding yeast. Activation of the checkpoint involves the recognition of ssDNA, stalled replication forks or DNA damage

(Tercero and Diffley, 2001). ssDNA intermediates can be generated by the resection of double-stranded breaks (DSBs) or uncoupling of the replicative helicase and DNA polymerase under replication stress condition (Byun et al., 2005). Once a signal is formed, Mec1 (PIKK related kinase ATR in humans) and Rad24 (Rad17 in humans) are recruited to the RPA (eukaryotic single-stranded DNA binding protein)-coated ssDNA region (Zou and Elledge, 2003). *In vitro* studies have shown that Rad24 can further recruit PCNA-like sliding clamp Rad17/Mec3/Ddc1 (Rad9/Rad1/Hus1 in mammals) (Majka and Burgers, 2003) to activate Mec1 (Majka et al., 2006). In addition to the checkpoint clamp system, the replication factor Dpb11 in yeast (TopBP1 in human) is also an important activator of Mec1/ATR (Navadgi-Patil and Burgers, 2008). These checkpoint proteins together form a platform at RPA-coated ssDNA for checkpoint activation.

Recognition of DNA damage activates the Mec1 kinase and starts the signal transduction pathway (reviewed in (Branzei and Foiani, 2009)). The S-phase checkpoint is comprised of two partially redundant pathways that each culminates in activation of Rad53. However, two different mediator proteins are used: Rad9 or Mrc1 (Alcasabas et al., 2001; Sanchez et al., 1996; Vialard et al., 1998) (Figure 4). Rad9 is recruited to the DNA double-stranded breaks; however, it does not respond efficiently to replication stress induced by nucleotide depletion. Rad9 functions as a checkpoint adaptor that interacts with the FHA domain of Rad53 and promotes the recognition of Rad53 by Mec1 (Sweeney et al., 2005; Toh and Lowndes, 2003). This pathway is called the DNA damage checkpoint (DDC) (Figure 7).

In contrast, Mrc1 responds to replication stress, such as nucleotide depletion induced by the ribonucleotide reductase (RNR) inhibitor hydroxyurea (HU) (Alcasabas et al., 2001). Under replication stress, Mrc1 is phosphorylated by Mec1 to activate Rad53 (Alcasabas et al., 2001).

Mutations that eliminate the serine/threonine clusters, the consensus sequence within Mrc1 for Mec1-phosphoryalation abolish Rad53 phosphorylation (i.e. *mrc1AQ*) (Osborn and Elledge, 2003). Recent studies have provided some insights into the molecular mechanism involved in the Mrc1 mediated pathway. It has been suggested that Mrc1 phosphorylation leads to a feedback loop that promotes Mec1 enrichment at the replication fork, in order to amplify the checkpoint signal (Naylor et al., 2009). The *MRC1*-mediated pathway is called the DNA replication checkpoint (DRC) (Figure 7).

The *RAD9* and *MRC1* mediated pathways are partially redundant. When one pathway is eliminated, the remaining one can largely complement its checkpoint function. However, when both pathways are ablated, Rad53 hyperphosphorylation is abolished and the cells are extremely sensitive to DNA damage (Alcasabas et al., 2001).

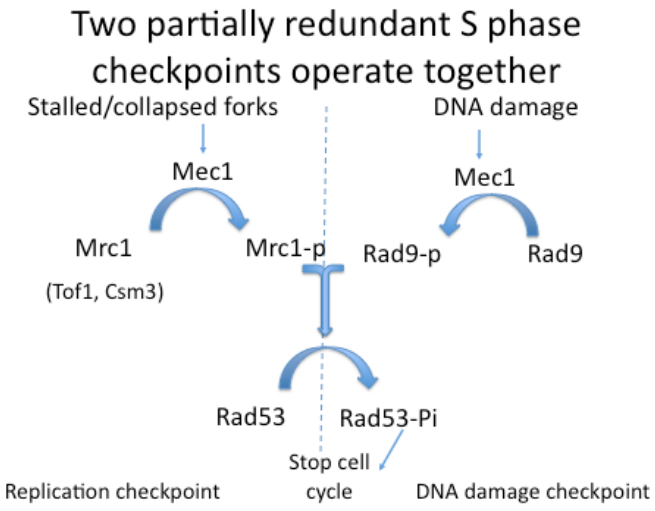

Figure 7. The S-phase checkpoint contains two partially redundant phosphorylation cascades

In response to stalled replication forks or double-stranded breaks, the S-phase checkpoint mediated by either *MRC1* or *RAD9* is activated, respectively. These pathways are partially redundant and compensate each other.

1.3.3 Other aspects of the S-phase checkpoint: regulation of the dNTP pools

The S-phase checkpoint responds to DNA damage or replication blocks by inducing transcription of genes that modulate the dNTP pools. Mec1-mediated phosphorylation of Rad53 activates the downstream protein kinase Dun1 leading to transcriptional induction of multiple genes (Allen et al., 1994). Dun1 phosphorylates Crt1 (Allen et al., 1994; Huang et al., 1998), a transcriptional repressor that binds to the promoter region of the *RNR* genes that encode the ribonucleotide reductase. During DNA damage, transcription derepression occurs as Crt1 is phosphorylated in a Mec1-dependent manner by and released from the promoter (Huang et al., 1998). This results in increased expression of the *RNR* gene. However, transcriptional response is not a crucial downstream effect because inhibition of protein synthesis in hydroxyurea (HU)-treated S-phase cells does not affect replication fork progression or viability (Tercero et al., 2003).

In addition to transcriptional control, RNR activity is also regulated by a small protein Sml1. Sml1 inhibits by binding to RNR, resulting in a downregulation of the dNTP pools (Zhao et al., 1998). In response to DNA damages, Sml1 is phosphorylated by the Dun1 kinase and rapidly degraded, resulting in the upregulation of the dNTP levels (Zhao and Rothstein, 2002). This regulation of Sml1 protein serves as a way to quickly increase the dNTP levels, as opposed to the slower transcriptional response.

Although it is natural to consider the increased dNTP pools as a mean to provide additional nucleotides for lesion repair, little is known regarding how dNTP pools affect DNA replication during replication stress. Interestingly, a recent study has shown that the upregulation of dNTP pools increases replication fork progression rate (Poli et al., 2012). Further, DNA precursors can also modulate origin usage, where higher levels of DNA precursors activate origin activations.

1.3.4 Other effect of the S-phase checkpoint: inhibition of late origin firing

During replication stress, the S-phase checkpoint inhibits the initiation of replication origins. In eukaryotic genomes, DNA replication is initiated at multiple discrete sites in order to allow the entire genome to be fully replicated within a reasonable time. While pre-replicative complexes (pre-RC) are formed at all origins, these origins fire following a pre-determined temporal order; some origins fire early in S-phase, and some origins fire late. In null mutants of *MRC1* or *RAD53*, all late origins fire prematurely during nucleotide depletion (Alcasabas et al., 2001; Crabbe et al., 2010; Feng et al., 2006; Santocanale and Diffley, 1998) (Figure 8). While the underlying mechanism of the repression of late origin firing is not clear for Mrc1, it has been reported that Rad53 suppresses late origin firing by inhibiting the initiator proteins Sld3 and Dbf4 via phosphorylation (Lopez-Mosqueda et al., 2010; Zegerman and Diffley, 2010). This inhibition blocks both the CDK and DDK pathways that are required for the activation of the replicative helicase. Thus, the S-phase checkpoint maintains the temporal order of origin firing.

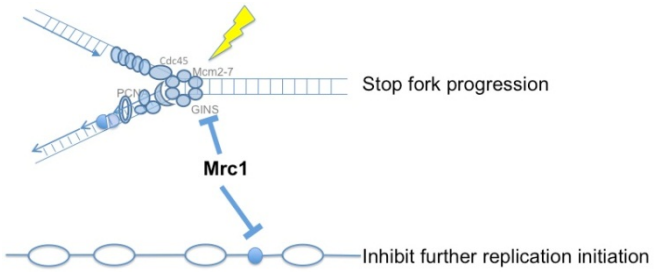

Figure 8. The S phase checkpoint stops cell cycle progression during DNA damage

S phase checkpoint inhibits cell cycle progression by inhibiting replication fork proression and additional replication initiation from late replication origins.

1.3.5 Other effect of the S-phase checkpoint: replication forks stabilization

When DNA replication forks encounters damage, the S-phase checkpoint maintains replication fork stability to preserve replisome integrity at the replication fork. Experiments using heavy isotope substitution to assay replication fork progression showed that replication forks in checkpoint mutants *rad53* and *mec1* terminate irreversibly in the presence of DNA damage caused by the alkylating agent methyl-methane sulfonate (MMS) (Tercero and Diffley, 2001). As the replicative helicase Mcm2-7 cannot be reloaded once forks collapse; this leads to incomplete replication and cell death (Tercero and Diffley, 2001). Also, ChIP experiments show that polymerase ε dissociates with replication forks in checkpoint mutants during replication stress (Cobb et al., 2003; Lucca et al., 2004). In addition to the dissociation of replication factors from the fork, under nucleotide depletion conditions, aberrant DNA structures have been observed (Lopes et al., 2001). Using electron microscopy, pathological DNA structures

correspond to collapsed, reversed forks or excess accumulation of ssDNAs have been identified (Sogo et al., 2002). Therefore, the S-phase checkpoint is important for maintaining stable forks. The generation of aberrant recombinogenic DNA structures can cause genomic instability.

Although the mechanism of replication fork stabilization is unknown, it may prevent the accumulation of aberrant DNA structures. For example, the deletion of *EXO1*, an exonuclease, suppresses irreversible replication fork termination in *rad53* but not *mec1* mutant (Segurado and Diffley, 2008). Exo1 is recruited to stalled replication forks to counteract reversed forks. Therefore, the inhibition of Exo1 by Rad53 may stabilize replication forks and prevent the generation of excess ssDNA (Morin et al., 2008). On the other hand, the mechanism of Mec1 in stabilizing replication fork is less clear. As *mec1* mutants generally have lower viability than *rad53* mutants, and are more sensitive to DNA damage (Tercero and Diffley, 2001), Mec1 may have an additional Rad53-independent function. As shown by ChIP experiments, Mec1 but not Rad53 is required to promote polymerase ε stability at the fork (Cobb et al., 2003; Lucca et al., 2004).

In addition to Mec1 and Rad53, Mrc1 is required to maintain a tight coupling between the replication factors during replication stress (Katou et al., 2003). With a specially engineered budding yeast strain that can transport and incorporate exogenous BrdU into DNA, ChIP to both replication proteins and new DNA synthesis could be assayed simultaneously. In null mutants of *MRC1*, uncoupling of the replicative helicase Mcm2-7 (and Cdc45) from DNA synthesis was observed at a single origin of replication (Katou et al., 2003) (Figure 8). This study suggested that the S-phase checkpoint may target Mcm2-7 to promote replication fork stability and coordinate DNA unwinding with DNA synthesis. Alternatively, being part of the replication

fork, loss of Mrc1 generates fragile forks that are prone to collapse under replication stress (Szyjka et al., 2005).

Although the role of checkpoint proteins in maintaining replication fork stability has been the long standing model based on the evidences described above, one recent study has challenged this view (De Piccoli et al., 2012). It has been shown by co-immunoprecipitation that the replisome remains intact during hydroxyurea arrest (De Piccoli et al., 2012). Also, it was demonstrated by ChIP-seq analyses that a subunit of the replicative helicase Mcm4 and DNA Pol1 do not uncouple during replication stress condition (De Piccoli et al., 2012). Future experiments using single molecular technique (Fu et al., 2011) may be required to directly address the replisome stability issue.

1.3.6 Potential targets of the S-phase checkpoint in the replication fork

Since the S-phase checkpoint regulates replication fork stability, it is likely that its direct target is the replisome. The Mcm2-7 complex central to much known regulation, seems a likely target. In *S. pombe*, Mcm4 physically interacts with the checkpoint proteins Cds1 (Rad53 in budding yeast), and is phosphorylated in a Cds1-dependent manner (Bailis et al., 2008), suggesting that Mcm2-7 is a downstream target of Rad53. In budding yeast, a mutation in the C-terminal AAA+ domain of Mcm6 has been identified that abolishes its interaction with Mrc1; *mcm6* mutants that no longer bind Mrc1 (*mcm6IL*) are defective for checkpoint signaling (Komata et al., 2009). *In vitro* experiments have shown that human Mcms can be phosphorylated by the checkpoint kinases ATM (Mec1 in yeast) and ATR (Tel1) (Cortez et al., 2004); however, there is no evidence that these phosphorylation events directly regulate the activity of Mcm2-7 during DNA

damage *in vivo*. Together, these studies suggest that the Mcm2-7 complex may be a target of the S-phase checkpoint. This possibility will be addressed in **Thesis Overview**.

1.4 SISTER CHROMATID COHESION

In addition to generating new sister chromatids, DNA replication is coupled to an additional event needed for proper mitosis—sister chromatid cohesion (SCC). During S phase, newly replicated sister chromatids are physically paired by the ring-shaped cohesin complex (Figure 9). SCC is essential for proper chromosomal segregation, as tension between sister chromatids is needed for proper bipolar attachment. In the absence of SCC, premature sister chromatid separation occurs, resulting in chromosome missegregation. Proteolysis of cohesins by separase resolves the tension between sister chromatids, allowing proper segregation of sister chromatids into each daughter cell during anaphase (Onn et al., 2008). SCC is also required for DNA damage induced recombinational repair in G2 (Sjögren and Ström, 2010).

Although new cohesins are loaded onto chromosomes in G1; DNA replication forks are required in some unknown manner to couple together the new sister chromatids (establishment) (Onn et al., 2008). Multiple genetic screens have revealed interactions among factors involved in DNA replication, SCC, and DRC, suggesting an interplay among these processes (Warren et al., 2004; Xu et al., 2004). However, simultaneous examination of all three processes has not been carried out, and this interconnection has only recently begun to be appreciated. To understand these problems, the following topics will be discussed: the composition and architecture of cohesin, the influence of replication licensing on the association of cohesin with DNA, and how factors associating with the replication forks influence SCC and DRC.

1.4.1 Architecture and composition of cohesin

Cohesin is a highly conserved multi-subunit ring-shaped complex formed from two Smc (Structural Maintenance of Chromosome) proteins (Smc1 and Smc3) and two non-Smc proteins (Scc1 and Scc3) (Haering et al., 2002). Smc proteins are evolutionarily conserved throughout bacteria, archaea and eukaryotes and contain five domains: two elongated antiparallel coiled-coil segments that interact intramolecularly, a dimerization domain, and N- and C-terminal domains that together form an ATPase active site (Figure 9). Smc1 and Smc3 form a heterodimer at the hinge domain, and their ATPase domains heads are bridged by cohesin's Scc1 subunit through its N- and C-terminal domain, respectively (Gruber et al., 2003; Haering et al., 2002) (Figure 9). ATP hydrolysis within Smc1 and Smc3's ATPase domain is needed for the cohesins to stably associate with the chromosomes (Arumugam et al., 2003; Weitzer et al., 2003). Scc3 interacts with accessory factor Rad61 (Wapl in human), and perhaps indirectly with Pds5 through Rad61 (Rowland, 2009). Rad61/Wapl appears to play different roles in yeast and higher eukaryotes. Human Wapl is required for prophase removal of cohesins from the chromosome arm, allowing resolution of sister chromatids (Gandhi et al., 2006; Kueng et al., 2006). In budding yeast, Rad61 appears promote the association of cohesin with chromosome arms (Rowland, 2009; Sutani et al., 2009). Pds5 is required for maintaining SCC (Hartman et al., 2000; Losada et al., 2005; Panizza et al., 2000). EM studies have shown that the cohesin ring complex has a diameter of roughly 40nM, which is large enough to accommodate two DNA duplexes (Haering et al., 2002). These features suggest that cohesin complex may encircle both sister chromatids in a highly regulated manner to ensure accurate chromosomal segregation (reviewed in (Nasmyth and Haering, 2009)). However, alternative models have been proposed to describe the mechanism of cohesin ring association with DNA (reviewed in (Nasmyth and Haering, 2009)).

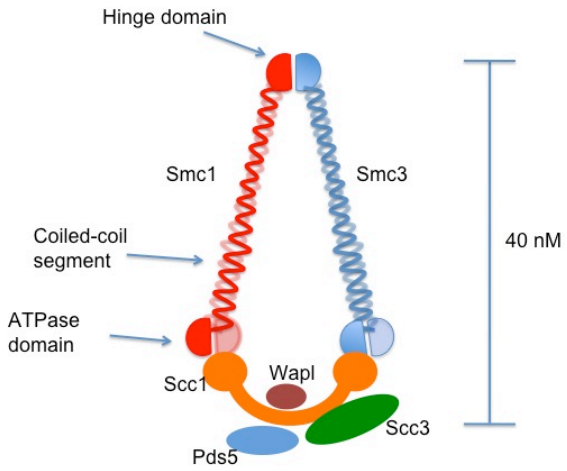

Figure 9. Cohesin architecture

Cohesin is a ring-shaped complex composed of Smc1, Smc3, Scc1 and Scc3. Smc1 and Smc3 form heterodimer and are connected by Scc1at their N- and C-terminal domains respectively. Pds5 and Wapl are accessory factors.

1.4.2 Cohesin loading prior to S-phase

Cohesins are loaded onto chromosomes during G1 by Scc2 and Scc4, which are not themselves part of the cohesin complex (Bernard et al., 2006; Ciosk et al., 2000; Neuwald and Hirano, 2000) (Figure 10). Scc2 and Scc4 are highly conserved (Tonkin et al., 2004; Watrin et al., 2006), and form a dimeric complex (Seitan et al., 2006; Takahashi et al., 2008). In *scc2* and *scc4* mutants, the cohesin complex is still formed, but does not associate with DNA (Ciosk et al., 2000). Once initial cohesin loading is achieved and DNA replication is completed, Scc2 and Scc4 are not required to maintain SCC during metaphase and anaphase (Lengronne et al., 2006). Recently, these observations have been biochemically reconstituted *in vitro* (Onn and Koshland, 2011).

In addition to Scc2 and Scc4, replication licensing by pre-RC formation is also required for the loading of the cohesin complex. In *Xenopus*, all the components in the pre-RC, including Orc, Cdc6, Cdt1, and Mcm2-7, are required to load both the cohesin complex and Scc2 in a DDK dependent manner (Takahashi et al., 2008; Takahashi et al., 2004). Cohesin loading occurs after pre-RC formation and before Cdc45 loading, thus, only origin licensing but not initial unwinding is required (Takahashi et al., 2004). However, a similar mechanism has not been observed in budding yeast. Cdc6 depletion in budding yeast does not affect cohesin association with DNA (Uhlmann and Nasmyth, 1998), suggesting that the link between replication initiation and SCC may not be conserved. The cohesin complexes are loaded every 11kb along the chromosome where each cohesin association site (CAR) site spans 1kb (Blat and Kleckner, 1999; Glynn et al., 2004; Laloraya et al., 2000). However, as replication origins in budding yeast are 30kb apart on average (Wyrick et al., 2001), it is likely that each replication fork will encounter at least one cohesin complex.

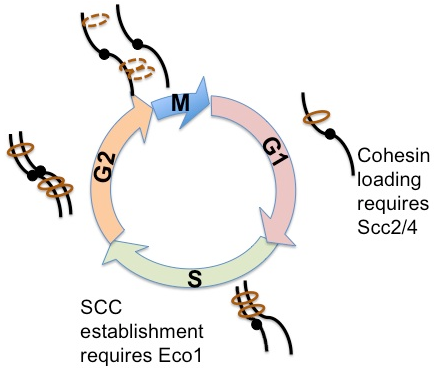

Figure 10. SCC loading and establishment are cell cycle dependent

1.4.3 SCC establishment during S-phase

After cohesin's loading in G1, SCC is likely established between during DNA replication. Indeed, a conserved protein, Eco1, is essential to establish SCC in S phase (Figure 10), and its activity is limited to S-phase via Cdk1 mediated degradation during metaphase (Lyons and Morgan, 2011; Skibbens et al., 1999; Tóth et al., 1999). Once DNA replication is complete, Eco1 is no longer needed since inactivation of a temperature-sensitive *ECO1* allele in G2 neither compromises cell viability nor blocks SCC (Lengronne et al., 2006). Eco1 has acetyltransferase activity (Ivanov et al., 2002), and acetylates cohesin subunit Smc3 at the key residues K112 and K113 (K105 and K106 in human), that are in close proximity to the ATP binding site of Smc3 (Ben-Shahar, 2008; Rowland, 2009; Ünal et al., 2008; Zhang, 2008). This acetylation is thought to promote SCC by counteracting the inhibitory function of Pds5, Wap1, and Scc3 (Rowland et al., 2009; Sutani et al., 2009; Tanaka et al., 2001). Recently, yeast genetic studies have implicated the role of acetylation in regulating the ATP hydrolysis activity of Smc3, thus regulating cohesin (Scc1) binding (Heidinger-Pauli et al., 2010). This study opens the question of whether other accessory factors such as Pds5 and Scc3 are regulated similarly, and if ATP hydrolysis affects conformational changes of the cohesin subunits. These studies suggest that establishment of SCC in S-phase requires reorganization of the cohesin ring.

1.4.4 Many DNA replication factors are required for SCC

DNA replication is linked to SCC not only during replication licensing as described above but also during elongation. Overexpression of polymerase processivity factor PCNA suppresses lethality of an *eco1* (*ctf7-203*) mutant at non-permissive temperature (Skibbens et al., 1999).

Interestingly, Eco1 is also found to physically interact with PCNA, and disruption of this interaction leads to defective SCC (Moldovan et al., 2006). Furthermore, null mutant of *ctf18*, an alternative clamp loader involved in DNA damage repair and recombination (Naiki et al., 2001), is synthetically lethal with an *eco1* mutant (Skibbens et al., 1999). A null mutant of *CTF4/AND-1*, which physically links Mcm2-7 to lagging strand DNA polymerase δ, is also defective in SCC (Hanna et al., 2001). Finally, mutants of *CHL1/CHLR1*, which is implicated in lagging strand synthesis, are also compromised in SCC (Petronczki et al., 2004). Although the involvement of these replication proteins clearly suggests an interplay between SCC and DNA replication, the mechanisms involved are largely unknown.

1.4.5 SCC establishment during DNA damage

Although SCC is normally established during S phase in the presence of active replication forks, recent studies have shown that SCC can also be established in G2, in order to facilitate double strand break (DSB) repair (Ström et al., 2007; Ünal et al., 2007). In both budding yeasts and human cells, cohesins are recruited to DSB sites in G2 (Kim et al., 2002; Ström et al., 2004; Ünal et al., 2004). Presumably, this DNA damage dependent SCC facilitates recombinational repairs, since sister chromatids are the preferred substrates for post-replicative recombinational repair in G2 in yeast (Kadyk and Hartwell, 1992).

DNA damage-induced SCC is mediated by the DNA damage response pathway. Early studies have shown that Smc1 and Smc3 are phosphorylated by the sensor checkpoint kinase ATM (Mec1 in yeast), upon exposure to ionizing irradiation in human cells (Kitagawa et al., 2004). This suggests a link between cohesin and the S-phase checkpoint signal transduction pathway. Eco1 and APRIN (human homolog of budding yeast Pds5) are substrates of

ATM/ATR (Matsuoka et al., 2007). Two independent groups have specifically tested whether DNA damage-induced SCC occurs independent of DNA replication (Ström et al., 2007; Ünal et al., 2007). In one study, budding yeast strains expressing a temperature sensitive cohesin subunit *scc1* (S-cohesin) during S phase (Ünal et al., 2007). Two HO endonuclease cleavage sites were introduced into chromosome III (one is upstream of *SRD1* and the other is the *MAT* locus), which breaks the chromosome into a 60 kb *SRD1-MAT* fragment and two larger fragments (Ünal et al., 2007). Upon HO endonuclease cleavage, the S-cohesin was degraded at non-permissive temperature, and wild type Scc1 was expressed. Using this strategy, it was found that DNA damaged-induced SCC can be established during G2/M in the absence of DNA replication (Ünal et al., 2007). Similar results have been obtained using temperature sensitive *smc1-259* cohesin allele and wild type Smc1, and DNA damage was generated by γ-irradiation treatment (Ström et al., 2007). Furthermore, Mec1 is required for damage-induced SCC in G2, while Tel1, H2A and Rad53 are only partially required (Ström et al., 2007; Ünal et al., 2007). As in S-phase, Eco1 is also required for the establishment of SCC in G2. Most importantly, cohesin recruitment is not limited to DSB site but occurs globally among all chromosomes. These findings show that at least part of the DNA replication checkpoint signal transduction pathway is required for SCC in response to DNA damage.

1.4.6 Many S-phase checkpoint proteins are required for SCC

The S-phase checkpoint is also required for normal SCC. Various non-essential genes with both SCC and checkpoint defects have been identified from the yeast genetic screens. These include *MRC1*, *TOF1*, *CSM3*, *CTF4* and *CTF18* (Mayer et al., 2004; Warren et al., 2004; Xu et al., 2004) (Figure 11). Mrc1, Tof1 and Csm3 are S-phase checkpoint proteins that are required for both

replication fork pausing during replication stress (reviewed in (Branzei and Foiani, 2009)), and as normal constituents of the replication fork during unchallenged S-phase (reviewed in (Zegerman and Diffley, 2009)). This suggests that SCC is linked to both DNA replication as well as the S-phase checkpoint. Synthetic lethality among *MRC1*, *TOF1*, and *CSM3* suggests the possibility of parallel pathways for cohesin establishment (Mayer et al., 2004; Warren et al., 2004; Xu et al., 2007).

Conversely, SCC proteins may play a role in the DRC. Two recent studies reported that Ctf18, first identified by involvement in SCC, is also required to regulate late origin firing during replication stress (Crabbe et al., 2010; Kubota et al., 2011). These results again implicate the coordination among the S-phase checkpoint and sister chromatid cohesion.

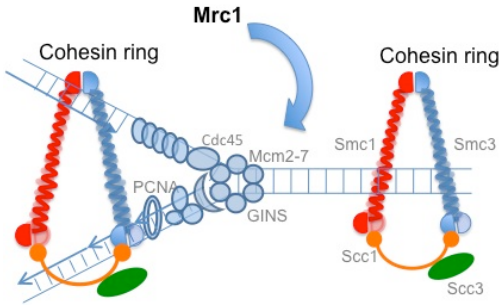

Figure 11. S-phase checkpoint protein Mrc1 is required for SCC establishment

1.4.7 Relationships between DNA replication, S-phase checkpoint, and SCC

Many of the proteins coordinately required for DNA replication, SCC and DRC are directly or indirectly associated with Mcm2-7. Ctf4 links Mcm2-7 to the lagging strand polymerase α (Gambus et al., 2009). In contrast, Mrc1 links Mcm2-7 to the leading strand polymerase ε (Lou et al., 2008). Furthermore, Tof1 and Csm3 form a heterotrimeric complex with Mrc1, and are reported to physically interact with Mcm2-7 as well (Bando et al., 2009). It is possible that Mcm2-7 is the actual focus of these processes and coordinates SCC, DNA replication checkpoint and DNA replication (See **Thesis Overview**.) Thus for many of these proteins, their classification as DRC factors, replication factors or SCC factors is completely arbitrary. Table 1 lists genes required for each cellular process and the corresponding references.

Table 1. Genes involved in DNA replication, DRC or SCC

Note: Genes are divided into three categories: 1) DNA replication, 2) DNA replication checkpoint and 3) sister chromatid cohesion. The genes listed below are all required for additional roles in functions other than the roles they were originally characterized; these are marked in the table and the corresponding references are listed. The alleles responsible for the corresponding phenotypes are also noted. If no allele is given, the wild type gene or protein was tested in the given study. "?" denotes that the gene function in fork association, initiation, DRC or SCC is not known.

	Gene name	Associate with the fork?	Initiation	DRC	SCC
DNA replication	*MCM2*	Gambus et al., 2006	*mcm2-1* Sinha et al., 1986	?	?
	MCM4	Gambus et al., 2006	*mcm4*$^{\Delta 74-174}$ Sheu and Stillman 2010 Sheu and Stillman 2006	?	?
	MCM6	Gambus et al., 2006	Forsburg 2004	*mcm6IL* Komata et al., 2009	?
	ORC2	?	Aparicio et al., 1997	*orc2-1* Shimada et al., 2002	orc2-1 depletion Shimada and Gasser 2007
	ORC5	?	Bell and Dutta 2002	?	*orc5-1* Suter et al., 2004
	POL2	Aparicio et al., 1997	?	*POL2N* Lou et al., 2008	*pol2-12* Edwards et al., 2003
	TRF4	Edwards et al., 2003	?	?	*trf4-236, trf4*Δ Wang et al., 2000
	TRF5	Edwards et al., 2003	?	?	*trf5*Δ Edwards et al., 2003
	RFA1	Alani et al., 1992 Brill and Stillman, 1991 Longhese et al., 1994	?	*rfa1-t11* Zou and Elledge, 2003	?
	POL30	Hingorani and O'Donnell 2000	?	?	PCNA^{K127,164R} Moldovan et al., 2006
DNA replication checkpoint	*MEC1*	no	Randell et al., 2010	*mec1-1* Paulovich and Hartwell, 1995	*mec1*Δ*sml1*Δ Ström et al., 2007 Ünal et al., 2007 Ünal et al., 2004
	MRC1	Gambus et al., 2006	*mrc1*Δ Katou et al., 2003	*mrc1*Δ Alcasabas et al., 2001 *mrc1AQ* Osborn and Elledge, 2003	*mrc1*Δ Xu et al., 2004 Warren et al., 2004

	TOF1	Gambus et al., 2006 Katou et al., 2003	?	*tof1*Δ Foss, 2001	*tof1*Δ Mayer et al., 2004
	CSM3	Gambus et al., 2006	?	*csm3*Δ Calzada et al., 2005	*csm3*Δ Mayer et al., 2004
Sister chromatid cohesion	*CTF4*	Gambus et al., 2009	*ctf4*Δ Ma et al., 2010	?	*ctf4*Δ Mayer et al., 2001 Hanna et al., 2001
	CTF18	Lengronne et al., 2006	*ctf18*Δ Ma et al., 2010	*ctf18*Δ Crabbe et al., 2010 Kubota et al., 2011	*ctf18*Δ Mayer et al., 2001 Hanna et al., 2001
	CHL1	?	*chl1*Δ Ma et al., 2010	?	*chl1*Δ Petronczki et al., 2004

1.5 THESIS OVERVIEW

As described above, DRC, SCC, and DNA replication may be coordinated through the regulation of Mcm2-7. As all six Mcm subunits are essential (Schwacha and Bell, 2001), a role for Mcm2-7 in either DRC or SCC function may have escaped notice. Although a role of Mcm2-7 in the DRC has been demonstrated in some studies (Komata et al., 2009), its involvement in the SCC process is unknown. The goal of this thesis project is to elucidate the relationship among these cellular processes using a biochemically well characterized *mcm* ATPase allele. This allele is viable and carries substitution mutation DE→NQ in the conserved residues of the Walker B motif of Mcm2 (*mcm2DENQ*). This mutation likely ablates ATP hydrolysis from the Mcm6/2 ATPase active site. The *DENQ* mutation has been studied in the Mcm3/7 dimer where it abolishes ATP hydrolysis of the site (Bochman et al., 2008). Since the *in vitro* helicase activity is only slightly affected in the *mcm2DENQ* mutant in the Mcm2-7 complex (Bochman and Schwacha, 2010), the role of the Mcm6/2 active site may be regulatory. To further examine the role of Mcm2-7 with DRC and SCC, I also examined additional well-studied *mcm* alleles where

necessary. The *mcm2-1* (*mcm2E392K*) allele was originally isolated from the minichromosome maintenance screen (Maine et al., 1984). *mcm2-1* has an initiation defect and may affect ATP hydrolysis in Mcm6/2 active site (see **Chapter 3** for detail). The *mcm4chaos3* (*mcm4F345I*) allele was isolated from a forward genetic screen in mice (Shima et al., 2007), and causes unstable replication forks, genomic instability and cancer in mice (Kawabata et al., 2011). The analogous *mcm4chaos3* mutation in budding yeast (*mcm4F391I*) has also been shown to cause genomic instability (Li et al., 2009).

1.5.1 The involvement of Mcm2-7 in DRC signaling

To determine whether Mcm2-7 is involved in the DRC, I first tested whether the *mcm* mutants display any classic checkpoint mutant phenotypes, including drug sensitivity, spindle elongation defect, and cell cycle arrest during DNA damage. To understand the role of Mcm2-7 in the DRC signaling cascade, I asked whether the S-phase checkpoint activation is impaired in response to replication stress or DNA damage in the *mcm* mutants. Furthermore, the late origin firing profile was also studied and compared to known DRC mutants. These experiments allow me to clearly address whether Mcm2-7 directly participates in the DRC.

1.5.2 The role of Mcm2-7 in DNA replication initiation, SCC and accurate chromosomal segregation

mcm2-1 was originally isolated as a DNA replication intiation mutant from the minichromosome maintenance screen (Maine et al., 1984). I tested whether *mcm2DENQ* and *mcm4chaos3* are similarly defective in DNA replication initiation. SCC is tightly related to DNA replication and

achieved upon the commencement of DNA unwinding and synthesis. Many S-phase checkpoint mutants have been revealed for additional roles in maintaining SCC. My goal was to test whether Mcm2-7 is similarly required for SCC, using a well-established assay. This assay utilizes a lac operator array integrated into a yeast chromosome arm and a GFP-tagged lac repressor; binding of the lac repressor to the chromosome allows direct chromosome visualization. To determine the relationship between DRC and SCC, components in the DRC pathway were also tested for SCC maintenance. To directly examine the transmission of replicated plasmids, I also used a modified SCC assay to follow plasmid segregation cytologically.

1.5.3 The role of Mcm2-7 in maintaining replication fork stability

Unstable replication forks are often found in checkpoint mutants. I examined double strand break (DSB) formation in *mcm* mutants to determine whether replication forks collapse. DSB formation was examined in parallel with cell cycle progression studies by flow cytometry. In order to determine whether DSB formation occurs during S phase or requires entry into mitosis, I tested DSB formation at multiple time points during synchronized growth. I compared the formation of DSB in *mcm* mutants with a checkpoint mutant *mrc1*Δ, which is known to cause fork collapse (Szyjka et al., 2005).

2.0 MATERIALS AND METHODS

2.1 MATERIALS

2.1.1 Yeast strains

S. cerevisiae strains are listed below in Tables 2. Except as noted, strains are isogenic derivatives of W303 (Thomas and Rothstein, 1989).

Table 2. Yeast strains used in this study

Strain	Genotype	Source
YLV11	*MATa, W303, ade2-1, ura3-1, his3-11,15, can1-100, cdc21Δ::KanMX, trp1-1::TRP1 GAL-dNK, leu2-3,112::LEU2 GAL-hENT1*	Vernis *et al*., 2003
M359	*MATa, ade2-1, ura3-1, his3-11,15, trp1-1, leu2-3,112, can1-100, mcm2-1 (backcrossed 4x to W303)*	Weinreich and Stillman, 1999
OAY481	*MATa, ade2-1, ura3-11, his3-11,15, leu2-3,112, can-100, trp1-1, cdc6-1 (backcrossed to W303)*	S.P. Bell
PS807	*MATa, ade2-1, ura3-11, his3-11,15, leu2-3,112, can-100, trp1-1, cdc9-1 (backcrossed to W303)*	P. Sorger
RDKY3615	*MATa, S288C, ura3-52, leu2Δ1, trp1Δ63, his3Δ200, lys2ΔBgl, hom3-10, ade2Δ1, ade8, yel069::URA3*	Chen and Kolodner, 1999
K7542	*MATa + ade2-1, can1-100, ura3::3XURA3tet O 112, leu2-3,12::LEU2 tetR-GFP, his3-11,15, eco1-1, trp1-1::TRP1-PDS1-myc18 (K.lactis)*	Tóth et al., 1999
W303a	*MATa, ade2-1, ura3-1, his3-11,15, leu2-3,112, can-100, trp1-1*	S.P. Bell
W303α	*MATα, ade2-1, trp1-1, ura3-1, his3-11,15, leu2-3,112, can1-100*	S.P. Bell

UPY412	W303a + *rad9Δ::loxP-his5^{+}-loxP, mcm4Δ::hisG,* pUP193 (*ARS/CEN, URA3, MCM4*)	This study
UPY421	*W303a + rad9Δ::loxP-his5^{+}-loxP, mcm2Δ::hisG + pUP191 (ARS/CEN, URA3, MCM2)*	This study
UPY428.1	*W303a +mrc1Δ:: loxP-his5^{+}-loxP, mcm2Δ::hisG + pUP191 (ARS/CEN, URA3, MCM2)*	This study
UPY438	W303a + *mrc1Δ::loxP-his5^{+}-loxP, mcm4Δ::hisG,* pUP193 (*ARS/CEN, URA3, MCM4*)	This study
UPY464	*W303a + bar1::hisG*	This study
UPY493	*YLV11 + bar1::hisG, ARS305Δ (plasmid shuffle of ARS305Δ)*	This study
UPY499	*W303a + bar1::hisG, mcm2DENQ (plasmid shuffle of pUP849)*	This study
UPY524	*YLV11 + bar1::hisG, ARS305Δ, mcm2DENQ (plasmid shuffle of pUP849)*	This study
UPY535	*W303a + bar1::hisG, ade3Δ::hisG, mcm2DENQ*	This study
UPY572	*W303a +bar1::hisG, lys2::hisG, cdc15-2 (ts)*	This study
UPY606	*W303a + bar1::hisG, ade3Δ::hisG, mcm2DENQ, his3-11,15::GFP-LacI-HIS3(KanMX), ChrIV(932137)::lacO (NAT+)*	This study
UPY610	*W303a + bar1::hisG, ade3Δ::hisG*	This study
UPY613	*W303a + bar1::hisG, ade3Δ::hisG, his3-11,15::lacI-GFP(KanMX), ChrIV(932137)::lacO (NAT+) (integration of pDB030 and pCM46)*	This study
UPY630	*W303a + bar1::hisG, rad9Δ:: loxP-his5^{+}-loxP*	This study
UPY631	*W303a + tof1Δ:: loxP-his5^{+}-loxP, mcm2Δ::hisG + pUP191 (ARS/CEN URA, MCM2)*	This study
UPY632	*W303a + csm3Δ:: loxP-his5^{+}-loxP, mcm2Δ::hisG/pUP191 (ARS/CEN URA, MCM2)*	This study
UPY634	*W303a + bar1::hisG, rad9Δ:: loxP-his5^{+}-loxP, mcm2DENQ*	This study
UPY636	*W303a + mrc1Δ::loxP, sml1Δ:: loxP-his5^{+}-loxP, mcm2Δ::hisG + pUP191 (ARS/CEN URA3 MCM2)*	This study
UPY637	*W303a + mrc1Δ:: loxP-his5^{+}-loxP, MCM6::MCM6-MRC1(LEU2), mcm2Δ::hisG + pUP191 (ARS/CEN URA3 MCM2) (Integration of plasmid pUP998)*	This study
UPY638	*W303a + bar1::hisG, mcm4Chaos3 (plasmid shuffle of pUP992)*	This study
UPY641	*W303a + mrc1Δ:: loxP-his5^{+}-loxP, MCM6::MCM6IL-MRC1(LEU2), mcm2Δ::hisG + pUP191 (ARS/CEN URA3 MCM2) (Integration of* 168C IL Mrc1 fusion)	This study
UPY644	*W303a + mcm4Δ::hisG, csm3Δ:: loxP-his5^{+}-loxP + pUP193 (ARS/CEN URA3 MCM4)*	This study
UPY646	*W303a + bar1::hisG, leu2-3,112::LEU2-MRC13XHA (Integration of pUP985)*	This study
UPY647	*W303a + bar1::hisG, leu2-3,112::LEU2-MRC13XHA,*	This study

	mcm2DENQ	
UPY648	*W303a + bar1::hisG, leu2-3,112::LEU2 RAD9-3XHA (Integration of pUP986)*	This study
UPY649	*W303a + bar1::hisG, leu2-3,112::LEU2 RAD9-3XHA, mcm2DENQ*	This study
UPY659	*W303a + bar1::hisG, rad9Δ::loxP-his5^{+}-loxP, leu2-3,112::LEU2-MRC13XHA*	This study
UPY660	*W303a + bar1::hisG, rad9Δ:: loxP-his5^{+}-loxP, leu2-3,112::LEU2-MRC13XHA, mcm2DENQ*	This study
UPY666-1	*W303a + bar1::hisG, ade3Δ::hisG, cdc6-1 (plasmid shuffle of pUP1002)*	This study
UPY667-1	*W303a + bar1::hisG, ade3Δ::hisG, cdc9-1 (plasmid shuffle of pUP1003)*	This study
UPY676	*W303a + mrc1Δ:: loxP-his5^{+}-loxP, leu2-3,112::LEU2-mrc1AQ, mcm2Δ::hisG + pUP191 (ARS/CEN URA3 MCM2) (Integration of pUP1017)*	This study
UPY687	*S288C ura3-52, leu2Δ1, trp1Δ63, his3Δ200, lys2ΔBgl, hom3-10, ade2Δ1, ade8, yel069::URA3, Mcm2::mcm2DENQ-NatMX4*	This study
UPY694	*S288Ca ura3-52, leu2Δ1, trp1Δ63, his3Δ200, lys2ΔBgl, hom3-10, ade2Δ1, ade8, yel069::URA3, rad50Δ:: loxP-his5^{+}-loxP*	This study
UPY696	*W303a + tof1Δ:: loxP-his5+-loxP, mcm4Δ::hisG + pUP193 (ARS/CEN URA3 MCM4)*	This study
UPY698	*S288Ca ura3-52, leu2Δ1, trp1Δ63, his3Δ200, lys2ΔBgl, hom3-10, ade2Δ1, ade8, yel069::URA3, mrc1Δ::loxP-his5^{+}-loxP*	This study
UPY700	*W303a + bar1::hisG, ade3Δ::hisG, mrc1Δ::loxP-URA3-loxP*	This study
UPY713	*W303a + bar1::hisG, mrc1Δ:: loxP-his5^{+}-loxP*	This study
UPY715	*W303a + bar1::hisG, rad9Δ:: loxP-his5^{+}-loxP, sml1Δ:: loxP-his5^{+}-loxP, mrc1Δ::loxP*	This study
UPY720	*W303α + bar1::hisG, rad9Δ:: loxP-his5^{+}-loxP, sml1Δ:: loxP-his5^{+}-loxP, mrc1Δ::loxP,leu2-3,112::LEU2-MRC1-3XHA (Integration of pUP985)*	This study
UPY721	*W303α + bar1::hisG, rad9Δ:: loxP-his5^{+}-loxP, sml1Δ:: loxP-his5+-loxP, mrc1Δ::loxP, leu2-3,112::LEU2-RAD9-3XHA (Integration of pUP985)*	This study
UPY722	*YLV11 + bar1::hisG, ars305Δ, mrc1Δ:: loxP-his5^{+}-loxP*	This study
UPY732	*W303a + rad9Δ::loxP-his5^{+}-loxP, sml1Δ:: loxP-his5^{+}-loxP, bar1::hisG, mcm2DENQ*	This study
UPY734	*W303a + rad9Δ::loxP-his5^{+}-loxP, sml1Δ:: loxP-his5^{+}-loxP, bar1::hisG, MCM6::MCM6-MRC1(LEU2), mcm2Δ::hisG/pUP191 (ARS/CEN URA3 MCM2)*	This study

UPY735	*W303a + rad9Δ:: loxP-his5^{+}-loxP, sml1Δ:: loxP-his5^{+}-loxP, bar1::hisG, MCM6::MCM6IL-MRC1(LEU2), mcm2Δ::hisG/pUP191 (ARS/CEN URA3 MCM2)*	This study
UPY744	*W303a + bar1::hisG, ade3Δ::hisG, mrc1Δ::loxP-URA3-loxP, his3-11,15::lacI-GFP-HIS3(KanMX), ChrIV(932137)::lacO (NAT+)*	This study
UPY758	*W303a + bar1::hisG, leu2-3,112::LEU2-Mrc1AQ, mrc1Δ::loxP, mcm2DENQ*	This study
UPY769	*W303a + bar1::hisG, mcm2-1 (5th backcross into w303)*	This study
UPY770	*W303a + bar1::hisG, rad9Δ:: loxP-his5^{+}-loxP, mcm2-1 (5th backcross into W303)*	This study
UPY773	*W303a + mrc1Δ::loxP-his5^{+}-loxP, leu2-3, 112::LEU2-mrc1AQ*	This study
UPY781	*W303a + mrc1Δ:: loxP-his5^{+}-loxP, leu2-3,112::LEU2-MRC1, mcm2Δ::hisG + pUP191 (ARS/CEN URA3 MCM2)*	This study
UPY788	*W303a + bar1::hisG, rad9Δ::loxP-his5^{+}-loxP, mcm4chaos3*	This study
UPY790	*YLV11 + ars305Δ, bar1::hisG, mcm2-1 (6th backcross into w303)*	This study
UPY797	*YLV11 + ars305Δ, bar1::hisG, mcm4chaos3*	This study
UPY799	*W303a + bar1::hisG, mrc1Δ:: loxP-his5^{+}-loxP, mcm2-1*	This study
UPY800	*W303a +bar1::hisG, mrc1Δ:: loxP-his5^{+}-loxP, mcm4Chaos3*	This study
UPY839	*W303a + rad9Δ::loxP-his5^{+}-loxP, leu2-3,112::LEU2-MCM2, mcm2Δ::hisG + pUP191 (ARS/CEN URA3 MCM2) (integration of pUP1018)*	This study
UPY841	*W303a + rad9Δ::loxP-his5^{+}-loxP, leu2-3,112::LEU2-mcm2-1, mcm2Δ::hisG + pUP191 (ARS/CEN URA3 MCM2) integration of pUP1033)*	This study
UPY842	*W303a + mrc1Δ::loxP-his5^{+}-loxP, leu2-3,112::LEU2-MCM2, mcm2Δ::hisG + pUP191 (ARS/CEN URA3 MCM2) (integration of pUP1018)*	This study
UPY844	*W303a + mrc1Δ::loxP-his5^{+}-loxP, leu2-3,112::LEU2-mcm2-1, mcm2Δ::hisG + pUP191 (ARS/CEN URA3 MCM2) (integration of pUP1033)*	This study
UPY846	*W303a + bar1::hisG, mec1Δ:: loxP-URA3-loxP, sml1Δ:: loxP-his5^{+}-loxP, , his3-11,15::lacI-GFP-HIS3 (KanMX), ChrIV(932137)::lacO (NAT+,LEU2)*	This study
UPY848	*W303a + bar1::hisG, rad53Δ::loxP-URA3-loxP, sml1Δ:: loxP-his5^{+}-loxP, his3-11,15::lacI-GFP(KanMX), ChrIV(932137)::lacO (NAT+,ARS/CEN LEU2) (integration of pUP951)*	This study
UPY860	*W303a +bar1::hisG, his3-11,15::lacI-GFP(KanMX), ChrIV(932137)::lacO (NAT+,ARS/CEN LEU2) (integration of pUP951)*	This study
UPY863	*W303a +bar1::hisG, mrc1Δ:: loxP-his5^{+}-loxP, his3-*	This study

	11,15::lacI-GFP(KanMX), ChrIV(932137)::lacO (NAT+,ARS/CEN LEU2) (integration of pUP951)	
UPY865	*W303a +bar1::hisG, mcm2DENQ, his3-11,15::lacI-GFP(KanMX), ChrIV(932137)::lacO (NAT+,ARS/CEN LEU2) (integration of pUP951)*	This study
UPY868	*W303a +bar1::hisG, mcm2-1, his3-11,15::lacI-GFP(KanMX), ChrIV(932137)::lacO (NAT+,ARS/CEN LEU2) (integration of pUP951)*	This study
UPY871	*W303a +bar1::hisG, mcm4Chaos3, his3-11,15::lacI-GFP(KanMX), ChrIV(932137)::lacO (NAT+,ARS/CEN LEU2) (integration of pUP951)*	This study
UPY872	*W303a + leu2-3,112::LEU2-MCM2, mcm2Δ::hisG + pUP191 (ARS/CEN URA3 MCM2) (integration of pUP1018)*	This study
UPY874	*W303a + leu2-3,112::LEU2-mcm2-1, mcm2Δ::hisG + pUP191 (ARS/CEN URA3 MCM2) (integration of pUP1033)*	This study
UPY878	*W303a + leu2-3,112::LEU2-MCM4, mcm4Δ::hisG + pUP193 (ARS/CEN URA3 MCM4) (integration of pUP1099)*	This study
UPY879	*W303a + leu2-3,112::LEU2-mcm4Chaos3, mcm4Δ::hisG + pUP193 (ARS/CEN URA3 MCM4) (integration of pUP1098)*	This study
UPY880	*W303a + rad9Δ:: loxP-his5^{+}-loxP, leu2-3,112::LEU2-MCM4, mcm4Δ::hisG + pUP193 (ARS/CEN URA3 MCM4) (integration of pUP1099)*	This study
UPY881	*W303a + rad9Δ:: loxP-his5^{+}-loxP, leu2-3,112::LEU2-mcm4Chaos3, mcm2Δ::hisG + pUP193 (ARS/CEN URA3 MCM4) (integration of pUP1098)*	This study
UPY882	*W303a + mrc1Δ:: loxP-his5^{+}-loxP, leu2-3,112::LEU2-MCM4, mcm4Δ::hisG + pUP193 (ARS/CEN URA3 MCM4) (integration of pUP1099)*	This study
UPY883	*W303a + mrc1Δ:: loxP-his5^{+}-loxP, leu2-3,112::LEU2-mcm4Chaos3, mcm4Δ::hisG + pUP193 (ARS/CEN URA3 MCM4) (integration of pUP1098)*	This study

2.1.2 Plasmids

Plasmids used are listed in Table 3.

Table 3. Plasmids used in this study

Plasmid name	Genes involved	Source
pDK243	*LEU2, ARS1, CEN3, ADE3-2p*	Hogan et al., 1992
pDK368-1	*LEU2, ARS1, CEN3, ADE3-2p, H4 ARS (7 copies)*	Hogan et al., 1992
pDB030	*AmpR, HIS3, KANMX, LacI-GFP*	Koshland lab
pCM46	*AmpR, NATR, lacOperator array::ChrIV(932137)*	Koshland lab
pMrc1	*AmpR, URA3, MRC1*	Osborn et al., 2003
pAO138	*AmpR, URA3, mrc1AQ*	Osborn et al., 2003
168C wt Mrc1 fusion	*AmpR, URA3, MCM6-MRC1 translational fusion*	Komata et al., 2009
168C IL Mrc1 fusion	*AmpR, URA3, Mcm6IL-MRC1 translational fusion*	Komata et al., 2009
ARS305dl	*AmpR, YIp5, ARS305 containing a deletion of BamHI-ClaI fragment*	Newlon
pUG27	*AmpR, S pombe loxP-HIS5^{+}-loxP*	Gueldener et al., 2002
pUG72	*AmpR, K lactis loxP-URA3-loxP*	Gueldener et al., 2002
pSH63	*AmpR, TRP1, GAL1::CRE*	Gueldener et al., 2002
CPY*-HA	*AmpR, URA3, CPY*-HA*	Bhamidipati et al., 2005
pUP191	*AmpR, URA3, MCM2, ARS/CEN*	Schwacha and Bell 2001
pUP193	*AmpR, URA3, MCM4, ARS/CEN*	Schwacha and Bell 2001
pUP197	*AmpR, TRP1, PMCM5-MCM2, ARS/CEN*	Bochman et al., 2008
pUP199	*AmpR, TRP1, PMCM5::mcm2DENQ, ARS/CEN*	Bochman et al., 2008
pUP849	*AmpR, URA3, mcm2DENQ integration*	This study
pUP932	*AmpR, LEU2, TOF1, 2µm*	This study
pUP933	*AmpR, LEU2, CSM3, 2µm*	This study
pUP961	*AmpR, TRP1, MRC1-3xHA, Integration vector*	This study
pUP966	*AmpR, TRP1, RAD9-3xHA, Integration vector*	This study

pUP991	*AmpR, TRP1, mcm4Chaos3, ARS/CEN (PCR mutagenesis to introduce the Chaos3 mutation)*	This study
pUP992	*AmpR, URA3, mcm4Chaos3*	This study
pUP1016	*AmpR, LEU2, MRC1*	This study
pUP1017	*AmpR, LEU2, mrc1AQ*	This study
pUP1018	*AmpR, LEU2, MCM2*	This study
pUP1032	*AmpR, TRP1, ARS/CEN, mcm2-1*	This study
pUP1033	*AmpR, LEU2, mcm2-1*	This study
pUP1098	*AmpR, LEU2, mcm4Chaos3*	This study
pUP1099	*AmpR, LEU2, MCM4*	This study
pUP1108	*AmpR, LEU2, ARS/CEN, NAT+, lacOperator array::ChrIV(932137)*	This study

2.2 METHODS

2.2.1 α-factor arrest and release.

Cell cycle synchronization using α-factor arrest and release was performed as previously described (Aparicio et al., 1997). To synchronize cells in G1, α-factor was typically added to log phase *bar1* cultures to a final concentration of 30 nM, and incubated with agitation at 23°C for 3 hours (>90% of the cells were unbudded). To release from the arrest, the culture was washed three times in YP media (Burke et al., 2000), where the first wash contains 0.1mg/ml Pronase E (Sigma), then resuspended in fresh YP media supplemented with 2% glucose.

2.2.2 Apoptosis assay

Apoptosis was assayed as previously described (Madeo et al., 1999). Briefly, asynchronous log phase cells were incubated with 10 μg/ml dihydrodichloro-fluorescein diacetate (DHCF) (Sigma,

prepared in 100% ethanol as 2.5mg/ml stock) for 2 hours at 30°C in the dark with gentle mixing. After incubation, cells were visualized using a Zeiss Axioskop 40 microscope equipped with a green filter set (Zeiss filter set #38) and a CCD camera for image acquisition. Live cells were spotted on polylysine coated slide immediately and examined under fluorescence microscope. >100 cells were counted for each sample.

2.2.3 Limited proteolysis

Purified wild-type and *mcm2DENQ* Mcm2-7 complexes were assayed with limited proteolysis as previously described using baculovirus infected insect cells (Pucci et al., 2007). Protein expression and purification was performed as previously described (Bochman and Schwacha, 2010). Both protein preps were extensively characterized for subunit stoichiometry by quantitative Western blotting and complex integrity by immunoprecipitation of Mcm4p (minimal hexamer content for wild-type Mcm2-7 preparation = 81%; for Mcm2-7 preparation containing mcm2DENQp = 59%) and the characterizations for these preparations have been published previously (Bochman and Schwacha, 2010). To perform limited proteolysis, 2 pmol of purified protein was incubated in binding buffer (25 mM K^+/HEPES, pH7.5, 100mM KCl, 5mM MgOAc, 50 μM ZnOAc, 10% glycerol, 100 μM EDTA, 0.1 % NP-40, 1 mM DTT) that contains 2.5μg/ml trypsin, 10mM MgOAc and 10mM ATP (as indicated) in a final volume of 5 μl. At each indicated time point, kill cocktail (1.6XSDS loading dye, 6.67 mM PMSF, 6.67 μg/ml TPCK in a total volume of 15 μl in S/0.1 buffer, which is the same as the binding buffer except NaCl is substituted for KCl) was added to stop the reaction and incubated on ice. At the end of the time course, reactions were boiled for 3 min and separated on a 7% SDS-PAGE gel. Protein bands were visualized by silver staining.

2.2.4 Western blot analysis

Protein extracts for Western blots were prepared by the trichloroacetic acid (TCA) precipitation method (Wright et al., 1989). Unless otherwise noted, protein extracts were separated on 7% SDS-PAGE, and Western blot was conducted using standard procedures. Briefly, proteins were transferred to nitrocellulose, blocked in TBS-t containing 5% dried milk, probed with primary antibodies overnight at 4°C, washed thrice in TBS-T, incubated with HRP-conjugated secondary for 30min at RT, washed thrice in TBS-T, developed using the ECL chemiluminescence kit (Femto kit, Pierce), and imaged using a Fuji LAS-3000 CCD, and quantified with ImageGauge software. Protein extracts for assaying Rad9-3XHA and Mrc1-3XHA were separated on 6% SDS-PAGE. The following antibodies/dilution were used respectively: 1:1000 goat anti-Rad53 (yC-19) antibody (Santa Cruz Biotechnology, sc-6749) in TBS-T, 1:100000 rabbit anti-G6PDH antibody (Sigma, A9521) in TBS-t containing 5% dried milk, 1:1000 goat anti-Mcm2 (yN-19) antibody in TBS-t in 5% dried milk (Santa Cruz Biotechnology, sc-6680), and 1:1000 mouse anti-HA antibody (Covance, HA-11) in TBS-t. The following HRP-conjugated secondary antibodies were used at 1:10000 dilution in TBS-t: donkey anti-goat antibody (Santa Cruz Biotechnology, sc2020), donkey anti-rabbit antibodies (G.E. Healthcare, NA934V) and sheep anti-mouse antibodies (G.E. Healthcare, NA931V).

2.2.5 Cyclohexamide chase assay

Cycloheximide chase experiment was performed as previously described (Bhamidipati et al., 2005). Briefly, cycloheximide was added to exponentially growing cells to a final concentration of 50 μg/ml at time zero. Culture aliquots were withdrawn at indicated times, and sodium azide

was added to 0.01% final concentration. The cells were immediately separated by centrifugation, and the cell pellets were each resuspended in 1 ml of ice-cold water containing fresh protease inhibitor (similarly prepared as described in the ChIP-seq method). The resuspension was flash frozen in liquid nitrogen and stored at -80°C until needed. To prepare for protein extracts, the cells were thawed on ice and processed as described in the Western blot analysis procedure.

2.2.6 FACS analysis

FACS analysis was performed as previously described (Bell et al., 1993). Culture aliquots were taken at indicated intervals, briefly sonicated (Branson model 250, 7 pulses at a setting of 2 output 35%), and fixed overnight by addition of ethanol to 70% V/V at 4°C. Fixed cells were washed twice in 50 mM sodium citrate (pH 7.4), and resuspended in 1 ml of 50 mM sodium citrate containing 0.25 mg/ml boiled RNAse A. Following incubation at 50°C for 1 hour, 50 µl of 20 mg/ml proteinase K was added and the incubation continued for another hour at 50°C. The cells were then centrifuged and resuspended in 1 ml of 50µg/ml propidium iodide (Sigma P4170). Stained cells were analyzed using a CyAn ADP analyzer (Beckman Coulter) with Summit Software (DAKO), and FACS analysis figures were generated using the FlowJo software (Tree Star, Ashland OR).

2.2.7 Immunoprecipitation and Western blot analysis of Rad53 phosphorylation

To verify that the slower migrating species results from Rad53 phosphorylation, phosphatase treatment of immunoprecipitated Rad53 was performed as previously described (Sanchez et al.,

1996). Briefly, 25ml of log phase cells were treated in the presence or absence of 0.1% MMS for 1 hr. Cell lysates were prepared by bead beating in the presence of phosphatase inhibitors (50mM of beta-glycerophosphate, 5mM of sodium vanadate, and 20mM of NaF). Immunoprecipitation was carried out with 6 µl of anti-Rad53 (Santa Cruz, sc-6749) for 2 hour at 4°C, followed by a 1 hour incubation with 30 µl of prewashed (washed in 1XPBS, 0.1% BSA) protein G beads (Gamma bind, GE Healthcare). After immunoprecipitation, the beads were washed thrice to remove non-specific binding. The beads were then incubated in the presence or absence of with 2 µl (20 units) of calf intestinal phosphatase (NEB) in 1X NEB buffer 3 for 45 minute at 37^{o}C. Following phosphatase treatment, proteins were eluted from beads by boiling for 3 minutes in 1X SDS buffer, and analyzed by SDS-PAGE gel followed by Western blot analysis.

2.2.8 ChIP-seq DNA preparation

ChIP sample preparation was performed as described (Aparicio et al., 1997; Katou et al., 2003) using yeast engineered for bromodeoxyuridine (BrdU) uptake (Vernis et al., 2003). For G1 experiments, strains were arrested in α-factor for 3 hours at 23^{o}C then processed for ChIP. For S-phase experiments, strain were similarly arrested with α-factor, then released into fresh media containing 400 µg/ml BrdU and 0.2M HU until cell budding reached 75% (100-110 minutes at 23°C), harvested, and processed for ChIP-seq. To assay MCM-bound DNA, ChIP-seq DNA preparation was performed as previously described (Aparicio et al., 1997). Formaldehyde was added to 50 ml of α-factor arrested cells to a final concentration of 1% and mixed for 15 minutes at room temperature. Crosslinking was quenched by addition of glycine to a final concentration of 125 mM and room temperature incubation for 5 minutes. Cells were

washed twice with 20 ml of ice-cold TBS (20mM Tris-HCl, pH7.6, 150mM NaCl) and the resulting cell pellet was frozen in liquid nitrogen and stored at -80^{o}C. The cell pellet was thawed on ice, resuspended in 250 µl of 1X lysis buffer (50 mM HEPES/KOH, pH 7.5, 140 mM NaCl, 1mM EDTA, 1% Triton X-100, and 0.1% Na-Deoxycholate) with fresh protease inhibitors (1 mM PMSF, 10 mM benzamidine, 0.1 mg/ml TPCK, 10 µg/ml aprotinin, 10 µg/ml leupeptin, 10 µg/ml pepstatin, 0.5 mg/ml bacitracin), and the cells were lysed following addition of glass beads and vortexing (cycles of 30 seconds on ice and 30 seconds vortexing for a total of 30 min) 250 µl of additional 1X lysis buffer was added and briefly mixed. Using a hot 27 gauge needle, a hole was poked into the bottom of the tube, and the cell lysates were separated from the glass beads by centrifugation into a fresh tube). The DNA in the lysate was then sheared using a Branson 250 model sonicator to yield an average DNA size of 700 bp with the following scheme: 12 pulses at 35% output and setting 2 (twice), 16 pulses at 35% output and setting 2, 12 pulses at 35% output and setting 4 (twice), 6 pulses at 35% output and setting 2, with a two-minute incubation on ice between the intervals. 6 µl of anti-Mcm2-7 antibody (UM174, Stephen P Bell, MIT) or 4 µl of anti-Mcm2 (sc6680, Santa Cruz,) was added to cell lysates and incubated at 4^{o}C for 2 hours as indicated. 30 µl of pre-washed protein G beads equilibrated in 1X PBS, 0.1%BSA (Gamma bind, GE Healthcare) were then added and incubated for an additional hour at 4°C. Following incubation, beads were washed twice with 1 ml of lysis buffer with fresh PMSF; then once each with 1 ml of lysis buffer containing 500 mM NaCl once, 1 ml of TLNNE (10mM Tris/HCl, pH8.0, 0.25 M LiCl, 0.5% NP-40, 0.5% Na-Deoxycholate, 1mM EDTA), then 1 ml of TE. Each wash was performed with 5 minutes of room temperature incubation with mixing. To elute the DNA, 100 µl of elution buffer (50 mM Tris/HCl pH8.0, 10 mM EDTA/1% SDS) was then added to the beads and incubated at 65°C for 15 min. Beads were removed by

centrifugation and the supernatant was transferred to a fresh tube. Beads were resuspended in 150 µl of TE containing 0.67% SDS and spun down again. The supernatants were pooled and incubated at 65°C overnight to reverse the protein-DNA crosslinks. The next morning 250 µl of TE, 5 µl of 20 mg/ml proteinase K, and 0.25 µl of 20 mg/ml glycogen was added and incubated at 37°C for 30 minutes. After incubation, 55 µl of 4M LiCl was added and the DNA was precipitated with ammonium acetate and ethanol. The dried DNA pellet was processed to construct the library for sequencing (see Materials and Methods). To assay BrdU incorporation, genomic DNA was prepared using standard procedures (Ryba et al., 2011), boiled and immunoprecipitated with anti-BrdU antibodies (555627, BD Bioscience). The resulting DNA pellet was subjected to sequencing library preparation. Sequencing libraries were generated from the above immunoprecipitated DNA using the Illumina sample prep kit and protocol. Genomic libraries were multiplexed and sequenced on a GAII Illumina sequencer and processed using SCS2.6 software. Approximately 5 million reads per experiment were obtained. All experiments were performed in duplicate (except for *mcm2-1* and *mcm4chaos3* where no significant late origin firing was observed), and the data was assembled and normalized using standard methods. In general, each experimental replica produces similar or identical results; the combined dataset is shown in results.

2.2.9 Genomic Analysis

2.2.9.1 Read mapping and normalization

Sequenced reads were aligned to the *S. cerevisiae* S288C reference genome (SacCer2, SGD June 2008) (Kent et al., 2002) using MAQ (Li et al., 2008) allowing up to three mismatched bases. Once mapped, only those reads with a Phred quality score of 35 or greater were used for

downstream analysis. For each experiment, reads were binned across the genome and RPKM (reads per kilobase per million mappable reads) was calculated for each bin. For all the BrdU ChIP-Seq experiments, bins of 5000 bp stepping every 1250 bp were used; and for all the Mcm ChIP-Seq experiments, bins of 1000 bp stepping every 250 bp were used. All *in silico* analyses were done in the R programming environment using the Bioconductor suite of packages (Gentleman et al., 2004; RDevelopmentCoreTeam, 2010). Experimental replicates were quantile normalized, and combined by calculating the mean score within each bin.

2.2.9.2 Peak identification

For each bin along a chromosome, a probability was assigned according to that chromosome's empirical cumulative distribution of RPKM. A threshold was determined, and bins with a probability greater than or equal to the cutoff were taken as peaks (the ranges of overlapping peaks were merged such that the resulting peaks represented the union of all enriched bins). For BrdU ChIP-Seq in HU arrested cells, the thresholds used were as follows: WT strains p >= 0.95, MRC1 p >= 0.75, and 2DENQ p >=0.75. For ChIP-Seq experiments in G1 arrested cells, a threshold of p >= 0.96 was used. Replicates were combined by taking the intersection of peak calls. When possible, peaks were assayed for concordance against analogous data previously reported (Crabbe et al., 2010).

2.2.9.3 Heatmaps

Reads within +/- 10kb of origins (identified in oriDB (Nieduszynski et al., 2007)) were binned into windows of 300 bp stepping every 100 bp and RPKM was determined. Early firing origins were determined by BrdU incorporation within +/- 5kb of each origin in the WT background and

identified via K-means clustering (k=3). For each experiment, data was aggregated by LOESS regression using a span of 0.01 (RDevelopmentCoreTeam, 2010).

Peak-widths determined from the aggregated BrdU signal +/- 20kb of early firing origins as described above. Peak edges where determined by identifying the initial inflection point of the first differential following and preceding the global maxima of the aggregated signal, the distance between edges was reported.

2.2.10 Plasmid loss assay

The plasmid loss assay was performed as previously described (Hogan and Koshland, 1992). This assay takes the advantage of color selection. Test plasmids carrying either one or seven origins of replication and an *ADE3* gene were transformed in to an *ade2-1ade3*Δ strains, and colonies that maintain test plasmids accumulate red pigment, whereas colonies that lose the plasmids are white (Hogan and Koshland, 1992). To test plasmid loss, a single colony was inoculated into CSM-leu media to select for retention of the test plasmid, incubated overnight at 30°C, briefly sonicated, and cell number counted using a hemocytometer. Known amounts of sonicated cells were spread onto CSM plates and incubated for 2 days at 30°C to determine the fraction of the cells in the population that carry plasmid (i.e., that form red colonies) at the start of the experiment. To examine plasmid loss, this overnight culture was diluted to 10^4 cells/ml in CSM complete media (NON-SELECTIVE) and incubated at 30°C for 22-28 hours. Cells were again counted, sonicated, and spread on CSM plates, and incubated for at least 2 days at 30°C to allow colony growth and color development. Average plasmid loss/generation was calculated (Lei et al., 1996).

2.2.11 Sister chromatid cohesion assay

The sister chromatid cohesion assay was performed as previously established (Straight et al., 1996). Test strains contain chromosome IV marked with Lac Operator array (pCM46) and express GFP-tagged Lac repressors (PDB030). Cells were arrested at G1 with α-factor for 3 hours, washed, and released into fresh YPD containing 15μg/ml of nocodazole for 2 hours. Aliquots were withdrawn for G1 and G2/M arrested cultures, and viewed under the Zeiss Axioskop 40 microscope. The number of cells displaying two separate GFP dots in close proximity was scored.

2.2.12 Cytological plasmid segregation assay

The plasmid segregation assay was performed as previously established with the following modifications (Megee and Koshland, 1999). Test strains contain a plasmid that encodes a Lac Operator array (pCM46), express GFP-tagged Lac repressors (PDB030), and carry *cdc15-2* mutation that allows telophase arrest at non-permissive temperature (Schweitzer and Philippsen, 1991; Straight et al., 1996). Cells were arrested at G1 with α-factor for 4.5 hours at 25°C, washed, released into fresh YPD for 1 hour at 25°C, and then shifted to 37°C for 2.5 hours. After incubation, cells were incubated in 2μg/ml of DAPI for additional 30 minutes in dark. Aliquots were withdrawn for G1 and telophase arrested cultures, and viewed under the Zeiss Axioskop 40 microscope. The number of GFP dots in each cell was scored.

2.2.13 Immunofluorescence

Immunofluorescence of γ-H2A(X) was performed as described (Nakamura, 2006). About $2x10^7$ cells were collected and fixed for 1 hour at room temperature in 1 ml of 40 mM potassium phosphate buffer (pH6.5) (0.5 mM $MgCl_2$) containing 1% formaldehyde, spun down and washed twice in 500 ul of the same buffer. The final pellet was resuspended in 100 µl of the above buffer containing 1.2 M sorbitol and 65 µg/ml zymolyase (ICN Biochemicals). Cells were incubated at room temperature for 16 minutes, washed twice in 500 µl of sorbitol buffer and resuspended in fresh sorbitol buffer. Digested cells were spotted on polylysine coated slides for 10 min at room temperature, then dehydrated by submersion into 100% methanol for 6 minutes followed by 100% acetone for 30 seconds (methanol and acetone were pre-stored at -20°C). Slides were air dried briefly, and blocked for 30 minutes at RT with blocking solution (1x PBS containing 1.5% BSA, 0.1% Triton X-100, and 0.5% Tween-20). The anti-γ-H2A(X) antibody (a generous gift from William Bonner) was diluted at 1:1000 in blocking solution and then added to the cells for overnight incubation at room temperature in a humidified chamber. Secondary antibodies (Alexa Fluor 546 rabbit anti-goat IgG (A21085)) were used at a concentration of 1:500 and incubated at room temperature for 1 hour in the dark. Following incubation, slides were briefly rinsed in blocking buffer and incubated in 1mg/ml DAPI (Sigma) to stain nuclear DNA. DAPI was rinsed away, and slides were mounted after anti-fade (SlowFade Gold anti-fade reagent, Invitrogen) was spotted on each well. To visualize spindle elongation, immunofluorescence were carried out as the γ-H2A(X) immunofluorescence assay described above, except that 1:350 anti-tubulin (rat monoclonal YOL 1/34, Serotec) and 1:500 Alexa Fluor 546 goat anti-rat IgG A11081 (Invitrogen) were used.

2.2.14 GCR assay

GCR assay was performed as previously described (Motegi et al., 2006). Test strains contain a *URA3* gene inserted at the non-essential *HXT13* gene (~21 kb from the end of the left arm of chromosome V), which is 8.5 kb apart from the endogenous *CAN1* gene (~32 kb from the end of the left arm of chromosome V) (Chen and Kolodner, 1999). This assay tests the simultaneous deletion of both markers by selecting cells that are resistant to both 5-FOA and L-canavanine. Since the point mutation rate for *URA3* or *CAN1* is 10^{-6} to 10^{-7} per generation, simultaneous point mutations occur for both of the genes would result in a rate of 10^{-12} to 10^{-14}, which is too rare to be detected. Therefore, cells losing both markers should result from deletion of the left arm of chromosome V by gross chromosomal rearrangement. To conduct this assay, a single colony was inoculated into 2 ml of YPD, incubated overnight at 30°C, then subcultured the following day into 50 ml of YPD media. The 50 ml culture was grown overnight to saturation to reach a cell density ~$1X10^8$ cells/ml. An aliquot was withdrawn, diluted, sonicated and spread onto YPD plate to access viable count. The culture was concentrated by centrifugation and spread onto 5-FOA (1mg/ml) CAN (60μg/ml) CSM-arg plates at roughly $4X10^8$ cells/plate to assay the rate of translocations. After 4 days of incubation, FOA-R CAN-R colonies were counted. Results reported for the *rad50*Δ (UPY694) strain were the average of two experiments, with each experiment containing three replicates from independent colonies. At least three colonies were tested for each of the wild type (RDKY3615), *mcm2DENQ* (UPY687), and *mrc1*Δ (UPY698) strains. The fluctuation test was performed based on Lea and Coulson's equation (Lea and Coulson, 1949).

3.0 THE MCM2-7 REPLICATIVE HELICASE HAS A CENTRAL ROLE IN BOTH THE DNA REPLICATION CHECKPOINT AND SISTER CHROMATID COHESION

Feng-Ling Tsai conducted this work with the following exceptions. Dr. Anthony Schwacha supervised the conduct of experiments. The genomic experiments were performed in collaboration with Dr. David MacAlpine from Duke University. Joseph Prinz carried out all the genomic analysis. Heather MacAlpine prepared the DNA library required for high-throughput sequencing.

3.1 SUMMARY

Various non-essential factors (e.g., Mrc1p) coordinately participate in DNA replication, the DNA replication checkpoint (DRC), and sister chromatid cohesion (SCC). Most lack known independent biochemical function but all physically associate with the Mcm2-7 replicative helicase, suggesting that DNA unwinding or its regulation may be the common mechanistic link among them. We re-examined existing *mcm* alleles and found that a Walker B allele in *MCM2* (*mcm2DENQ*) proved defective in all three processes. In the presence of DNA damage, wild type level of phosphorylation of an early protein of the DRC cascade (Mrc1p) was observed in *mcm2DENQ*, but the activation of the downstream effector kinase (Rad53p in *S. cerevisiae*) is defective, implicating Mcm2-7 as an integral member of the DRC cascade. We find that unlike

DRC, SCC does not depend upon Rad53, suggesting that this process co-opts a "sub-circuit" of the DRC ending with Mcm2-7. Finally, this mutant displays a classical plasmid loss phenotype which cannot be rescued by incorporating multiple origins on the plasmid, suggesting a replication initiation defect. Surprisingly, when plasmid transmission was examined using a cytology based method, it was revealed that a sister chromatid segregation defect also contributes to the plasmid loss defect. We show that this mutant forms stable replication forks at near normal levels, suggesting that the observed defects are a direct consequence of altered Mcm activity. These results underscore a direct role for Mcm2-7 not only in DNA replication, but also in chromosome inheritance and damage surveillance.

3.2 INTRODUCTION

Three processes essential for genome stability transpire during S-phase: DNA replication, the intra-S phase checkpoint, and the establishment of sister chromatid cohesion (SCC). Both genetic (Mayer et al., 2004; Warren et al., 2004; Xu et al., 2004) and physical association studies (Gambus et al., 2006; Komata et al., 2009; Segurado and Tercero, 2009) indicate that all three processes are coordinately assisted by several non-essential proteins that stabilize and constitutively associate with replication forks (e.g., Mrc1p, Tof1p, Csm3p, and Ctf18p) (reviewed in (Sherwood et al., 2010). These data imply that the three processes share a common mechanistic link.

The Mcm2-7 helicase is central to both eukaryotic DNA replication and its regulation (reviewed in (Bochman and Schwacha, 2009)), and physically interacts with both Ctf18p and a complex of Mrc1p, Tof1p and Csm3p (Bando et al., 2009; Lou et al., 2008). This toroidal

complex contains six different and individually essential subunits (Mcm2 → 7) that form six ATPase active sites at dimer interfaces. Although these sites are allosterically coupled, individual sites are biochemically distinct; some are essential for DNA unwinding, while others serve a regulatory role. Mcm2-7 activity may be regulated via a reversible structural discontinuity at the Mcm2/5 ATPase active site ("gate"): opening the gate blocks DNA unwinding, while closing the gate (putatively *in vivo* via the regulated loading of Cdc45 and GINS to form the CMG complex (Costa et al., 2011)) activates the helicase. The active sites that flank Mcm2/5 (i.e., Mcm3/5 and Mcm6/2) may modulate gate conformation (Bochman and Schwacha, 2010).

The intra-S phase checkpoint responds to DNA damage by suppressing cell cycle progression, initiation from unfired (late) origins, and ongoing elongation (reviewed in (Branzei and Foiani, 2009)**)**. It contains two overlapping signal transduction cascades: the DNA replication checkpoint (DRC) monitors replication fork integrity, while the DNA damage checkpoint (DDC) monitors genome integrity. In both cascades, DNA damage activates the ATR or ATM kinases (Mec1p and Tel1p in *S. cerevisiae*); these in turn activate (phosphorylate) the downstream effectors kinases CHK1 and CHK2 (Rad53p in *S. cerevisiae*). The two pathways differ in the transduction of Rad53p activation: the DDC proceeds through phosphorylation of Rad9p, whereas the DRC proceeds through phosphorylation of Mrc1p in the presence of Tof1p and Csm3p (reviewed in (Branzei and Foiani, 2009)). Although loss of either Mrc1 or Rad9 causes a modest checkpoint defect, loss of both factors ablates the intra-S phase checkpoint, and causes extreme DNA damage sensitivity (Alcasabas et al., 2001).

SCC physically pairs sister chromatids using proteins called cohesins; this process facilitates proper mitotic spindle assembly and faithful chromosome segregation (reviewed in

(Onn et al., 2008)). Cohesins load onto chromosomes during G1, but require passage of the replication fork to convert them into an active form (i.e., establishment). SCC persists until the onset of mitosis, during which cohesin degradation triggers chromatid segregation. Misregulation of SCC ultimately leads to chromosomal missegregation.

Elucidating the relationship among these processes has been hampered by several problems. First, complete gene deletions are often studied, an approach that excludes essential factors and makes the distinction between direct (i.e., loss of enzymatic function) and indirect effects (i.e., loss of protein-protein contacts leading to fork collapse) difficult. Second, such mutants are often highly pleiotropic, making defects with a common mechanistic basis difficult to distinguish from those having an unrelated basis. Third, the observed phenotypes span multiple research areas, which to date has stymied comprehensive analysis.

Mcm2-7 may be the linchpin connecting these three processes. Prior studies have demonstrated involvement of Mcm2-7 in replication initiation (Aparicio et al., 1997) and have implicated indirect roles for Mcm2-7 in checkpoint activation and SCC (Komata et al., 2009; Lengronne et al., 2006; Randell et al., 2010; Suter et al., 2004; Takahashi et al., 2004). Loss of physical interaction between Mrc1 and Mcm6 (*mcm6IL* allele) causes a DRC defect (Komata et al., 2009). Moreover, reduced Mcm levels (Kawabata et al., 2011) and specific *mcm* alleles cause DNA damage sensitivity (Stead et al., 2009).

To test the involvement of Mcm2-7 in SCC and DRC, we focused on a previously characterized viable allele of the Walker B ATPase motif of *S. cerevisiae* Mcm2 (*mcm2DENQ*) that ablates the activity of the Mcm6/2 active site, yet supports *in vitro* Mcm2-7 DNA unwinding (Bochman and Schwacha, 2010). To assist comparison, two additional well-studied alleles were also analyzed. The *mcm2-1* allele (*mcm2E392K*) has a replication initiation defect (Sinha et al.,

1986). The *mcm4Chaos3* allele (*mcm4F345I*) causes carcinogenesis in mice through replication fork collapse (Kawabata et al., 2011); the analogous allele in *S. cerevisiae* (*mcm4F391I,* henceforth called *Chaos3*) also causes genomic instability (Li et al., 2009).

We show that all three alleles are defective for DNA replication initiation, SCC and plasmid missegregation. We demonstrate the DNA replication initiation defect by plasmid loss assay. We find that the plasmid loss defect is partially attributed to a defect in chromosomal segregation, which is consistent with defective SCC observed in these mutants. However, some other phenotypes do not cosegregate in all three mutants. We show that the *mcm2DENQ* and *mcm2-1* mutants are defective in the DRC after Mrc1p phosphorylation and before Rad53p activation. Furthermore, we use a genomic approach to show that *mcm2DENQ* but not *mcm2-1* displays misregulation of late origin firing, similar to a known DRC allele *mrc1AQ* (Osborn and Elledge, 2003). This suggests that the *mcm2DENQ* allele is speficically resistant to the inbhibition of late origin firing. In the *mcm2DENQ* mutant, these defects are not caused by a reduction in either Mcm2-7 protein levels or stability, strongly suggesting that Mcm2-7 ATP turnover at a site distinct from DNA unwinding is the common mechanistic step required for all three processes.

3.3 RESULTS

3.3.1 *mcm2DENQ* has a DRC defect

The *mcm2DENQ* mutant grows slowly (below) and demonstrates elevated cell death (Figure 12A and B). Quantitative Western blot analysis of Mcm2p and mcm2DENQp demonstrates no

difference in steady-state levels (Figure 13A). The protein stability of Mcm2p and mcm2DENQp has no significant difference as shown by cyclohexamide chase experiment (Figure 13B). The mcm2DENQp subunit appears to fold properly and oligomerize well into Mcm2-7, as protease sensitivity experiments on purified Mcm2-7 complexes (Figure 13C) showed that the mutant subunit causes only a subtle change in the protection pattern.

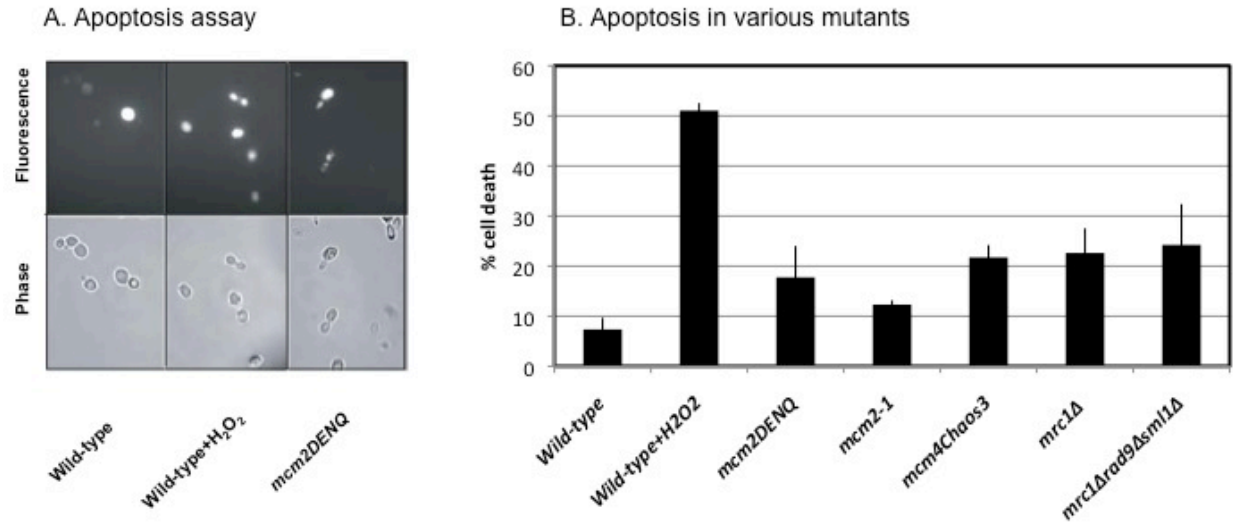

Figure 12. Cell death phenotype of *mcm2DENQ*

A) Apoptosis assay. Asynchronous cultures of wild-type (UPY464) or *mcm2DENQ* (UPY499) ± incubation in the presence of 3 mM hydrogen peroxide (positive control) were assayed for apoptosis as previously described (Madeo et al., 1999) (Methods). Fluorescin fluorescence (i.e., apoptosis) and phase contrast images are shown. B) Apoptosis levels of various mutants. Results represent at least 2 independent experiments.

A. Mcm2p/mcm2DENQp Western blot analysis

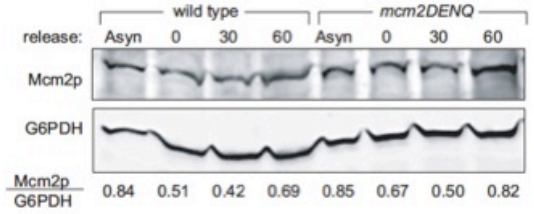

B. Mcm2p/mcm2DENQp protein stability– cyclohexamide chase

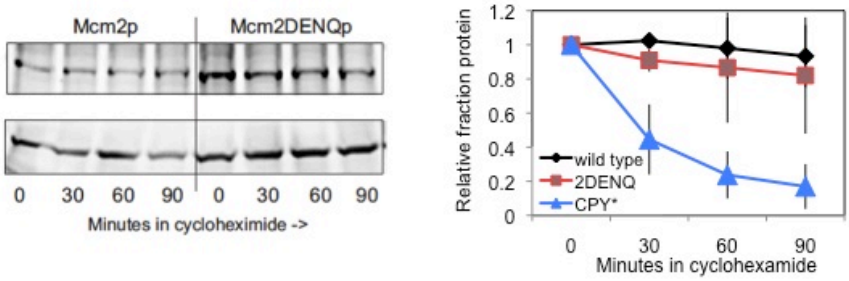

C. Trypsin proteolysis of purified Mcm2-7p

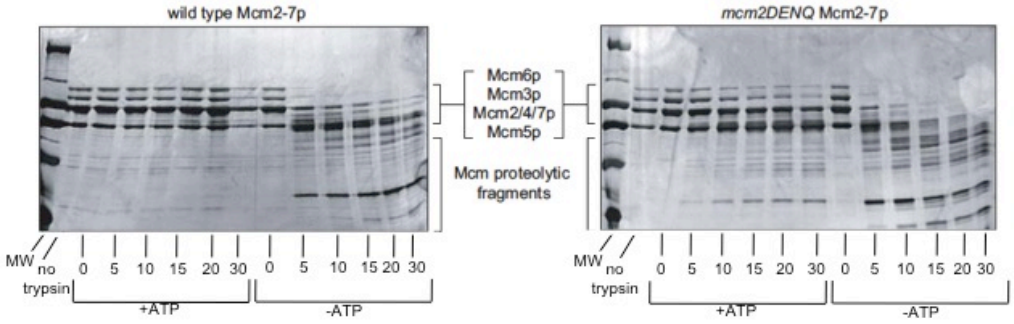

Figure 13. Protein stability of *mcm2DENQ*

A) Mcm2 protein levels. Wild type (UPY464) and *mcm2DENQ* (UPY499) strains were harvested following either asynchronous growth in rich media (Asyn) or following α-factor arrest in G1 at 0, 30, or 60 minutes after release into fresh media to examine protein levels during S phase. Cell extracts were made by a TCA-based method (Wright et al., 1989), and analyzed with quantitative Western blotting using antibodies either to Mcm2 (Sana Cruz SC-6680) or to the loading control glucose-6 phosphate dehydrogenase (G6PDH) (A9521, Sigma Chemical Company). Results were recorded using a CCD camera (Fuji LAS-3000) within the linear signal range, quantified using ImageGauge software (Fuji), and the signal ratios between Mcm2p/mcm2DENQp and the loading control (G6PDH) were calculated. B) Mcm2 protein stability. Cyclohexamide (CHX) was added to wild type (UPY464), mcm2DENQ (UPY499) and a wild type strain transformed with an ARS/CEN plasmid encoding carboxypeptidase Y (CPY*) (pUP1106) tagged with 3XHA (a well-characterized ER associated degradation substrate). Cultures were incubated at 30°C in CHX and aliquots were withdrawn at indicated times and processed for protein extraction as described Methods. Protein extracts were analyzed by Western blotting analysis similar to A), except that anti-HA antibodies were used to probe for CPY*. (left) representative blots. (right) graph of the average and standard deviation of protein stability. No statistical difference in stability was observed between Mcm2p and Mcm2DENQp. C) Protease sensitivity of Mcm2-7 complexes. Silver stained SDS-PAGE showing a time course of both purified wild type (top) and *mcm2DENQ* (bottom) Mcm2-7 hexamers treated with trypsin as described in Methods; numbers are the duration in minutes in the presence of active trypsin. Note that the Mcm2, 4, and 7 subunits co-migrate in the *S. cerevisiae* Mcm2-7 complex on SDS-PAGE. MW= molecular weight. ATP makes wild type Mcm2-7 relatively resistant to proteolysis (FT, observation), and the digests shown were conducted in both the presence (+ATP) and absence (-ATP) of 10 mM ATP.

To study this growth defect, we examined the DNA damage sensitivity of the *mcm2DENQ* mutant, to understand whether the Mcm6/2 active site plays a role in the S phase checkpoint. The S phase checkpoint is a partially redundant phosphorylation cascade composed of the DNA replication checkpoint (DRC) and the DNA damage checkpoint (DDC) (reviewed in (Branzei and Foiani, 2009)). The DRC transduces signals via Mrc1 phosphorylation in response to replication fork stalling (Alcasabas et al., 2001), while the DDC transduces signals via Rad9 phosphorylation in response to DNA double strand breaks (DSB) (Vialard et al., 1998). Both pathways contain a common sensor kinase Mec1 and effector kinase Rad53, which is phosphorylated during DNA damage and leads to cell cycle arrest. The *MRC1* and *RAD9* pathways can compensate each other; however, the lost of both pathways result in synthetic lethality (Alcasabas et al., 2001) (Figure 7).

Alone, *mcm2DENQ* resembles *mrc1*Δ; both form small colonies in the presence of the ribonucleotide reductase inhibitor hydroxyurea (HU) but are relatively resistant to the DNA damaging agent methyl methane sulfonate (MMS) (Figure 14A). However in combination with *rad9*Δ, *mcm2DENQ* is as sensitive as *rad9*Δ*/mrc1*Δ*/smlI*Δ to MMS and is similarly unable to resume cell cycle progression after MMS removal (Figure 14A and B) (*smlI*Δ suppresses lethality associated with ablation of the intra-S phase checkpoint (e.g., *mec1*Δ*, rad53*Δ), but otherwise causes no additional checkpoint phenotype (Zhao et al., 1998)).

In contrast, the *mcm2DENQ* allele caused synthetic lethality in combination with *mrc1*Δ, *tof1*Δ, or *csm3*Δ; at least with *mrc1*Δ the lethality was unsuppressed by *smlI*Δ (Figure 14F and legend). However, the *mcm2DENQ* allele could be combined with *mrc1AQ* (Figure 14F), a checkpoint defective allele of *MRC1* with normal DNA replication (Osborn and Elledge, 2003;

Szyjka et al., 2005). The double mutant showed no synergistic increase in DNA damage sensitivity with either HU or MMS (Figure 14A).

The synergistic DNA damage sensitivity in combination with *rad9*Δ but not *mrc1AQ* suggests that the *mcm2DENQ* mutant is specifically defective for the DRC. However, the *mcm2DENQ*/*rad9*Δ double mutant is much more HU resistant than the *mrc1*Δ*/rad9*Δ*/sml1*Δ triple mutant (Figure 14A), suggesting that *mcm2DENQ* does not completely ablate the intra-S phase checkpoint under these conditions. In addition, the genetic interactions between *mcm2DENQ* and *rad9*Δ do not require ablation of *SML1* for viability unlike *mrc1*Δ*/rad9*Δ (Figure 14A).

The DNA damage sensitivity was similarly tested in the *mcm2-1* and *chaos3* mutant. *mcm2-1* is slightly sensitive to hydroxyurea and forms smaller colonies similar to *mcm2DENQ*. Contrary, *chaos3* behaves similar to wild type when exposed to hydroxyurea (Figure 15A). When combined with *rad9*Δ, both the *mcm2-1/rad9*Δ and *chaos3/rad9*Δ double mutants are viable. Only *mcm2-1/rad9*Δ shows synergistic DNA damage sensitivity to MMS but not *chaos3/rad9*Δ (Figure 15A). Furthermore, *chaos3/rad9*Δ is more resistant to HU than *mcm2-1/rad9*Δ (Figure 15A). The genetic interaction of both alleles with *mrc1*Δ are synthetic lethal (Figure 15B and C). Overall, these results suggest that DNA damage response may be modulated through the Mcm2 subunit or the Mcm6/2 active site, and Mcm4 appears to play a lesser role in this process. The synthetic lethality between *chaos3/rad9* may reflect a common function in replication fork progression, rather than a defect in the S-phase checkpoint.

To validate the *mcm2DENQ* checkpoint defect, we examined cell cycle progression. G1 phase synchronized wild type cells released into MMS displays G2/M arrest and blocks spindle elongation (Komata et al., 2009) (Figure 14C and D). In the absence of MMS, the doubling time

of the *mcm2DENQ* mutant is approximately 20-30 minutes longer than wild type (compare the wild type (Mcm2) T=100 with the mutant (*mcm2DENQ*) T=120) (Figure 14C**)** with increases in both S (~10 minutes) and G2 phases (~10-20 minutes). However, in the presence of MMS, both *mcm2DENQ* and wild type proceed slowly through S-phase with identical kinetics (Figure 14C), suggesting that *mcm2DENQ* is less inhibited by DNA damage than wild type. A similar observation has been made for *mrc1*Δ (Alcasabas et al., 2001). Spindle elongation for the *mcm2DENQ* mutant is nearly indistinguishable from wild type under these conditions (Figure 14D).

The *mcm2DENQ/rad9*Δ double mutant was next assayed. In the presence of MMS, *rad9*Δ alone has a slight spindle defect (Figure 14D) and reaches a G2 DNA content with about a 20 minutes cell cycle delay (Figure 14C, compare *rad9*Δ ± MMS). However, the *mcm2DENQ/rad9*Δ double mutant is similar to *rad9*Δ*/mrc1*Δ/*sml*1Δ and nearly eliminates the MMS-induced block to cell cycle progression (< 10 minute) (Figure 14C, compare *mcm2DENQ/rad9*Δ ± MMS) and spindle elongation (Figure 14E). In total, these data confirm that *mcm2DENQ* is a DRC mutant.

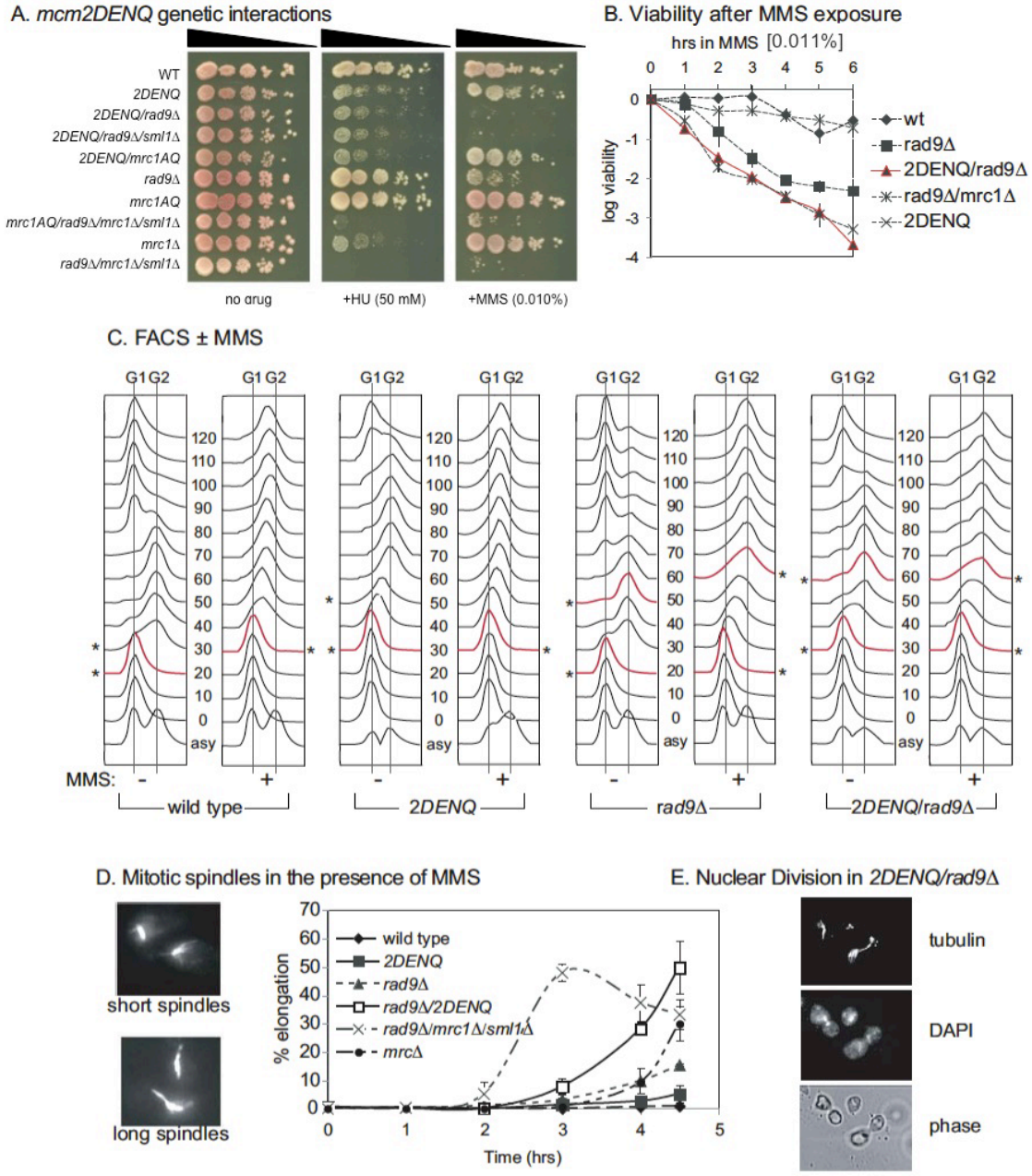
A. mcm2DENQ genetic interactions
WT
2DENQ
2DENQ/rad9Δ
2DENQ/rad9Δ/sml1Δ
2DENQ/mrc1AQ
rad9Δ
mrc1AQ
mrc1AQ/rad9Δ/mrc1Δ/sml1Δ
mrc1Δ
rad9Δ/mrc1Δ/sml1Δ
no drug
+HU (50 mM)
+MMS (0.010%)
B. Viability after MMS exposure
hrs in MMS [0.011%]
log viability
wt
rad9Δ
2DENQ/rad9Δ
rad9Δ/mrc1Δ
2DENQ
C. FACS ± MMS
G1 G2
asy
MMS:
wild type
2DENQ
rad9Δ
2DENQ/rad9Δ
D. Mitotic spindles in the presence of MMS
short spindles
long spindles
% elongation
wild type
2DENQ
rad9Δ
rad9Δ/2DENQ
rad9Δ/mrc1Δ/sml1Δ
mrcΔ
Time (hrs)
E. Nuclear Division in 2DENQ/rad9Δ
tubulin
DAPI
phase

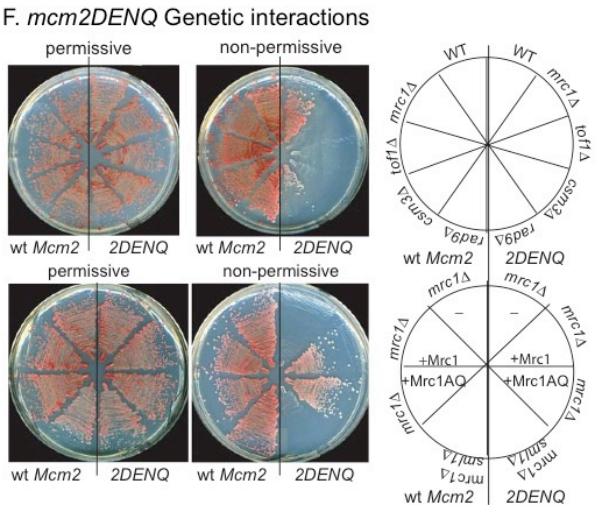

Figure 14. *mcm2DENQ* is defective in the DRC

A) The indicated isogenic strains (wild type, UPY464; *mcm2DENQ*, UPY499; *mcm2DENQ/rad9*Δ, UPY634; *mcm2DENQ/rad9*Δ*/smlI*Δ, UPY732: *mcm2DENQ/mrc1AQ*, UPY758; *mrc1AQ*, UPY773; *mrc1AQ/mrc1*Δ*/rad9*Δ*/sml1*Δ, UPY745, *rad9*Δ, UPY630; *mrc1*Δ, UPY713; *rad9*Δ*/mrc1*Δ*/smlI*Δ, UPY715) were grown to mid-log phase, their cell densities normalized, and 5 μl aliquots of ten-fold serial dilutions were spotted onto the indicated media. B) The listed strains (wild type, UPY464; *mcm2DENQ*, UPY499; *mcm2DENQ/rad9*Δ, UPY634; *mcm2DENQ/rad9*Δ*/smlI*Δ, UPY630; *mrc1*Δ, UPY713; *rad9*Δ*/mrc1*Δ*/smlI*Δ, UPY715) were arrested in α-factor, released into YPD + 0.011% (v/v) MMS, and colony forming units were measured at indicated intervals. The starting culture = "0" (=log1), and error bars are small and appear to be absent. C) FACS analysis (wild type, UPY464; *mcm2DENQ*, UPY499; *rad9*Δ, UPY630; *mcm2DENQ/rad9*Δ, UPY634) ± 0.033% MMS using a CyAn ADP analyzer (Beckman Coulter) and the FlowJo software package (Tree Star, Ashland OR). asy = asynchronous culture. D) The indicated strains (wild type, UPY464; *mcm2DENQ*, UPY499; *rad9*Δ, UPY630; *mcm2DENQ/rad9*Δ, UPY634; *rad9*Δ*/mrc1*Δ*/smlI*Δ, UPY715) were arrested in α-factor, released into YPD + 0.033% MMS, processed for tubulin immunofluorescence and the mitotic spindles scored. (Top) short spindles; (bottom) long spindles. Graph represents the percent long spindles from ≥ 100 cells vs. time. E) *mcm2DENQ/rad9*Δ *cells* dividing in YPD + 0.033% MMS. F) Synthetic lethal interactions between *mcm2DENQ* and various checkpoint alleles. Diagram on the right indicates the genetic makeup of each plate sector, with additional genetic markers outside the circle, and plasmids encoding genes other than *MCM2* or *mcm2ENQ* inside the circle. All strains contain a chromosomal

deletion of *Mcm2* covered with a *MCM2*$^{+}$*/URA3*$^{+}$ plasmid (pUP191). In addition, strains on the left side of the plate additionally contain a TRP1+ tester plasmid encoding MCM2p (pUP197), while strains on the right side contain a similar plasmid encoding mcm2DENQp (pUP199). Top: The strains contain additional chromosomal mutations as indicated: no additional markers (-, UPY110); *mrc1*Δ (UPY428.1); *tof1*Δ (UPY631); *csm3*Δ (UPY632); rad9Δ (UPY421). Left plate was grown on media that lacks uracil (permissive) to select for the wild type *MCM2* plasmid (pUP191), while the plate on the right contains 5-fluoroorotic acid (5-FOA) (non-permissive) and kills cells containing the pUP191. Under the non-permissive condition, either pUP197 (*MCM2*) or pUP199 (*mcm2DENQ*) provide *MCM2* function. Bottom: Test of *mrc1AQ* and *sml1*Δ to suppress the synthetic lethality between *mcm2DENQ* and *mrc1*Δ. The analysis is similar to the top panel, except that only strains carrying *mcm2*Δ and *mrc1*Δ were used. From top to bottom of the plate, four additional constructs were tested for their ability to rescue *mrc1*Δ*/mcm2DENQ* synthetic lethality: no additional construct (UPY428.1), *LEU2::MRC1* (UPY781), *LEU2::mrc1AQ* (UPY676), and *sml1*Δ (UPY636). Strains were grown under permissive and non-permissive (5-FOA) conditions as described above.

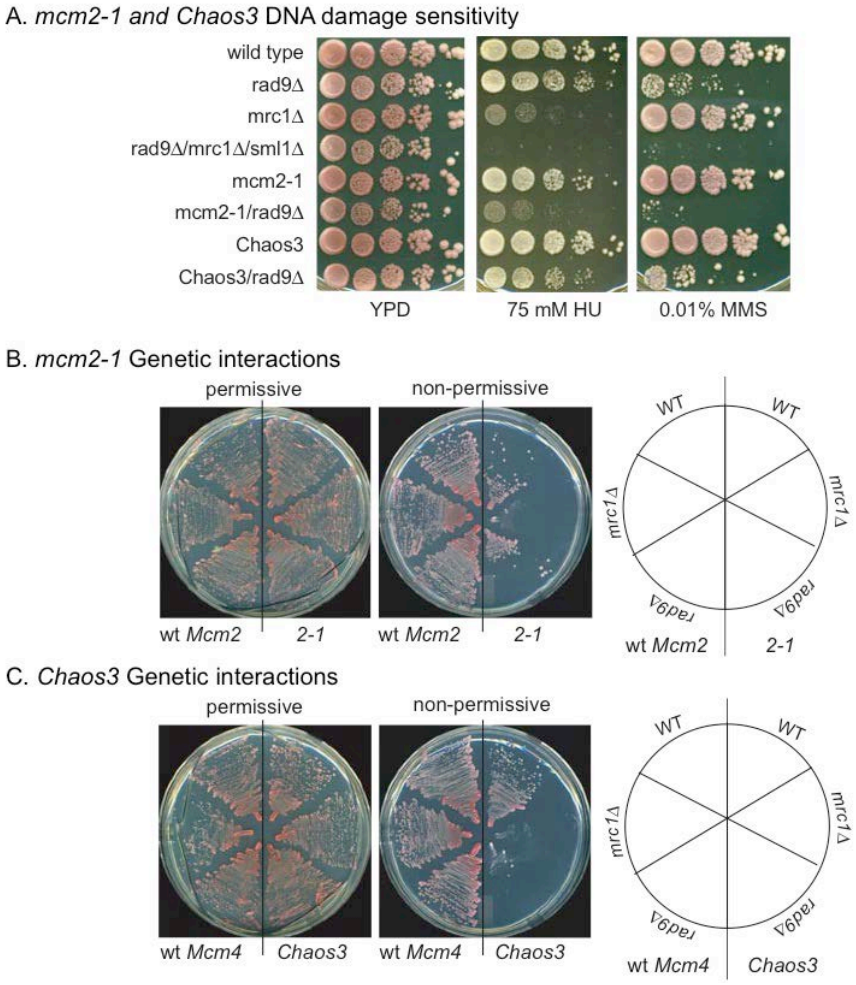

Figure 15. Characterization of *mcm2-1* and *Chaos3* involvement in the DRC

A) Sensitivity of *mcm2-1/chaos3* mutants in combination with the indicated checkpoint alleles to MMS or HU. Assay performed as described in Figure 14A. B) Genetic interactions between *mcm2-1* and *mrc1*Δ and *rad9*Δ were tested similar to Figure 14F, except that LEU2+ integrating plasmids that encode either Mcm2p (pUP1018) or mcm2-1p (pUP1033) was used instead of the *ARS/CEN TRP+* plasmids. C) Genetic interactions were tested similar to B), except that strains carrying *mcm4*Δ and integrating plasmids encoding Mcm4p (pUP1099) or mcm4chaos3p (pUP1098) on *LEU2+* integrating vectors were used. The strains tested were: no mutation (UPY114), *mrc1*Δ (UPY438), *rad9*Δ (UPY412).

3.3.2 The role of Mcm2-7 in the DRC signal transduction pathway

The intra-S phase checkpoint culminates in the (auto)phosphorylation and activation of Rad53p via the phosphorylation of Mrc1p (DRC), or Rad9p (DDC); phosphorylation causes a diagnostic molecular weight increase in each protein on SDS-PAGE (Figure 16A) (Alcasabas et al., 2001; Vialard et al., 1998).

To examine the DRC and DDC cascades, the phosphorylation of Rad53p, Mrc1p, and Rad9p was assayed following exposure to either HU or MMS. Most strains, including the *mcm2DENQ/mrc1AQ* double mutant, demonstrate normal Rad53p phosphorylation (~70% of Rad53p in one of several phosphorylated forms) relative to a strain completely devoid of the intra S-phase checkpoint (*mrc1*Δ*/rad9*Δ*/sml1*Δ) (Figure 16B). In contrast, combining either the *mcm2DENQ* or *mcm2-1* allele with *rad9*Δ (to eliminate DDR) causes a reproducible ~4 fold reduction in Rad53p phosphorylation (15%/17%) upon MMS exposure and a 2 fold reduction upon HU exposure (25%/28%) (Figure 16B), indicating that both *mcm2* alleles cause a defect in the DRC cascade. Unlike the *mcm2-1/rad9*Δ or *mcm2DENQ/rad9*Δ double mutant, *chaos3/rad9*Δ produces wild type level of Rad53 phosphorylation upon MMS or HU exposure (61%/65%) (Figure 16B), which is consistent with its HU and MMS resistance in the spot dilution test (Figure 14A). In contrast to Rad53p, a similar analysis of Mrc1p and Rad9p demonstrates that *mcm2DENQ* has normal phosphorylation of both proteins under DNA damage conditions, indicating that *mcm2DENQ* blocks after their phosphorylation (Figure 16C and D and legend) (the HA-tagged Mrc1p and Rad9p are verified to be functional (Figure 16E)).

These results warrant two conclusions: 1) The two *mcm2* alleles (but not *chaos3*) cause a DRC defect prior to Rad53p phosphorylation but not the *mcm4* allele; and 2) since Mrc1p phosphorylation is normal, these *mcm2* mutants sense DNA damage but signal transduction is

restricted after Mrc1p phosphorylation. Thus, Mcm2-7 is an integral member of the DRC cascade.

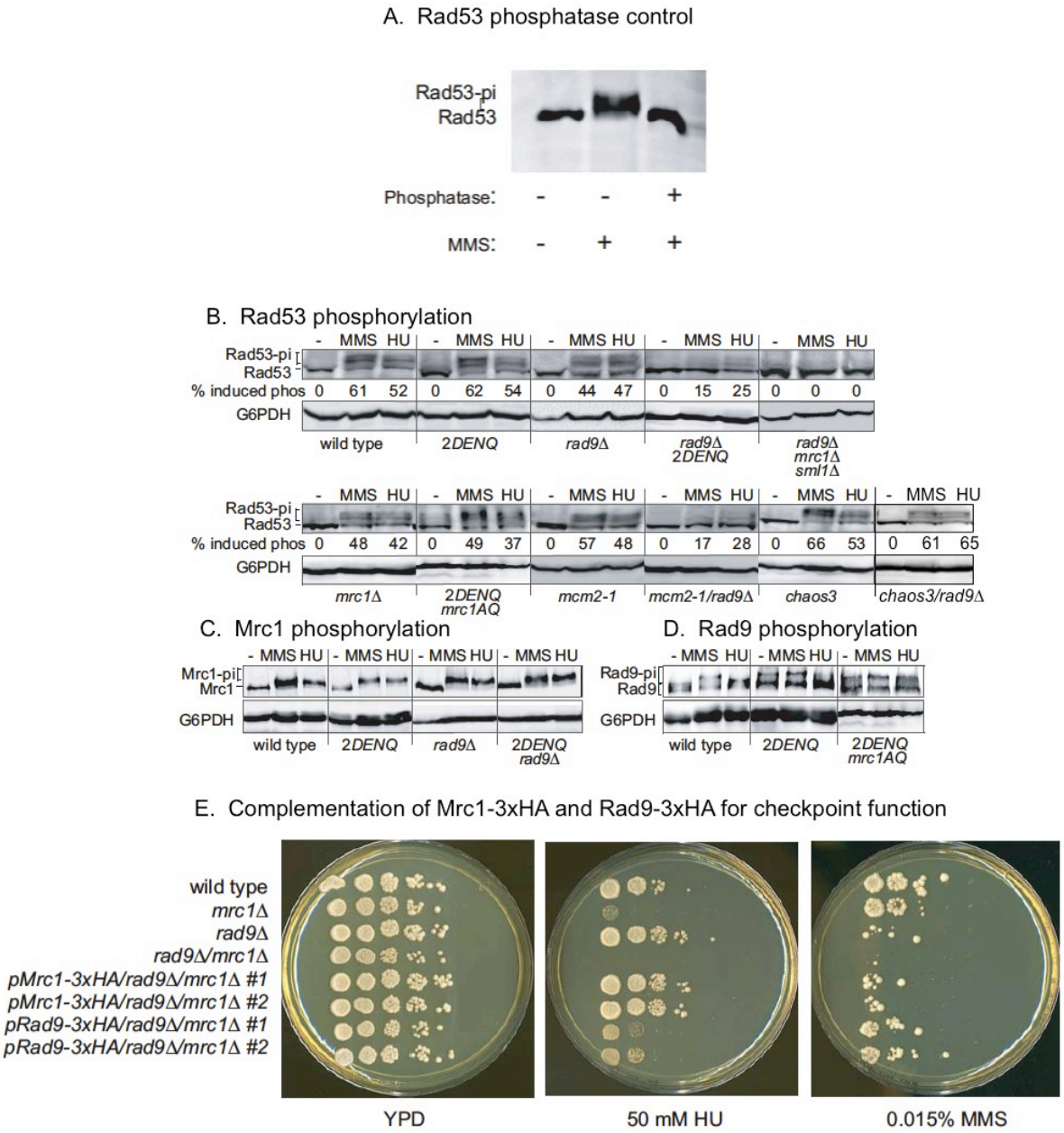

Figure 16. Mcm2-7 is part of the DRC cascade

A) Rad53p mobility shift is a result of phosphorylation. Wild-type (UPY464) cells were grown in the absence or presence of 0.1% MMS for 1hr. Protein extracts were prepared with appropriate phosphatase inhibitors and immunoprecipitated with anti-Rad53 antibodies (Methods). To confirm whether the slower migrating form is a result of phosphorylation, immunoprecipitated Rad53 was incubated in the absence or presence of calf intestinal phosphatase for 45 minutes at 37^{o}C. The resulting protein samples were subjected to SDS-PAGE electrophoresis and Western blot analysis probed with anti-Rad53 antibodies. B) Representative Western blots of Rad53p from asynchronous cultures (wild type, UPY464; *mcm2DENQ*, UPY499; *mcm2DENQ/rad9*Δ, UPY634; *mcm2DENQ/rad9*Δ*/smlI*Δ, UPY732: *mcm2DENQ/mrc1AQ*, UPY758; *rad9*Δ, UPY630; *mrc1*Δ, UPY713; *rad9*Δ*/mrc1*Δ*/smlI*Δ, UPY715; *mcm2-1,* UPY769; *mcm2-1/rad9*Δ, UPY770; *chaos3*, UPY638; *chaos3/rad9*Δ, UPY788) grown ± 200 mM HU or 0.033% MMS for 90 minutes as indicated; % phosphorylation = (slow mobility Rad53/total Rad53) X 100. These experiments have been repeated ≥ 3 times and in all cases the standard deviation is ≤ 10% of the listed phosphorylation values. C) Mrc1p or D) Rad9p phosphorylation was measured (Mrc1-3xHA: wild type, UPY646; *mcm2DENQ*, UPY647; *rad9*Δ, UPY659; *mcm2DENQ/rad9*Δ, UPY660; Rad9-3xHA: wild type, UPY648; *mcm2DENQ*, UPY649) as in A) except that a functional C-terminal 3xHA epitope tag was engineered into each protein and an anti-HA primary antibody was used. As previously observed in *mrc1* mutants (Alcasabas et al., 2001), *mcm2DENQ/mrc1AQ* demonstrates significant Rad53p and/or Rad9p phosphorylation in the absence of exogenous DNA damage, consistent with the spontaneous DSBs generated by these mutants (Alcasabas et al., 2001) and below)). HU causes minimal Rad9p phosphorylation in wild type as previously observed (Alcasabas et al., 2001). E) Complementation test of Rad9-3xHA and Mrc1-3xHA constructs. C-terminal 3XHA tags on Mrc1 and Rad9 do not cause a defect in checkpoint function. The indicated strains were spotted as ten fold dilution series on either rich media (YPD), or rich media containing either HU (50 mM) or methylmethane sulfonate (MMS) (0.015%). From top to bottom, the strains used: wild type (UPY464); *mrc1*Δ (UPY713); *rad9*Δ (UPY630); *rad9*Δ*mrc1*Δ*sml1*Δ (UPY715); Mrc1-3xHA integrated into UPY715 (colonies 1 and 2); Rad9-3xHA integrated into UPY715 (colonies1 and 2). Both the Mrc1-3xHA and Rad9-3xHA constructs were integrated into the LEU2 loci and express under the control of its own promoter.

3.3.3 The effects of *mcm2DENQ* on replication initiation and elongation

A ChIP-Seq approach was used to assay DNA replication in *mcm2DENQ*. Chromatin immunoprecipitation (ChIP) was performed using antibodies that either recognize all six Mcm subunits (Mcm2-7-pan) or is specific to Mcm2p (Mcm2p-specific), and the isolated DNA fragments were subjected to next-generation sequencing (**Chapter 2**).

To examine replication initiation, cultures were arrested in G1 with α-factor prior to sample preparation and analysis (Figure 17A). Aside from several dozen exceptional origins (Figure 17B and legend, discussed further in Figure 18A), peaks of Mcm association for wild type and *mcm2DENQ* are qualitatively similar and concordant with previously determined replication origins (oriDB, (Nieduszynski et al., 2007)). However, apparent localization efficiency is antibody dependent. With the Mcm2-7-pan antibody, wild type and *mcm2DENQ* have nearly identical Mcm association levels (≤7% average reduction in Mcm protein loading in *mcm2DENQ*, difference between wild type and *mcm2DENQ* origin association t=1.69, $p\text{-}_{value}$ 0.092) (Figure 17A and B). In contrast, experiments using the Mcm2p-specific antibody showed an average 25% reduction in mcm2DENQp origin association relative to Mcm2p (difference between *mcm2DENQ* and wild type Mcm2 loading, t=6.60 p-value=8.28e-11) (Figure 18A, Figure 17A and C). This reduction is consistent with independent quantitative ChIP experiments of several candidate origins (data not shown), and places a lower limit on mcm2DENQp origin association at ≥ 75% of wild type.

A. MCM G1 chromosome association: Mcm2 specific vs. Mcm2-7 pan antibody, chromosome XIV

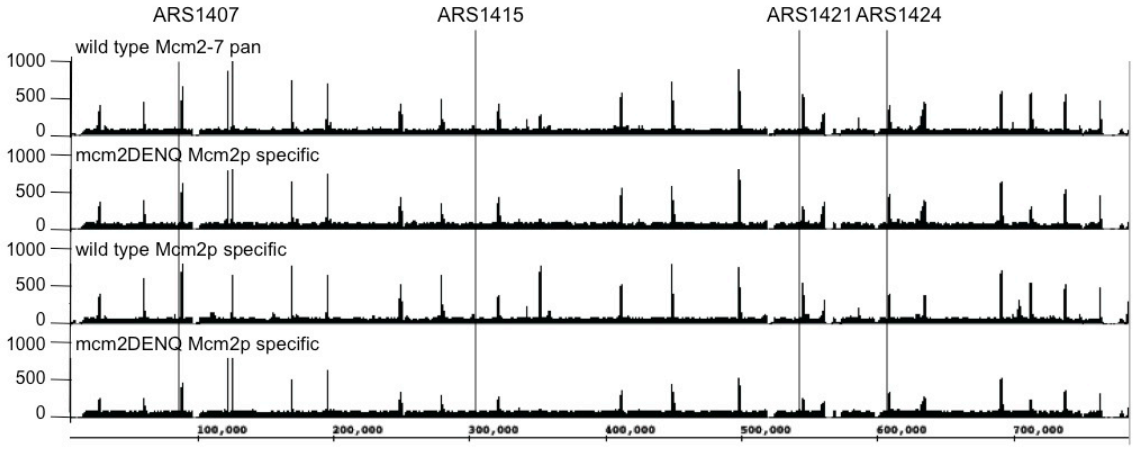

B. G1 chromosome association of Mcm2p and mcm2DENQp using Mcm2-7 pan antibody

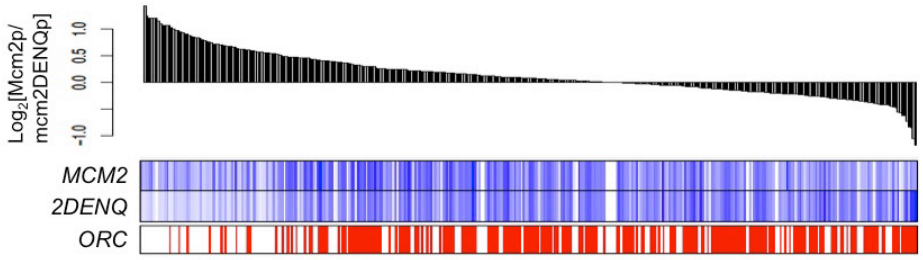

C. G1 chromosome association of Mcm2p and mcm2DENQp using Mcm2-specific antibody

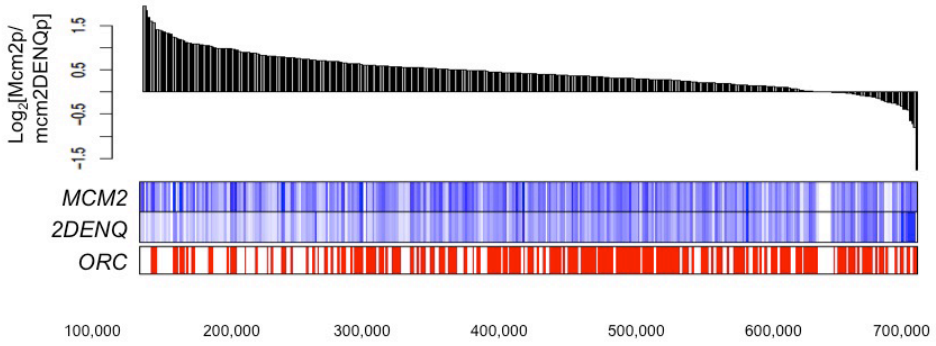

Figure 17. Mcm2-7 chromosome association during G1

A) Comparison of different ChIP-seq experiments using either the Mcm2-7 pan antibody (top), or the Mcm2 specific antibody (bottom). RPKM normalized results for the right arm of Chromosome XIV are shown. The pan Mcm2-7 antibody identifies 422 peaks in wildtype and 377 in *mcm2DENQ*, while the Mcm2 specific antibody recognizes 436 in wild type and 393 in *mcm2DENQ*. All identified peaks demonstrated > 90% overlap with previously validated origins (Eaton et al., 2010). B) HEAT maps showing ratios of Mcm origin enrichment for the wild-type and *mcm2DENQ* strains using the Mcm2-7 pan antibody. For both the wild-type and *mcm2DENQ* datasets, the average of the normalized-RPKM Mcm enrichment within 500bp +/- each "confirmed" ACS in the OriDB (Nieduszynski et al., 2007) was determined. Top panel: a plot of the ratio of wild type to mcm2DENQp association for each origin; positive values correspond to greater Mcm2p association, negative values correspond to more mcm2DENQp association. Log 2 scale is shown. Middle panel: relative levels of either wild-type Mcm2p or mcm2DENQp origin association used to create the top panel (white indicates no origin association, blue indicates the highest association). There is no statistical difference between Mcm2p and mcm2DENQp origin association using the Mcm2-7 pan antibody (t=1.685, p value =0.09). Bottom panel: although there is relatively little difference between the wild-type and *mcm2DENQ* strains in terms of Mcm association, there are a few origins in which the MCMs associate with at a much higher level in wild-type than *mcm2DENQ* (left side of middle panel). It should be noted that these origins tend to show little ORC association (lower panel, ORC binding sites in red from Eaton *et al*. (2010)). C). Same as in B), except the Mcm2 specific antibody was used. Using the mcm2 specific antibody, the levels of Mcm2p and mcm2DENQp origin association are statistically different (t=6.599, p value = 8.28×10^{-11})

We adapted our ChIP-Seq protocol to examine elongation. Following release of G1 synchronized cultures into S-phase, the nucleoside analog bromodeoxyuridine (BrdU) and HU were added to both label newly formed DNA and restrict replication to origin-proximal regions. ChIP was performed with antibodies specific to either BrdU or Mcm2-7 (using the more robust pan-Mcm2-7 antibody), and the isolated DNA fragments were processed as before.

The peaks of BrdU incorporation in wild type, *mcm2DENQ*, *mcm2-1*, *chaos3* and *mrc1*Δ localize to previously identified origins (Nieduszynski et al., 2007) (Figure 18B). Among early replication origins (i.e., those in wild type that fire in the presence of HU), the BrdU peak heights in *mcm2DENQ* are similar to the corresponding peaks in wild type (Figure 19B and C) and are consistent with mcm2DENQp association in G1 tested using pan-Mcm antibody. This data is in contrast to *mrc1*Δ, which demonstrates a ~70% reduction in peak height relative to wild type (Figure 19B and C). This data suggest that the average origin firing efficiency, at least in *mcm2DENQ*, is similar to that of wild type. *mcm2-1* and *Chaos3* appear to be similarly efficient in origin firing comparing to wild type (Figure 18D).

Second, *mcm2DENQ* is partially derepressed for late origin firing. DRC mutants (e.g., *mrc1*Δ) fire various subsets of additional origins (late origins) in an allele-specific manner (Crabbe et al., 2010; Katou et al., 2003), Figure 18B). In *mcm2DENQ*, origin usage is intermediate between wild type and *mrc1*Δ (Figure 18B); all early origins fire as well as a subset of late origins. Moreover, this usage resembles that of *mrc1AQ* (Crabbe et al., 2010), as 72% of the late origins that fire in *mrc1AQ* also fire in *mcm2DENQ* (Figure 18C). For *mcm2-1* and *chaos3*, repression of late origin firing is similar to wild type (Figure 18D).

The involvement of Mrc1 in coupling the replicative helicase and DNA polymerase during replication stress is controversial. Prior analysis of *mrc1*Δ using ChIP-chip suggests that

DNA polymerase (i.e., BrdU incorporation) physically uncouples from the replicative helicase (i.e., Mcmp or Cdc45p localization) at a few origins in the presence of HU (Crabbe et al., 2010; Katou et al., 2003). However, a recent study using the ChIP-seq technique suggests that replisome does not collapse in S phase checkpoint mutants *rad53*Δ and *mec1*Δ (De Piccoli et al., 2012). Our ChIP-seq methodology has considerably higher resolution than the previous ChIP-Chip studies, and we routinely observe bifurcation of the Mcm2-7 signal corresponding to bidirectional DNA replication (Figure 19A). However, re-examining the potential uncoupling issue using this methodology, we do not observe a systematic and global uncoupling in either *mcm2DENQ* or *mrc1*Δ, as Mcm2-7p discretely localizes to either edge of the BrdU incorporation zone flanking active origins of replication in these strains (Figure 19B).

In summary, *mcm2DENQ* is partially defective in the repression of late origins, a phenotype consistent with a DRC defect. *mcm2DENQ* is not defective in origin firing efficiency. This is consistent with the near to wild type level in chromosome association of mcm2DENQp during G1 (i.e., pre-replication complex formation (Wyrick et al., 2001)). The discrepancy between the G1 Mcm enrichment results obtained from pan-Mcm and Mcm2 specific antibodies may be due to the lack of epitope recognition caused by the *mcm2DENQ* mutation. We cannot completely exclude the possibility of minor pre-RC formation problems.

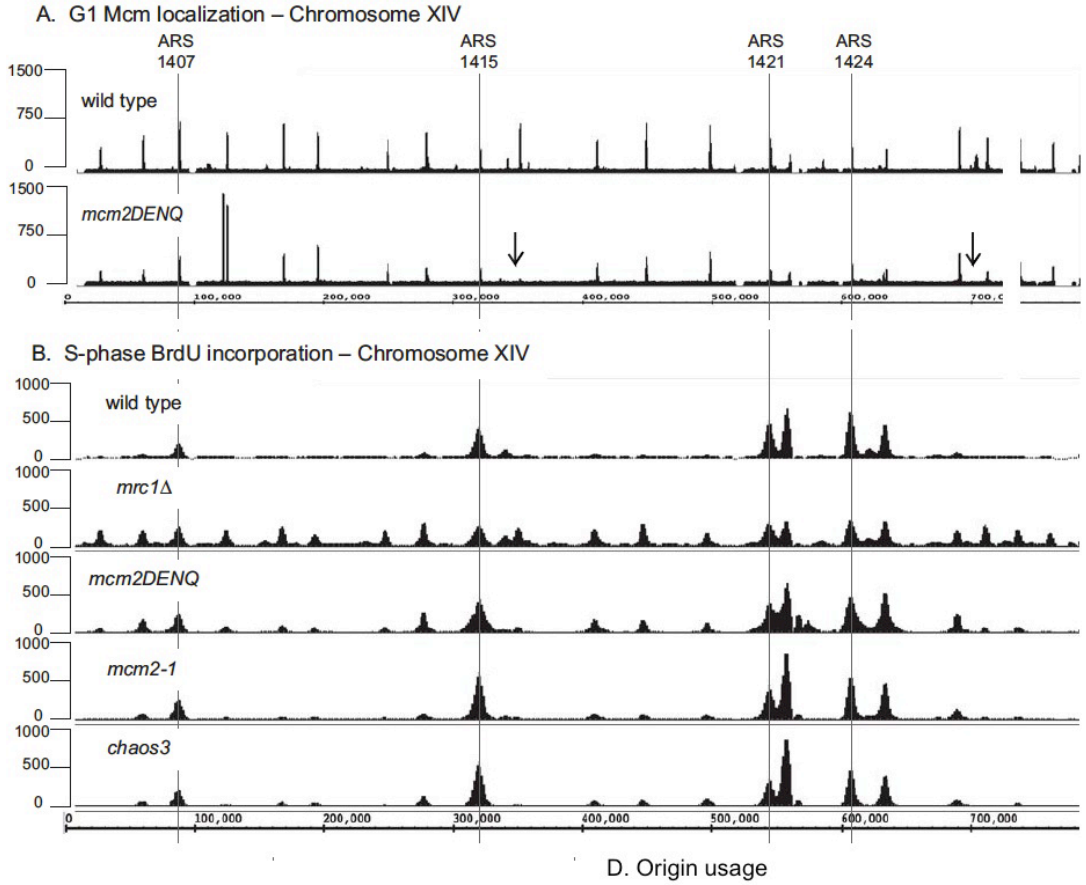
A. G1 Mcm localization – Chromosome XIV
ARS 1407
ARS 1415
ARS 1421
ARS 1424
wild type
mcm2DENQ
B. S-phase BrdU incorporation – Chromosome XIV
wild type
mrc1Δ
mcm2DENQ
mcm2-1
chaos3
100,000
200,000
300,000
400,000
500,000
600,000
700,000

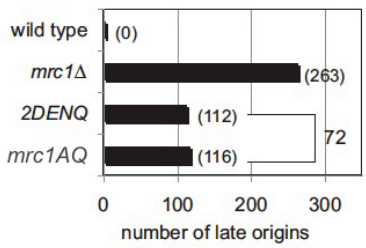
C. 2DENQ/mrc1AQ late origin comparison
wild type
mrc1Δ
2DENQ
mrc1AQ
(0)
(263)
(112)
(116)
72
number of late origins

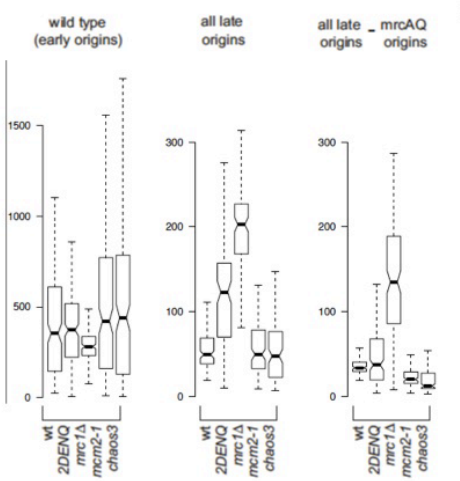
D. Origin usage
wild type (early origins)
all late origins
all late origins – mrcAQ origins
wt
2DENQ
mrc1Δ
mcm2-1
chaos3

Figure 18. *mcm2DENQ* partially loses repression of late origin firing

See Methods for analysis details. A) Mcm2 ChIP-seq of wild type (UPY493) and *mcm2DENQ* (UPY524) strains shows RPKM adjusted peaks of Mcm enrichment in G1 on the right arm of chromosome XIV using the Mcm2p-specific antibody. Arrows show regions that demonstrate Mcm loading in wild type but not *mcm2DENQ*. These putative origins may be nonfunctional in wild type, as they show exceptionally little ORC association (Eaton *et al*. (2010)). B) BrdU ChIP-seq of isogenic wild type (UPY493), *mcm2DENQ* (UPY524), *mrc1*Δ (UPY722), *mcm2-1* (UPY790) and *chaos3* (UPY797) strains following RPKM normalization (combined dataset). The right arm of Chromosome XIV is shown. C) Histogram showing the relationship between late origins that fire in wild type, *mrc1AQ* (red) and *mcm2DENQ*. Numbers in parenthesis are the number of origins; 72 corresponds to the number of origins that fire in common between *mrc1AQ* and *mcm2DENQ*. Results for the *mrc1AQ* are from (Crabbe et al., 2010). D) Origin utilization is similar between *mcm2DENQ* and *mrc1AQ*. Results shown are the combined dataset from both replicate experiments. Replication origins that were utilized in the presence of HU identified by Crabbe *et al*. (2010) were divided into three categories: i) Early origins active in wild type cells, ii) all late origins (origins activated in *mrc1*Δ – origins activated in wild type) and iii) late origins activated in *mrc1*Δ but not in *mrc1AQ*. For each subset of origins the median BrdU enrichment (RPKM) observed in our strains (wt, *2DENQ*, and *mrc1*Δ) was calculated and displayed the range of median values as box and whisker plots. Early origins (left) exhibited similar levels of usage in each strain. All late origins (center, (Crabbe et al., 2010)) were also found specifically enriched in our *mcm2DENQ* or *mrc1*Δ strain but not wild type. Late origins that activate in *mrc1*Δ but not *mrc1AQ* (Crabbe et al., 2010) activate in our *mrc1*Δ strain but not in *mcm2DENQ (right)*. p-values were determined by Wilcoxon rank sum test and are shown in Appendix. The notches represent 95% confidence for the medians.

A. Mcm association during S phase – chromosome XIV in HU

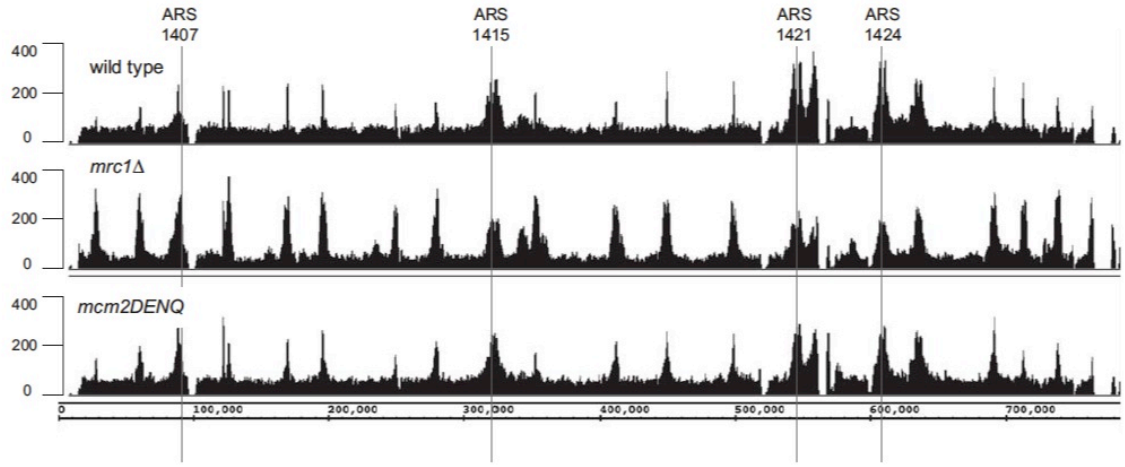

B. Fork Architecture

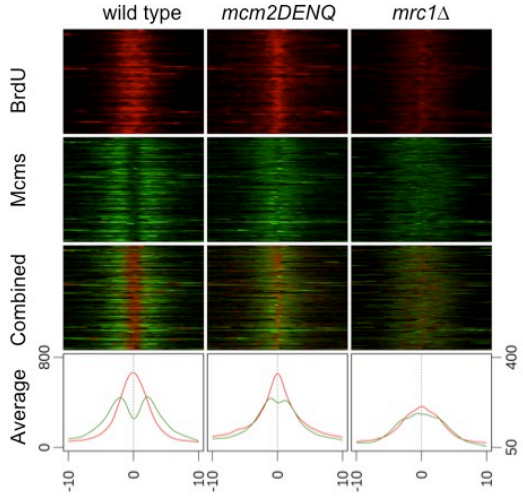

C. Average BrdU peak widths

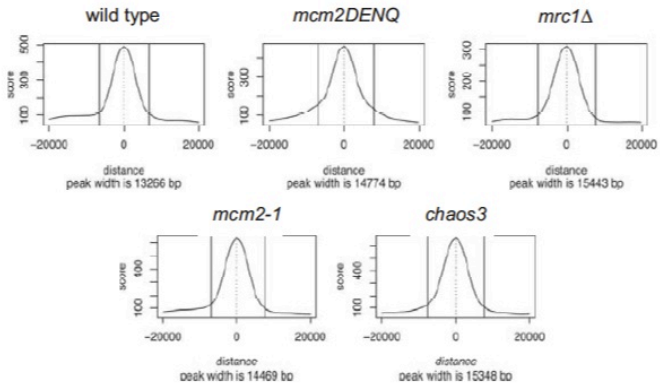

Figure 19. Mcm enrichment at the replication fork

A) Mcm ChIP-seq in HU arrested cells (combined replicates 1 and 2) following RPKM normalization. Analysis used the pan-Mcm2-7 antibody as described in Methods; cultures were synchronized with α-factor and released into 0.2M HU at 23^{o}C until the budding index reached 75% (wild type: 100 minutes, *mrc1*Δ: 105 minutes, *mcm2DENQ*: 105 minutes) and then processed for ChIP-Seq. RPKM normalized Mcm enrichment for chromosome XIV is shown. B) Relationship between Mcm and BrdU enrichment of wild type (UPY493), *mcm2DENQ* (UPY524), *mrc1*Δ (UPY722) in HU (combined dataset). Left, HEAT map of all early origins for BrdU enrichment (red), Mcm enrichment (green), and the composite of the two signals; Right, a composite of Mcm and BrdU localization for each strain. The BrdU scale is from 0-800; the Mcm scale is from 50-400. C) Fork progression of wild type (UPY493), *mcm2DENQ* (UPY524), *mrc1*Δ (UPY722), *mcm2-1* (UPY790) and *chaos3* (UPY797) (combined dataset). Shown above are peak width deteremined from aggregate of BrdU signal +/-20kb of early firing origins.

3.3.4 Minichromosome maintenance revisited

Mutants defective for DNA replication display high plasmid loss phenotype (Sinha et al., 1986). To distinguish whether the defect arises from DNA replication initiation or elongation, plasmids containing either single or multiple origins of replication can be tested. If the plasmid loss phenotype is caused by a defect in DNA replication initiation, it can be suppressed by incorporation of additional replication origins, similar to previously studied initiation mutants (Hogan and Koshland, 1992). In this assay, test plasmids carrying a *ADE3* gene were transformed in to an *ade2-1ade3*Δ strain, and colonies containing test plasmids accumulate red pigment, whereas colonies lack the plasmids are white (Hogan and Koshland, 1992) (Figure 20A). As controls, we assayed *cdc6-1* and *cdc9-1*, encoding for a DNA replication initiation

factor and a DNA ligase respectively, for plasmid loss phenotype. Consistent with the above logic, the plasmid loss defect of *cdc6-1* is suppressed to near wild type level when multiple origins are incorporated into the test plasmid. However, the plasmid loss defect in *cdc9-1* remains six fold higher than the wild type using either a single origin or multiple origin plasmid (Figure 20B). Similar to *mcm2-1* (Sinha et al., 1986) and *chaos3* (Shima et al., 2007), *mcm2DENQ* has a plasmid loss rate 10 fold higher rate than wild type (Figure 20A and B). These results are consistent with the reduced G1 origin association of mcm2DENQp when assayed with Mcm2 specific antibodies (Figure 17A). Furthermore, overexpression of mcm2DENQp does not rescue the plasmid loss phenotype, indicating that mcm2DENQp is not limiting.

Defective SCC (as observed in DRC mutants (Warren et al., 2004; Xu et al., 2004)) should also cause defective plasmid segregation. However, initiation and SCC defects are distinguishable: initiation defects cause plasmid loss (1:0 segregation), whereas SCC defects cause plasmid mis-segregation (2:0 segregation). SCC can be assayed by integrating a lac operator array that tightly binds an expressed GFP-laci fusion protein into a test chromosome (Figure 20C) (Straight et al., 1996). Following G2/M arrest, the number of GFP foci/cell is determined: haploid cells with a single focus represent closely paired sister chromatids with normal cohesion, while two distinct foci/cell represent loss of SCC (Michaelis et al., 1997). All three *mcm* mutants demonstrate a loss of SCC that is ~4-7 fold higher than that observed in wildtype (Figure 20D). These values are similar to that previously observed for *mrc1*Δ (Figure 20D, (Xu et al., 2004)) and much less severe than the observed ~ 30% loss of SCC in cohesin mutant *eco1-1* (Figure 20D, (Michaelis et al., 1997)). Over-expression of *mcm2DENQ* did not

reduce the SCC defect, demonstrating that mcm2p is not limiting for this phenotype (Figure 20D).

To further define the relationship between the DRC and SCC, additional mutants were examined. The DRC cascade upstream of *mcm2DENQ* is needed as both *mrc1AQ* and *mec1*Δ demonstrate SCC defects (Figure 20D). In contrast, activation of the entire checkpoint cascade is unnecessary, as a *rad53-11* mutant demonstrates normal SCC, and a *rad53*Δ mutant has only ~ a 2 fold increase in SCC (Figure 20D). These results suggest that Mec1 kinase activity is required for SCC even in the absence of exogenous DNA damage and/or Rad53 activation.

A. Plasmid loss assay

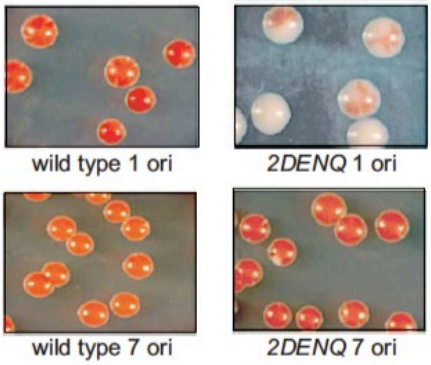

B. Plasmid loss

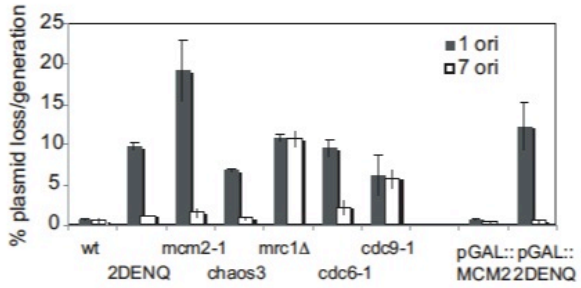

C. SCC assay

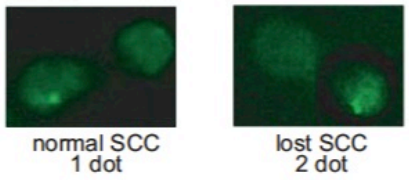

D. Sister chromatid cohesion

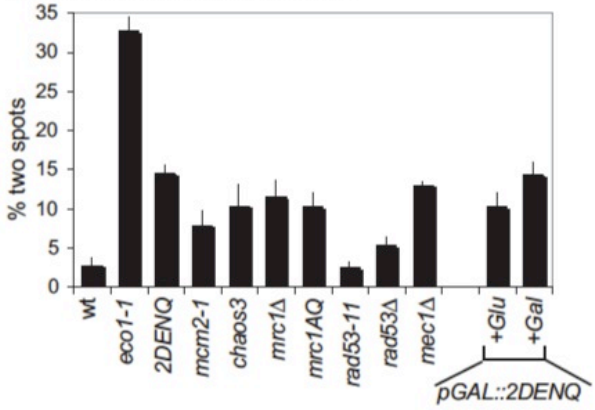

Figure 20. *mcm2DENQ* causes genomic instability

A) Plasmid segregation assay of wild type (UPY610) and *mcm2DENQ* (UPY535); red colonies contain the test plasmid (*LEU2*$^+$*ADE3*$^+$ plasmids carrying either one (pDK243) or seven (pDK368-1) origins), white colonies lack the test plasmid. B) Plasmid loss/generation. Both red and sectored colonies are treated as plasmid-containing. Conditional *cdc6-1* (UPY666-1) and *cdc9-1* (UPY667-1) strains were shifted to 37°C (non-permissive) for 3 hours prior to plating. C) SCC assay of wild type (UPY613) and *mrc1*Δ (UPY744). D) SCC was assayed in wild type (UPY613), *mcm2DENQ* (UPY606), *mcm2-1* (UPY814), *chaos3* (UPY835), *mrc1*Δ (UPY744), *mrc1AQ* (UPY822), *mec1*Δ (UPY846), *rad53*Δ (UPY848), and *eco1-1* (UPY831).

The high plasmid loss rate observed in *mcm2DENQ* contrasts with our genomic results, which show that early origin firing has wild type level efficiency. Because both DNA replication defect and plasmid segregation defect can result in high plasmid loss rate, we directly tested plasmid segregation. To directly visualize plasmid segregation, we modified the SCC assay to use a lac operator containing test plasmid (Megee and Koshland, 1999). To examine the products of individual mitotic events, the test strains contained a temperature sensitive *cdc15-2* allele; under nonpermissive conditions, *cdc15-2* causes telophase arrest with connected daughter cells and fully segregation chromosomes (Schweitzer and Philippsen, 1991). Cells were arrested in G1, released into S phase, arrested at telophase by shifting to 37°C, and the copy number of the ARS/CEN plasmid that each cell contains was cytologically assayed (see Methods).

Although individual cultures demonstrate considerable variability, close examination revealed good corresponence between the plasmid numbers in G1 and in telophase. Data from the wild type strain could provide a baseline for DNA replication or segregation defect, and is discussed first as an example. In the first culsture of wild type strain, we observed that ~78% of

the cells carry one plasmid during G1 and 22% carry two plasmids, visualized as GFP dots. During telophase arrest, ~71% of the cells carry two plasmids with each plasmid colocalizing to DAPI staining in separate buds (i.e. 1:1). ~19% of cells contains two GFP dots in the same bud but only one GFP dot in the opposite bud (i.e. 1:2) (Figure 21). These results make several points: 1) our assay is functional and the number of GFP dots observed in G1 is comparable to that of G2, 2) assuming only one round of DNA replication occurs, the 19% of 3-dot containing (1:2) cells in the telophase should arise from the 22% of cells that has 2-dot in G1, 3) the 3-dot (1:2) cells are a result of DNA replication defect, currently we do not know why the cells initially containing two plasmids are more prone to the DNA replication defect, and 4) the wild type cells do not exhibit any plasmid segregation defect.

Using this assay, we tested our mutant strains. We observed that the first culture of *mrc1*Δ is largely defective for DNA replication because many cells display 1:2 ratio (35%) for the GFP dots. On the other hand, the *mcm* mutants display elevated frequency of 1:0, 1:2 cells and 2:0 cells (Figure 21). To avoid an overestminate of plasmid segregation, we assume that both 1:0 and 1:2 arise from only putative replication defect. The cells display 2:0 ratio, however, can arise from both putative DNA replication and plasmid segregation defect. In principle, if the sum of frequencies of 2:2 and 1:2 in telophase is equal to the frequency of 2 dots in G1, then the 2:0 segregation likely results from a plasmid segregation defect (i.e. the 1 spot cells in G1 have successfully replicated but failed to segregate).

We statistically tested our data to determine whether the 2:0 results from missegregation. The possibility that both of the two plasmids in a G1 cell fails to replication would be equal to the square of the probability that a single plasmid fails to replication. The expected number of 2:0 cells can be calculated based on either the 1:0 or 1:2 frequencies and compared with our

observed number of cells. Chi square analysis between the expected and observed 2:0 frequency can be performed. We observed that in the *mcm* mutant strains, most but not all of differences between the observed and expected frequencies of the DNA replication defect are statistically significant (p-values for 0.053-0.49 are not statistically significant and p-values for 0.05 - <0.0001 are statistically significant) (Table 4). This demonstrates that the 2:0 ratio likely results from a plasmid segregation defect.

The relative contribution of DNA replication defect and plasmid segregation defect were also determined. We assume that the sum of the 1:0 and 1:2 ratios consist of non-replication, and estimate the frequency of non-segregation by substrating the observed frequencies of 2:0 by the expected frequencies. Using this approach, the wild type strain display <1% mis-segregation and the mutant strains display 2-18%. Overall, the plasmid loss phenotype observed can be account for by both DNA replication and plasmid segregation defect.

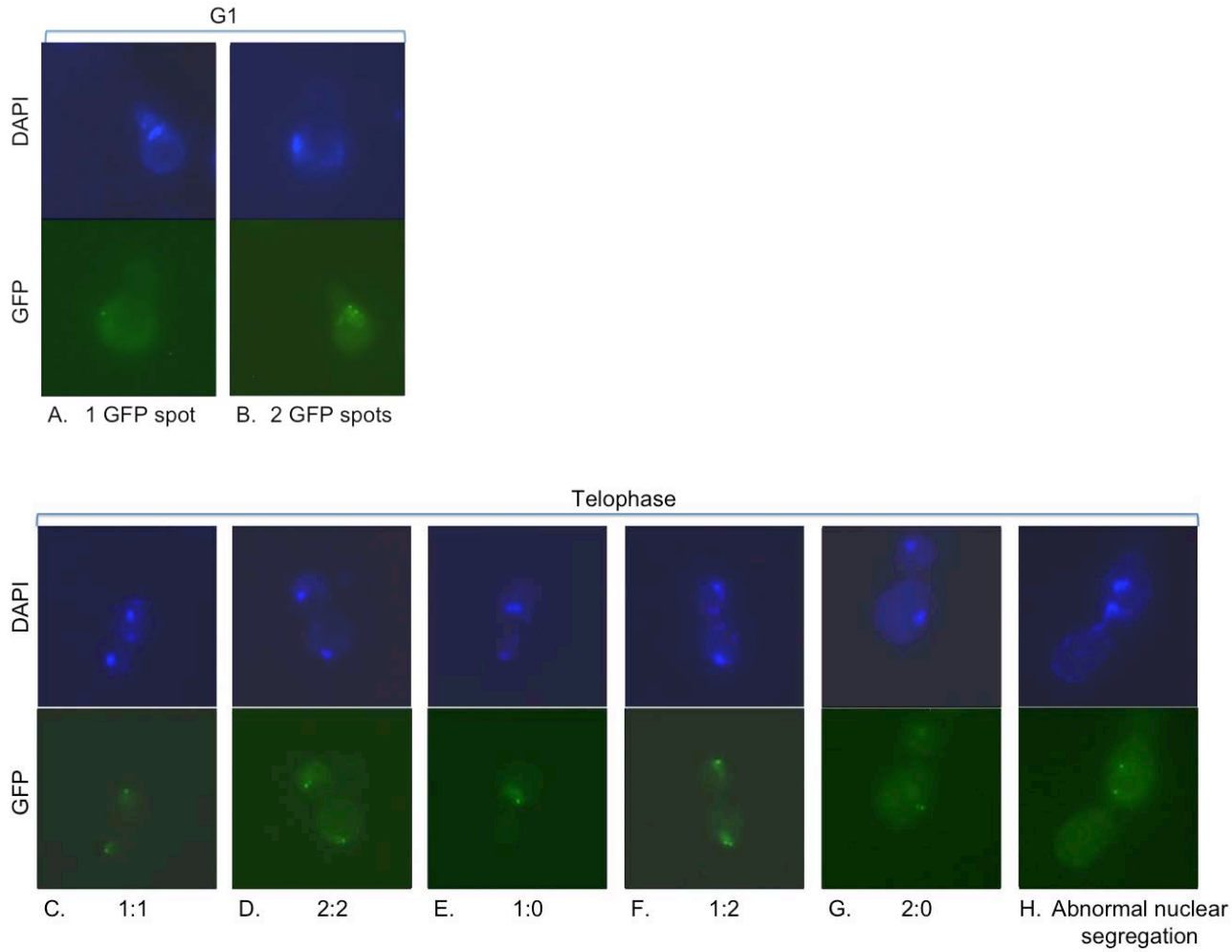

Figure 21. Cytological plasmid sgregation assay

Representative pictures of each type of plasmid segregation is shown. A) G1 cell with one plasmid B) G1 cell with two plasmids C-G) Telophase cells with 1:1, 2:2, 1:0, 1:2, and 2:0 plasmid segregation, respectively. F) Abnormal nuclear segregation (DAPI staining).

Table 4. Plasmid segregation

Observed frequencies of different categories of GFP spot is reported below. **N** indicates the total number of cells assayed in G1 or telophase.
A = the expected frequency of 2:0 based on the square of the 1:0 frequency, Chi square analysis of expected vs. observed 2:0 yielded the listed p value
B= the expected frequency of 2:0 based on the square of the 1:2 frequency, Chi square analysis of expected vs. observed 2:0 yielded the listed p value
C= the observed frequency of non-replication (frequency of 1:0 + frequency of 1:2)
D= minimum frequency of observed mis-segregation (observed frequency of 2:0 – expected frequency of 2:0 (using larger of the 2 estimated values).

Strain		G1 arrest			Telophase arrest						
		1 spot %	2 spot %	**N**	1:1 %	2:2 %	1:0 %	1:2 %	2:0 %	Nuclear mis-segregation	**N**
Wild type (UPY860)	Culture #1	78	22	**77**	71	10	0	19	0	0	**63**
	Culture #2	39	61	**59**	48	38	0	12	2	0	**42**
*mrc1*Δ (UPY863)	Culture #1	82	18	**50**	47	12	0	35	6	0	**51**
	Culture #2	59	41	**41**	47	25	6	9.5	3	9.5	**64**
2DENQ (UPY865)	Culture #1	100	0	**61**	40	0	47	0	13	0	**60**
	Culture #2	88	12	**50**	43	0	23	11	23	0	**70**
mcm2-1 (UPY868)	Culture #1	74	26	**61**	34	13	21	18	13	0	**38**
	Culture #2	80	20	**50**	34	3	29	14	6	14	**70**
chaos3 (UPY871)	Culture #1	93	7	**54**	33	2	30	7	14	14	**43**
	Culture #2	90	10	**67**	49	7	10	7	17	10	**41**

Table 4. Continued

Strain		Results			
		(1:0)[2]% p value[A]	**(1:2)[2]% p value[B]**	**No rep %[C]**	**No seg %[D]**
Wild type (UPY860)	Culture #1	**NA**	**3.6 (0.16)**	**19**	**0**
	Culture #2	**NA**	**1.4 (0.32)**	**12**	**<1**
*mrc1*Δ (UPY863)	Culture #1	**NA**	**12.25 (0.22)**	**35**	**<1**
	Culture #2	**0.36 (0.0002)**	**0.9 (0.11)**	**15.5**	**2**
2DENQ (UPY865)	Culture #1	**22 (0.053)**	**NA**	**47**	**?**
	Culture #2	**5.3 (<0.0001)**	**1.2 (<0.0001)**	**34**	**18**
mcm2-1 (UPY868)	Culture #1	**4.4 (0.011)**	**3.2 (0.0006)**	**39**	**9**
	Culture #2	**8.4 (0.49)**	**2 (0.018)**	**43**	**?**
chaos3 (UPY871)	Culture #1	**9 (0.27)**	**0.5 (<0.0001)**	**37**	**5**
	Culture #2	**1 (<0.0001)**	**0.5 (<0.0001)**	**17**	**16**

3.3.5 *mcm2DENQ* causes DSBs unrelated to replication fork collapse

mcm2DENQ demonstrates elevated cell death (Figure 12A and B), S and G2 phase cell cycle delays (Figure 14C), and Rad9p phosphorylation in the absence of exogenous DNA damage (Figure 16D). Other checkpoint alleles that have similar phenotypes (Kawabata et al., 2011; Lopes et al., 2001) often attributed to unstable replication forks that collapse and form DNA double strand breaks (DSBs) in S phase.

DSBs were assayed by immunofluorescence to γ-H2AX, a phosphorylated histone variant widely used as a DSB cytological marker (Nakamura, 2006). During unchallenged asynchronous growth, few wild type cells (<1%) demonstrate γ-H2AX foci; however MMS exposure substantially stimulates foci production (Figure 22A). In *mcm2DENQ*, ~25% of the cells contain γ-H2AX foci during unchallenged asynchronous growth (Figure 22A).

To examine DSBs during the cell cycle, synchronized cultures were analyzed (Figure 22C). DSBs occur in *mcm2DENQ* largely after S-phase and peak in mid G2 phase (Figure 22B and C). Upon mcm2DENQp over-expression, the abundance of DSBs formation remains similar; the delay in DSBs formation is likely due to the slightly slower growth in galactose media (Figure 22C). This demonstrates that DSBs formation does not result from limiting mcm2DENQp levels. The G2 phase appearance of γ-H2AX foci is not due to a time lag between DSB formation and γ-H2AX phosphorylation, as foci in *mrc1*Δ (known to cause S phase fork collapse (Szyjka et al., 2005) peak during S-phase (Figure 22C).

The origin of these DSBs was further delineated. If DSBs result from unstable replication forks, HU, a chemical that causes replication fork stress, should stimulate foci formation. This possibility in *mcm2DENQ* was ruled out, as HU incubation for up to 130 minutes completely blocks γ-H2AX foci formation whereas in *mrc1*Δ it stimulates and stabilizes

them (Figure 22C and D). This result strongly suggests that *mcm2DENQ* does not physically destabilize Mcm2-7. If in contrast DSBs depend upon mitosis, addition of the microtubule inhibitor nocodazole would prevent DSB formation. Nocodazole completely blocks foci formation in *mcm2DENQ*, whereas analogous treatment of *mrc1*Δ has no effect (Figure 22C and D). Although the magnitude of the effect is much smaller, both *mcm2-1* and *chaos3* make γ-H2AX foci that can be partially suppressed by nocodazole and HU (Figure 22E). Together, these data suggest that DSBs in these *mcm* mutants do not arise from unstable forks, but from attempted mitosis in the presence of incomplete DNA replication.

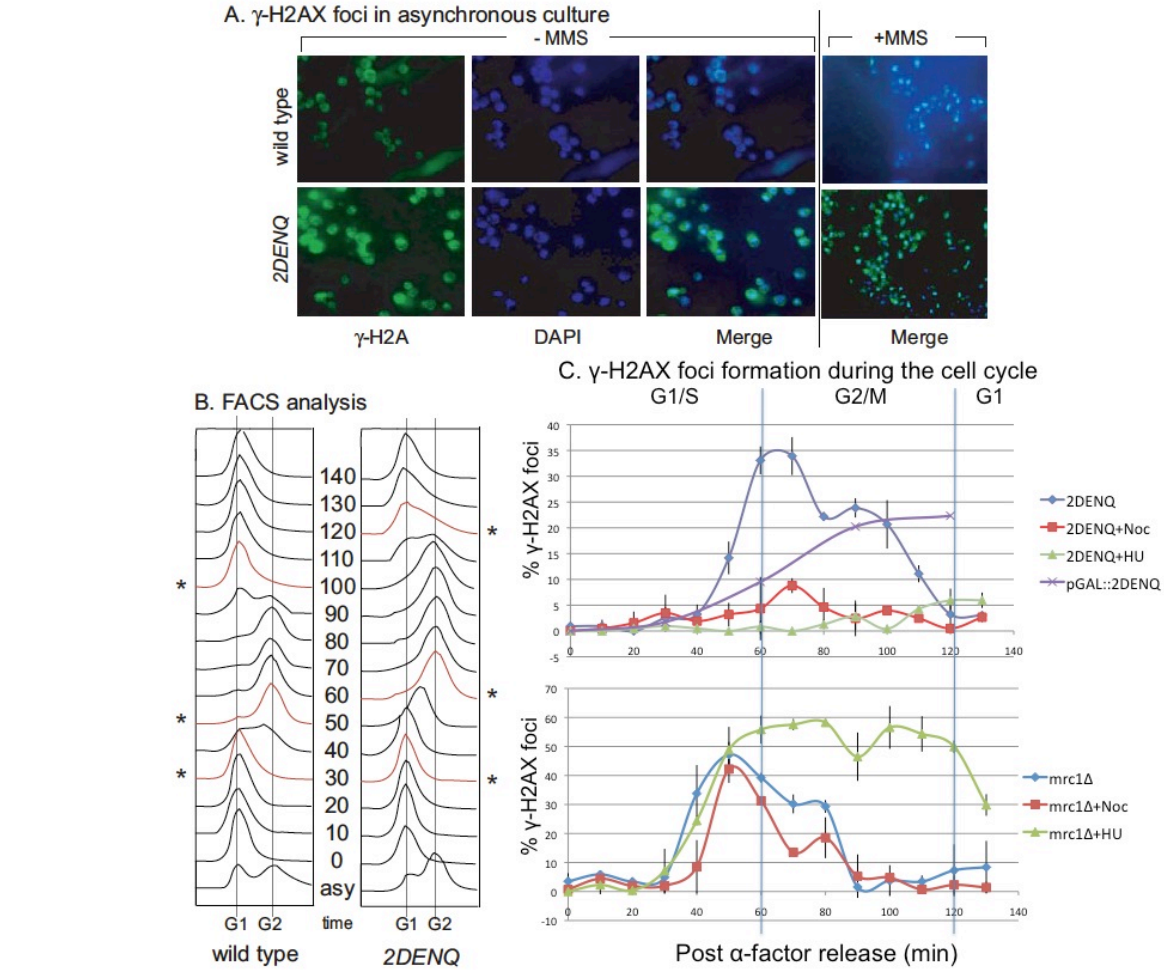
A. γ-H2AX foci in asynchronous culture
- MMS
+MMS
wild type
2DENQ
γ-H2A
DAPI
Merge
Merge
B. FACS analysis
140
130
120
110
100
90
80
70
60
50
40
30
20
10
0
asy
G1 G2
time
G1 G2
wild type
2DENQ
C. γ-H2AX foci formation during the cell cycle
G1/S
G2/M
G1
% γ-H2AX foci
2DENQ
2DENQ+Noc
2DENQ+HU
pGAL::2DENQ
mrc1Δ
mrc1Δ+Noc
mrc1Δ+HU
Post α-factor release (min)

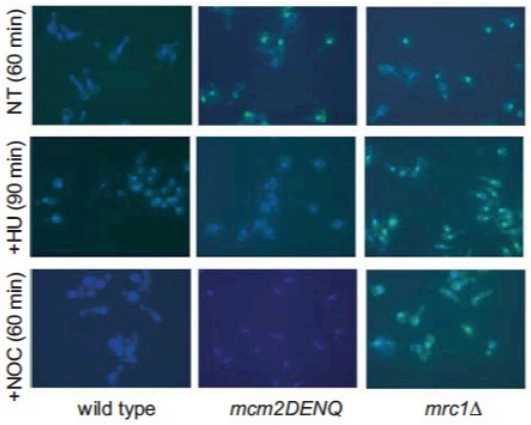
D. γ-H2AX foci
NT (60 min)
+HU (90 min)
+NOC (60 min)
wild type
mcm2DENQ
mrc1Δ

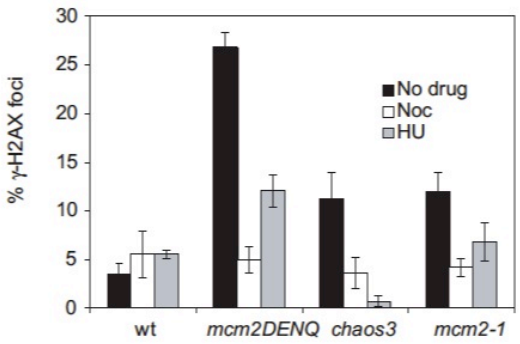
E. mcm2-1 and mcm4Chaos3 DSBs
% γ-H2AX foci
No drug
Noc
HU
wt
mcm2DENQ
chaos3
mcm2-1

Figure 22. DSB formation in replication mutants

A) Controls for γ-H2A(X) staining. Left: Asynchronous culture of either wild type (UPY464) or *mcm2DENQ* (UPY499) cells were processed and visualized for γ-H2A(X) immunofluorescence and DAPI staining (Supplemental Methods). Right: To validate that the γ -H2A(X) assay detects DSBs, asynchronous wild-type cells (UPY262) were treated with 0.01% MMS (to induce DSBs) in rich media for two hours, then processed for γ-H2A(X) immunofluorescence. Although in principle this assay should visualize discrete nuclear foci, the small size of the yeast nucleus and the extensive spreading of γ-H2A(X) neighboring a DSB site (~ 50 kb on each side of the break, (Kim et al., 2007)) generates nearly complete nuclear staining under our conditions. B) FACS analysis during unchallenged synchronized growth of wild type (UPY464) and *mcm2DENQ* (UPY499). This panel is the control for the DSB time courses in the absence of nocodazole shown in C). C) Immunofluorescence of γ-H2AX. Cultures of either *mcm2DENQ* (UPY499) or *mrc1*Δ (UPY713) were synchronized with α-factor, released into fresh YPD ± nocodazole as indicated, and samples processed for γ-H2AX immunofluorescence and FACS analysis as shown in A) and B). D) γ-H2AX immunofluorescence of wild type (UPY464), *mcm2DENQ* (UPY499) and *mrc1*Δ (UPY713) ± HU (90 minutes) or nocodazole (60 minutes) after α-factor release. E) γ-H2A(X) DSB foci formation in of *mcm* mutant strains is most prominent in *mcm2DENQ* cells. Asynchronous cultures of indicated strains (wildtype, UPY464; *mcm2DENQ*, UPY499; *mcm2-1*, UPY769; *mcm4Chaos3*, UPY638) were treated with no drug, 15μg/ml of nocodazole, or 0.2M hydroxyurea and incubated at 30°C for 2hr. Cells were then harvested and processed for γ-H2A(X) immunofluorescence as described in Materials and Methods.

Consistent with the DSB phenotype, *mcm2DENQ* causes gross chromosome rearrangements (GCRs). Using specially constructed strains, loss of a non-essential chromosome arm by simultaneous selection for loss of *URA3* and *CAN1* was measured; reconstruction experiments indicate that ~50% of the resulting $5FOA^r/CAN^r$ colonies correspond to translocations (Chen and Kolodner, 1999). Relative to the wild type rate (2.41×10^{-10}, Table 5) *mcm2DENQ* generates GCR at a 96-fold higher rate. This contrasts with *rad50*Δ, which was previously shown to have a 657-fold increase in GCR (Chen and Kolodner, 1999) (667 fold > wildtype, Table 5), and *mrc1*Δ that has a < 10-fold rate of GCR (Putnam et al., 2009) (9 fold > wild type, Table 5).

Table 5. Effect of *mcm2DENQ* mutation on the gross chromosomal rearrangement rate

Gross chromosomal rearrangement rates reported below are calculated using fluctuation test based on Lea and Coulson equation (Lea and Coulson, 1949) and previously published method (Motegi and Myung, 2007). Numbers within [ ] are the observed highest and lowest rates. ( ) indicates fold increase of GCR rate relative to wild type. At least three independent cultures were assayed in each strain.

Relevant genotype	Strain	Rate GCR (relative to wild type)
Wild type	UPY622	$2.41[1.91\text{-}8.93]\times10^{-10}$ (1X)
mcm2DENQ	UPY687	$2.31[1.09\text{-}4.00]\times10^{-8}$ (96X)
*mrc1*Δ	UPY698	$2.06[1.44\text{-}2.65]\times10^{-9}$ (9x)
*rad50*Δ	UPY694	$1.61[0.36\text{-}3.43]\times10^{-7}$ (667x)

3.4 DISCUSSION

We show for the first time that Mcm2-7 is coordinately involved in replication initiation, SCC, and DRC incidental to its role in DNA unwinding. With *mcm2DENQ*, these phenotypes do not result from a reduction in mcm2p levels or stability. Genomic analysis suggests that these alleles cause little or no loss in early origin efficiency. As *mcm2DENQ* specifically ablates the Walker B motif of Mcm2, reduced ATP hydrolysis at the Mcm6/2 active site is the likely mechanistic link among these three defects. One other *mcm2* allele (*mcm2-1*) shares these phenotypes, except for behaving wild type level repression of late origin firing during hydroxyurea arrest. This result indicates the ATP hydrolysis is directly involved in medating DRC and regulating DNA replication initiation during replication stress (discuss below). Our results demonstrate that genomic instability in *mcm* mutants not only arises as a passive consequence of reduced DNA replication, but by loss of active participation in checkpoint and mitotic functions. Our data reveal that *mcm* mutants display plasmid loss defect, and by following plasmid transmission within a single cell cycle using cytological method, we discovered that part of the plasmid loss phenotype is due to a plasmid segregation defect.

3.4.1 Reduced DNA replication versus loss of specific Mcm function

Although DNA replication mutants often have genomic instability, this phenotype usually represents aberrant DNA replication caused by reduced levels or stability of the mutant protein (Shimada et al., 2002). For example, in mouse embryonic fibroblasts, *mcm4Chaos3* yielded phenotypes broadly similar to ours (Kawabata et al., 2011); this allele in metazoans causes aberrant elongation by producing physically unstable Mcm2-7 complexes. This leads to

incomplete chromosome replication, G2 DSBs, and chromosome mis-segregation with a concomitant increase in translocations (Kawabata et al., 2011).

As the intra S-phase checkpoint requires active replication and functional forks (Tercero et al., 2003), initiation mutants can cause checkpoint defects through a reduction in the number of total replication forks rather than defective elongation *per se*. The optimal threshold level of replication may be quite high, as an estimated 30% reduction in the number of active replication forks in the *orc2-1* mutant correlates with a nearly complete loss of the intra-S checkpoint (Shimada et al., 2002). However, unlike *mcm2DENQ*, *orc2-1* is defective in both the DRC and the DDC.

The *mcm2DENQ* defects have a different basis: *in vivo* it has nearly normal Mcm2p expression and stability (Figure 13A and B). Overexpression does not reduce plasmid loss, SCC or DSB formation. *In vitro*, mcm2DENQp causes little or no decrease in Mcm2-7 stability (Figure 13C). Moreover, *mcm2DENQ* replication forks are stable, as HU, an agent that causes replication fork stress, inhibits DSB formation rather than stimulates it (Figure 22C). Unlike *orc2-1*, *mcm2DENQ* demonstrates near to wild type level of early origin efficiency. In addition, the *mcm2DENQ* SCC defect is difficult to explain as a consequence of reduced DNA replication, as our assay can only register a defect after replication through the lacI/GFP operator sites has occurred. Moreover, although *rad53*Δ causes defective DNA replication (Lopes et al., 2001), it has minimal effect on SCC (Figure 20D), indicating that the SCC defects have no obligatory connection to defective DNA replication.

3.4.2 Mcm2-7 mediates the DRC signaling pathway

We have carefully examined each component in the DRC signaling pathway. In the absence of exogenous stress, *mcm2DENQ* displays a phosphorylation in Rad9 and a slight increase in Rad53 phosphorylation. This is consistent with the DSBs observed in the absence of exogenous DNA damage (Figure 22C). As the S-phase checkpoint is partially redundant, we further assay Rad53 phosphorylation in *mcm2DENQ/rad9*Δ. We observed that *mcm2DENQ/rad9*Δ fails to undergo Rad53 activation upon exposure to MMS. Furthermore, Mrc1p is phosphorylated in *mcm2DENQ/rad9* upon MMS or HU exposure. The *mcm2-1/rad9*Δ double mutant similarly blocks Rad53 phosphoryaltion under the above conditions. These data indicate that Mcm6/2 active site mediates the DRC (more below), and functions downstream of *MRC1* in the checkpoint cascade.

Although Rad9 activation is observed in *mcm2DENQ* during MMS treatment, we consistently did not observe Rad9 activation upon hydroxyurea exposure. We reason that the *RAD9* pathway is less sensitive to hydroxyurea (Vialard et al., 1998) and the *MRC1* pathway is more readily activated upon hydroxyurea exposure (Alcasabas et al., 2001). Indeed, when *mrc1AQ*, which abolishes the *MRC1* pathway, is introduced in to the *mcm2DENQ* strain we were able to observe Rad9 phosphorylation in *mcm2DENQ* upon hydroxyurea treatment. Together, these data reinforce the notion that Mcm6/2 functions in the DRC, and is parallele to the *RAD9* pathway.

3.4.3 Possible role of Mcm2-7 ATP hydrolysis in DRC and SCC

The *mcm2DENQ* allele ablates conserved residues within the Walker B ATPase motif (Bochman et al., 2008). Interestingly, the *mcm2-1* allele is likely to disrupt the same active site. The analogous universally-conserved glutamate residue is located within the dimer interface of the *Sulfolobus* Mcm crystal structure (Barry et al., 2009) (and in a PYMOL model of the Mcm6/2 dimer interface, Figure 19). In archaea, mutations in this region (allosteric control loop, ACL) ablate allosteric interactions between ATPase active sites (Barry et al., 2009), and mutation of this specific residue (*mcmE182R*) yields a stable homohexamer with greatly reduced ATPase and helicase activity (Haugland et al., 2008).

The possible involvement of *chaos3* in Mcm ATP hydrolysis is less clear. This allele is a mutation of a conserved residue buried within the N terminus of Mcm4 five amino acids N-terminal to the ACL (Figure 23) and as such could conceivably disrupt allosteric interactions within the complex similar to *mcm2-1*. Although Mcm4 is not part of the Mcm6/2 active site, Mcm2-7 ATPase active sites are interdependent (Schwacha and Bell, 2001). As perturbations anywhere within the complex have the potential to globally disrupt ATP hydrolysis, the possibility that *chaos3* indirectly affects Mcm6/2 activity cannot be discounted. Alternatively, this mutation may affect hexamer-hexamer interaction (Kawabata et al., 2011). *chaos3* is located in close proximity to the zinc finger motif. In *M. thermoautotrophicum* Mcms, the zinc finger motif was reported to mediate interactions among the Mcms (Fletcher et al., 2003).

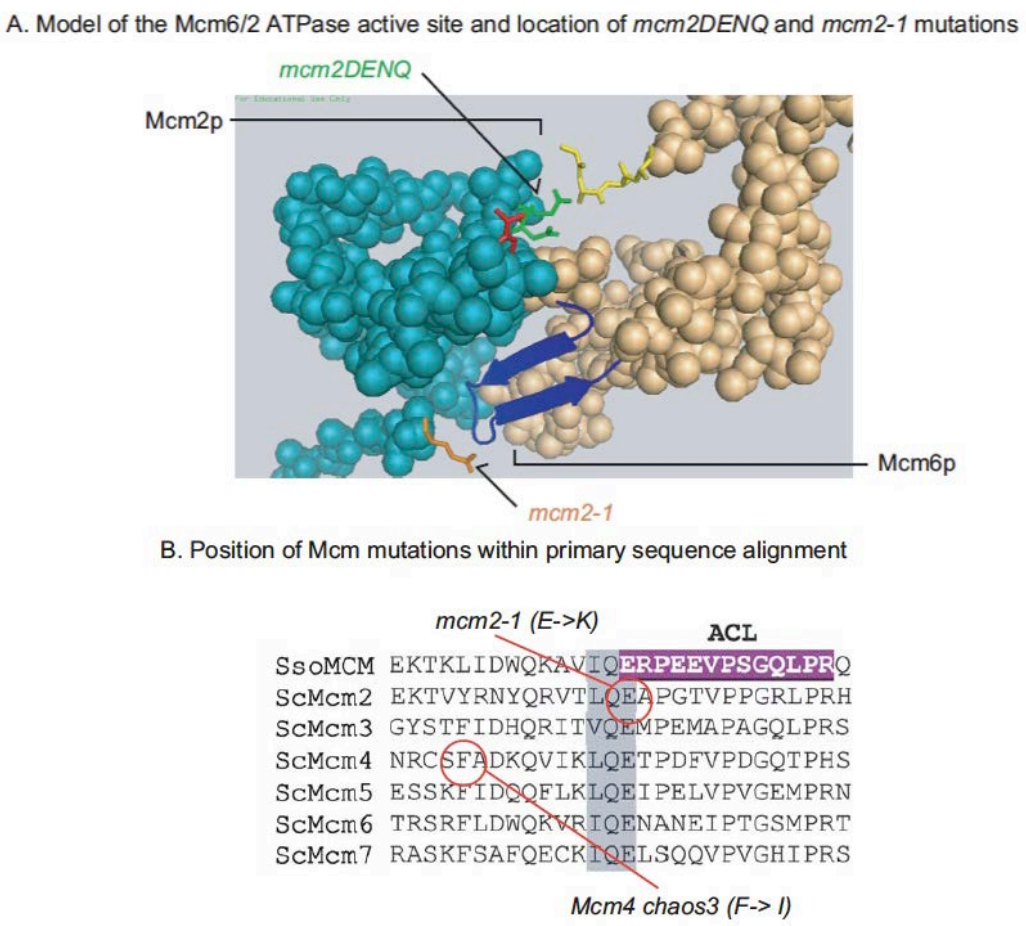

Figure 23. Mcm2-7 structural consequence of the *mcm* alleles

A) PYMOL visualization of the Mcm6/2 interface to localize the *mcm2-1* and *mcm2DENQ* amino acid changes (courtesy of Sriram Vijayraghavan). The yeast Mcm2 and Mcm6 protein structures were derived using the PHYRE2 fold recognition and homology modeling server (www.sbg.bio.ic.ac.uk/phyre2/), and were modeled on the *S.solfataricus* MCM crystal structure (PDB ID 2VL6, (Liu et al., 2008)) using PYMOL. Teal Blue = Mcm2; light orange = Mcm6; red sticks represent the Walker A conserved Lys in Mcm2; Green sticks represent the conserved Walker B Asp, Glu residues in Mcm2 that are mutated to Asn, Gln, and yellow sticks represent the arginine finger of Mcm6; blue hairpin represents the Mcm6 pre-sensor I hairpin, and orange stick represents the Mcm2 Glu 392 residue that is mutated to a lysine in *mcm2-1*. Various amino acid residues in both subunits have been removed to provide clarity. B) Multiple alignment of *Sulfolobus* MCM and the six yeast Mcms in the regions surrounding the ACL (Bochman and Schwacha, 2009). Positions of the *mcm2-1* and *mcm4Chaos3* mutations are indicated.

Our viable *mcm* alleles only incompletely disrupt DRC and SCC, as complete loss of either the intra-S phase checkpoint (Alcasabas et al., 2001) or SCC (Michaelis et al., 1997) is lethal. This partial phenotype may be attributed to branching redundancies within each pathway. Unlike *mrc1*Δ, two independent alleles, *mcm2DENQ* and *mcm6IL* (that ablates physical interaction between Mcm6 and Mrc1, (Komata et al., 2009)) have similar partial DRC phenotypes. These data suggest that Mrc1p has additional functions in the DRC besides its interaction with Mcm6p. Likewise, genetic analysis suggests that SCC can be achieved through several redundant means (Xu et al., 2007). Alternatively, the partial DRC and SCC phenotypes may reflect a defect in the regulation of these processes rather than a defect in the structural components of the pathway.

3.4.4 The basis of the DRC defect

mcm2DENQ and *mcm2-1* mutants both show a defect in the DRC; however, only the former initiates late origin firing prematurely (Figure 18B and C). This suggests that the derepression of late origin firing in *mcm2DENQ* may be independent of its DRC defect. Furthermore, the repression of late origin firing may specifically require the Mcm6/2 active site.

Our current data do not suggest fork uncoupling between Mcm localization and DNA synthesis. Although this has been previously shown in *mrc1*Δ mutants (Katou et al., 2003), we do not observe any uncoupling in *mcm2DENQ*, similar to a recent publication (De Piccoli et al., 2012). In our genomic analysis, Mcm2-7 bifurcates to the leading edge of BrdU incorporation and does not travel further (Figure 19B). Close examination of the data shows uncoupling at only a single origin, but not a global effect. As our ChIP-seq approach is more sensitive than the previous ChIP-chip approach, uncoupling is likely not the cause of a DRC defect. Furthermore,

in a second study where fork uncoupling was observed, closer examination revealed that Cdc45 enrichment signal was quite low, and perhaps the uncoupling seen was resulting from the scaling process. Therefore, it is possible that fork uncoupling cannot be observed at this level of analysis, and single molecule experiment with higher sensitivity may be needed to address this question.

3.4.5 Mcm2-7 is required for SCC and accurate chromosomal segregation

Our data show that *mcm* mutants are defective in SCC (Figure 20D). We currently do not know the basis responsible for the SCC defect. One possibility is that *mcm* mutants may be defective for cohesin loading, as previous studies in *Xenopus* has shown that ORC, Cdc6, Cdt1, and Mcm2-7 are required for cohesin loading during G1 (Takahashi et al., 2004). Although studies in *S. cerevisiae* show that Cdc6 is dispensible for cohesin recruitment (Uhlmann and Nasmyth, 1998), it is not known whether other components of the pre-RC (i.e. Mcm2-7) are similarly dispensible. Alternatively, Mcm2-7 may be required for SCC establishment during DNA replication elongation. A recent study shows that Mcm2-7 physically interacts with cohesin (Guillou et al., 2010). It is possible that fork progression of the *mcm2DENQ* mutant is impeded by cohesins.

As a consequence of defective SCC, we observed missegregation of chromosomal segregation in the *mcm* mutants (Figure 21). We followed the transmission of plasmids cytologically within a single cell cycle from G1 phase to telophase. In our analysis, we have made the assumption the DNA replication occurs only once under these experimental conditions. We could not disprove some other interpretations for the GFP dot segregation. For example, during telophase arrest, 1:2 segregation could also be interpreted as both replication initiation

defect and chromosomal segregation defect, if the two dots within the same bud represent two plasmids arise from a common parent. Because we are adopting a conservative approach and only scoring these GFP dot patterns as DNA replication initiation defect only, our results may underrepresent the actual missegregation events being scored. Furthermore, in the occurrence of plasmid missegregation, it will only be observed at 50% of the time. Therefore, the actual plasmid missegregation rate may be even higher. Our results indicate that a plasmid loss defect does not always reflect only a DNA replication initiation defect (Table 4). As we have shown, a plasmid segregation defect would also be observed as a plasmid loss defect.

Between our plasmid loss assay and genomic experiment, an apparent discrepancy lies within the G1 loading defect. Our genomic approach suggests that a subtle but global Mcm loading defect is observed in *mcm2DENQ*, and this may be due to insufficient epitope recognition by the Mcm2p antibody (Figure 17A). However, our plasmid loss assay shows a ~10-fold higher loss rate in *mcm2DENQ* relative to wild type (Figure 20B). One likely reason to account for this difference is that this particular origin assayed in the plasmid loss assay is slightly less efficient compared to the others. Another possibility is that the genomic experiment is not sensitive enough to detect subtle changes. Or, the α-factor arrest treatment may allow additional time for pre-RC formation to compensate any potential defect in chromosome binding.

3.4.6 Plasmid loss reflects a defect in replication initiation and chromosomal segregation, but not insufficient protein expression

Previous studies have suggested a dosage effect on minichromosome maintenance, in which a diploid strain carrying only one copy of the *MCM* gene displays a higher rate of plasmid loss (Lei M, 1996). To determine whether the plasmid loss defect observed in *mcm2DENQ* is due to

a dosage effect, we overexpressed mcm2DENQp under galactose promoter. Our result shows that overexpression of mcm2DENQp does not suppress plasmid loss (Figure 20B). This indicates that the plasmid loss defect does not result from insufficient protein expression.

3.4.7 Unequal roles of Mcm2-7 subunits

Our simultaneous examination of three *mcm* mutants reveals that each Mcm subunit is not functionally equal. This is consistent with previous studies that show functional distinction among subunits (Bochman et al., 2008; Schwacha and Bell, 2001). Our studies show that the ATP hydrolysis of the Mcm6/2 active site is specifically required for mediating the DRC. Howeer, we do not find any evidence that Mcm4 has a role in this process.

All three alleles are required for SCC. Previous studies have shown that the S-phase checkpoint is required for SCC establishment in G2 during DNA damage (Ström et al., 2007; Ünal et al., 2007). We show that *MCM2* is required for SCC, perhaps this is because *MCM2* actively participates in the DRC (Figure 20D). Furthermore, we show that without exogenous stress, only *MEC1* but not *RAD53* is required for SCC (Figure 20D). Our studies provide evidence that the S-phase checkpoint subcircuit is utilized to regulate SCC during normal cell cycles. The involvement of *MCM4* in SCC may arise from a different basis. Finally, our data show that all three subunits/active site are similarly required for DNA replication initiation and plasmid segregation, as a consequence of defective SCC.

3.4.8 Model for Mcm2-7 involvement in initiation, the DRC, and SCC

We propose that the commonality among these processes is regulation of the Mcm2/5 gate. Initiation likely requires gate opening to load Mcm2-7 onto DNA and gate closure during subsequent helicase activation (Costa et al., 2011). Likewise, the DRC blocks elongation upon exposure to DNA damage, and opening the Mcm2/5 gate would be a plausible mechanism. Although less is known about the relationship between SCC and DNA replication, transient regulation of fork progression (putatively through Mcm2-7) may be required to provide a temporal window for cohesion establishment.

If true, *mcm2DENQ* fork progression should be unregulated, and possibly result in uncoupling from DNA polymerase during replication stress in HU. Our efforts to test this using a genomic approach have been unsuccessful. Although previous lower-resolution studies demonstrating uncoupling in *mrc1*Δ (Crabbe et al., 2010; Katou et al., 2003), a recent study suggests that replisome remains intact in checkpoint mutants *rad53*Δ and *mec1*Δ (De Piccoli et al., 2012). Although 2D electrophoresis has been used to study replication forks, it provides information on fork stability rather than dynamics (Lopes et al., 2001). A true test of polymerase uncoupling will require development of sophisticated biochemical or single molecule approaches (e.g., (Fu et al., 2011)).

In vitro, mcm2DENQp biases Mcm2-7 into the gate-closed (active) conformation (Bochman and Schwacha, 2010), suggesting that ATP hydrolysis at this site may regulate gate conformation. This putative regulation may not involve Rad53p, as *rad53*Δ has little effect on SCC. This potential DRC "sub-circuit" may be advantageously used to quickly and transiently modulate progression at individual forks. Rad53p activation would then be saved for severe

problems requiring a global response. This may explain why *mec1* alleles are more deleterious than *rad53* alleles (Segurado and Diffley, 2008).

Mrc1p may regulate Mcm6/2 ATP hydrolysis (Figure 25). It physically interacts with the C-terminus of Mcm6p and loss of this interaction (*mcm6IL*) causes a DRC defect resembling *mcm2DENQ* (Komata et al., 2009). Interestingly, a translational fusion between Mcm6ILp and Mrc1p complements *mcm6IL* (Komata et al., 2009), but not *mcm2DENQ* (Figure 24), suggesting that the primary mcm2DENQ defect is not lost association with Mrc1. As phosphorylation of Mrc1p is necessary for Rad53p recruitment and activation (Osborn and Elledge, 2003), we suggest that Mrc1/Mcm2-7 interactions are likely involved in this step.

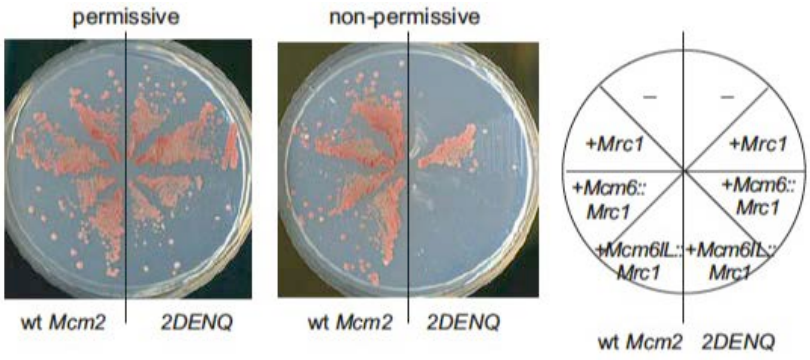

Figure 24. *Mcm6::Mrc1* fusion does not suppress *2DENQ*/*mrc1*Δ lethality

Synthetic lethality between *mcm2DENQ* and the *MCM6::MRC1* and *mcm6IL::MRC1* fusion constructs. Both fusions are reported to be functionally active for the replication checkpoint and Mcm6 (Komata et al., 2009), the *mcm6IL* mutation removes the Mcm6-binding site for MRC1. All strains shown contain deletions in *Rad9*, *Sml1*, and *Mcm2*, with viability being maintained by a plasmid containing the wild-type *MCM2* gene (pUP191). The indicated strains contain either the *MCM6-MRC1* or *MCM6IL-MRC1* fusion constructs integrated into and replacing the wild-type *MCM6* gene, as well as TRP1+ tester plasmids encoding either *MCM2* (pUP197) or *mcm2DENQ*

(pUP197). Plate on the left was grown on media lacking uracil (csm-URA, Permissive) to select for the wild-type MCM2 plasmids, while media on the right contains 5-FOA and selects against the URA plasmid (Non-permissive). Under the non-permissive condition, either pUP197 (*MCM2*) or pUP199 (*mcm2DENQ*) provide MCM2 function. Note that the apparently synthetic lethality between *MCM6-MRC1* and *mcm2DENQ* appears to be dominant as these strains contain the wild-type *MRC1* gene.

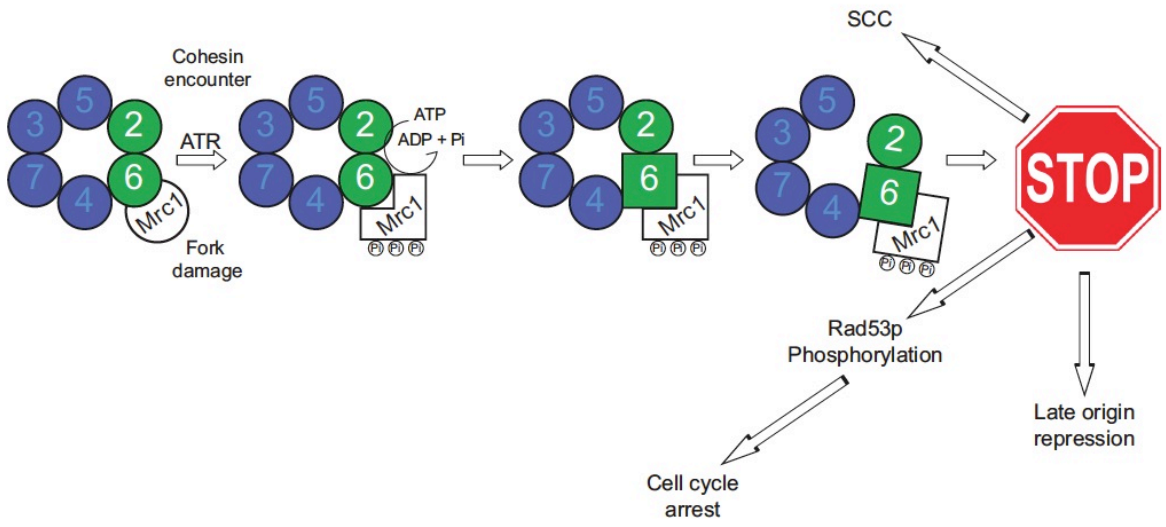

Figure 25. ATP hydrolysis within the Mcm6/2 ATPase active site coordinates DRC and SCC with DNA replication

Model of Mcm2-7 involvement in the DRC and SCC. See text for details.

4.0 DISCUSSION, CONCLUSIONS, AND FUTURE CONSIDERATIONS

4.1 MCM2-7 HAS REGULATORY FUNCTIONS BEYOND DNA UNWINDING

Studies from the past to present have consistently shown that Mcm4/6/7 subunits function as the catalytic core of the Mcm2-7 helicase, and Mcm2/3/5 subunits serve regulatory roles (reviewed in (Bochman and Schwacha, 2009)). *In vitro* work has provided biochemical and physical evidence that Mcm2 and Mcm5 form a structural discontinuity in the Mcm2-7 ring (Bochman and Schwacha, 2008; Costa et al., 2011). One potential function of the gate is to load Mcm2-7 onto DNA. However, no *in vivo* work has been conducted extensively to uncover the role of the ATPase active sites that are not involved in robust catalytic activities. My studies provide the first evidence that the regulatory subunits are important for both DRC and SCC simultaneously in addition to DNA replication initiation.

4.1.1 The Mcm6/2 active site is required for DRC signaling

Mcm2-7 has been proposed as a potential target for the DRC. *In vitro* studies have shown that human Mcm2-7 is phosphorylated by checkpoint kinases ATM and ATR (Cortez et al., 2004). These studies suggested that during DNA damage S-phase checkpoint is activated, which then targets Mcm2-7. However, there is no *in vivo* evidence to support this view. In budding yeast, Mec1 phosphorylates Mcm2-7 to prime Mcm2-7 for Cdc7 kinase phosphorylation. However,

this phosphoryaltion is required during DNA replication initiation for modulating origin firing (Randell et al., 2010). These priming phosphorylation events are not likely required for the checkpoint response, as priming site mutants are not sensitive to hydroxyurea (Randell et al., 2010). In budding yeast, *mcm6IL* mutation that abolishes the physical interaction of Mcm6 with Mrc1 abrogates Rad53 activation (Komata et al., 2009). These studies suggest that checkpoint activation requires localization of Mrc1 to the Mcm2-7 complex. Howeer, it remains unclear whether Mcm2-7 is mediating or getting targed by the DRC cascade.

Contrary to evidence suggesting that Mcm2-7 is a downstream target of DRC, We show that in fact, Mcm2-7 is an integral part of the DRC cascade. Analyses of both ATPase active site mutants (Walker B allele of *MCM2*) and the *mcm2-1* mutant (*mcm2-1* mutation is in close proximity to the Mcm6/2 active site) demonstrate that ATP hydrolysis at the Mcm6/2 active site is directly involved in the DRC signaling (**Chapter 3**). Similar to known DRC mutant such as *mrc1*Δ, *mcm2DENQ* and *mcm2-1* fail to arrest, are extremely sensitive, and result in a high lethality upon exposure to DNA damaging agents in the absence of the *Rad9* back up pathway. Furthermore, *mcm2DENQ*, but not *mcm2-1*, displays a premature late origin firing phenotype similar to *mrc1AQ*. A direct examination of the DRC pathway revealed that both the *mcm2DENQ/rad9*Δ and *mcm2-1/rad9*Δ double mutants largely block downstream effector checkpoint kinase activation in the presence of DNA damaging agent. On the other hand, *mcm2DENQ/mrc1AQ* does not show any synergistic sensitivity to DNA damaging drugs. However, *mcm4chaos3/rad9*Δ has wild type levels of Rad53 activation. Therefore, these results are consistent with the notion that ATP hydrolysis at the Mcm6/2 active site mediates the DRC and is an integral part of the surveillance system that ensures genome integrity.

4.1.2 Mcm2-7 is required for sister chromatid cohesion

While many DRC mutants demonstrate an intermediate loss of SCC (Warren et al., 2004; Xu et al., 2004), the involvement of Mcm2-7 in maintaining SCC has not been examined before. We show here for the first time that the *mcm* mutants are defective for SCC (**Chapter 3**). The intermediate levels of SCC defect are consistent with the notion that these *mcm* mutants are viable. In addition, these results also suggest that SCC is maintained via redundant pathways, as previously shown (Xu et al., 2007). Therefore, our results suggest that the Mcm2-7 complex, as part of the DRC, is required for SCC, and also provide evidence for a direct connection between DNA replication and SCC. Currently, our assay does not distinguish whether the SCC defect arise from cohesin loading or SCC establishment.

4.1.3 Mcm2-7 regulates chromosomal segregation

Regulation of DNA replication is essential to ensure that the entire genome is replicated once and only once during each cell cycle (Remus and Diffley, 2009). All *mcm* mutants examined display an initiation defect rather than an elongation defect as defined by the plasmid loss assay (**Chapter 3**). However, using a genomic approach, pre-RC formation and replication origin firing efficiency does not seem to differ significantly between wild type and *mcm* mutants. Since a plasmid loss defect can arise from either an initiation defect or a segregation defect, direct assay of plasmid transmission is required to distinguish between these two possibilities. Using a plasmid carrying Lac operator array that can be bound by GFP-tagged Lac repressor, we observed that *mcm* mutant strains fail to segregate and replicate their plasmids (**Chapter 3**).

Thus, the plasmid loss defect observed in *mcm* mutants is partially due to missegregation as a consequence of the SCC defect.

4.2 MCM2-7 IS THE MECHANISTIC LINK THAT COORDINATES DNA REPLICATION INITIATION, DRC AND SCC

4.2.1 Mcm2-7 is regulated via the Mcm2/5 gate

The coordination between initiation, DRC and SCC is likely achieved through the Mcm2/5 gate of Mcm2-7. *In vitro* studies show that neighboring ATPase active site of the Mcm2/5 gate, the Mcm6/2 site, modulates the regulation of Mcm2/5 gate (Bochman and Schwacha, 2010). Mutational analysis shows that the *mcm2DENQ* mutation favors a closed-ring conformation. This is also consistent with the allosteric regulation of Mcm complex (Schwacha and Bell, 2001). *In vivo*, *mcm2DENQ* and *mcm2-1* mutants are defective for DRC and SCC as discussed above (**Chapter 3**). It is likely that in response to DNA damage or upon encountering cohesins, the Mcm6/2 active site modulates gate opening and gate closure, thereby controlling the helicase activity of Mcm2/7 complex.

The Mcm6/2 gate may also be regulated upon the binding of accessory factors. Nucleotide hydrolases are often regulated by accessory factors. One well studied example is the regulation of GTPase by GAP and GEF (Scheffzek and Ahmadian, 2005). Mrc1 is a potential regulator, as the interaction between Mrc1 and Mcm6 is required to modulate the DRC response (Komata et al., 2009). In addition to that, *MRC1* also genetically interact with *MCM2* (**Chapter 3**). Since Mcm6/2 active site mediates the DRC and SCC, we propose that Mrc1 modulates the

activity of Mcm6/2 active site during DNA damage and SCC (Figure 25). Furthermore, this modulation could regulate the Mcm2/5 gate.

4.2.2 The mutual dependencies among initiation, DRC and SCC

Emerging evidences have suggested the coordinations between DNA replication, DRC and SCC (Sjögren and Ström, 2010). Ctf18, which is a clamp loader at the replication fork, is required for SCC, DRC and replication initiation (Crabbe et al., 2010; Hanna et al., 2001; Ma et al., 2010). Numerous other examples of genes involved in multiple cellular processes are shown in Table 1. However, this interconnection has not been established and simultaneously tested. Here, we show that a subcircuit of the replication checkpoint signaling pathway—*MEC1*, *MRC1*, and *MCM2-7*, is required to maintain SCC in the absence of DNA damage (**Chapter 3**). Furthermore, defective initiation observed in *mcm* mutants may cause an SCC defect. It has previously been shown in *Xenopus* that pre-RC is required for cohesin loading (Takahashi et al., 2004). We show that the checkpoint defect is not due to insufficient origin firing or unstable forks as reported for the *orc2-1* mutant (Shimada et al., 2002). Rather, these defects arise from a specific block of the Mcm6/2 ATPase active site (**Chapter 3**). Overall, our simultaneous examination of DNA replication, DRC and SCC shows that these processes must be tightly regulated and coordinated through a common target, Mcm2-7.

4.2.3 DRC, SCC and initiation may be mechanistically linked to leading strand and lagging strand synthesis

Leading strand and lagging strand synthesis are tightly coupled and coordinated processes that required the action of the replicative helicase, DNA polymerase and primase. These molecular motors each needs to coordinate with one another's enzymatic activities to ensure the integrity of the fork. In the T7 replication system, it has been shown that the helicase improves the priming activity of the primase by physical interaction (Frick and Richardson, 2001). Conversely, the primase could improve the processivity of the helicase. Furthermore, the coupling between the replicative helicase and DNA polymerase is required for efficient replication and high processivity (Dong et al., 1996; Stano et al., 2005). However, the coordination involves several issues that the replisome has to overcome. First, primer synthesis occurs at a much slower rate than the leading strand synthesis. To address this question, it has been shown by single molecule studies in a simpler replication system (i.e. phage T7) that primer synthesis may act as a molecular brake to pause the DNA unwinding and leading strand synthesis (Lee et al., 2006). More recently, studies of the T4 and T7 replisome show that priming loops are formed during primer synthesis, independent of leading strand and lagging strand synthesis (Manosas et al., 2009; Pandey et al., 2009). This allows primer synthesis to occur ahead of time so that the speed of lagging strand synthesis can catch up with that of the leading strand. Second, the lagging strand DNA polymerases are constantly recycling, therefore the cells must modulate the speed of leading strand and lagging strand synthesis by some means to ensure that the fork is not ripped apart. It has been shown that the lagging strand polymerase synthesizes at a much faster rate than the leading strand polymerase (Pandey et al., 2009). Despite advances in viral systems such as T4 or T7, little is known about how replication forks are coordinated in eukaryotes.

We propose that initiation, DRC, and SCC are commonly coordinated with DNA synthesis and DNA unwinding. Many proteins that link the replicative helicase and DNA polymerase are involved in DRC or SCC. For example, Mrc1, that required for DRC, links Mcm2-7 and DNA polymerase ε (Lou et al., 2008). Similarly, Ctf4 that is required for SCC links Mcm2-7 and polymerase α (Gambus et al., 2009). It is likely that these factors promote the tight coupling between DNA synthesis and unwinding.

4.3 FUTURE CONSIDERATIONS

4.3.1 Misregulation of Mcm2-7 leads to genomic instability

Misregulation of Mcm2-7 complex has been shown to result in tumorigenesis. *mcm4Chaos3* mutation that was originally isolated from a mouse genetic screen causes missegregation, chromosomal translocation and tumorigensis in mice (Kawabata et al., 2011; Li et al., 2009). Recently, it has been shown that overexpression of Mcm7 is cancer causing (Toyokawa et al., 2011). Here, we provide evidence that the *mcm2DENQ* mutation causes gross chromosomal rearrangements that are ~100 fold higher than wild type (**Chapter 3**). Furthermore, all *mcm* mutants are defective for SCC and chromosomal segregation. These genomic instabilities are characteristics of cancer. Future work is required to further understand the basis of genomic instabilities.

4.3.2 Coordination between DNA replication fork progression and SCC

Replication fork progression can be regulated by post-translational modification of cohesins (Terret et al., 2009). In this study, we have not tested replication fork progression upon encountering cohesins. To delineate the relationship between replication forks and cohesins, various aspects of replication fork progression (i.e. replication fork progression rate, fork stability, and the distance forks travel) must be examined in the context of conditional mutant alleles of cohesins and Mcms. A detail study of these parameters will provide insight into the regulation of Mcm2-7 during SCC establishment.

4.3.3 How did ATPase active sites evolve into functions beyond DNA replication?

One feature that makes the eukaryotic replicative helicase distinct from the other helicases is its heterohexameric composition, in contrast to the homohexameric Mcm complexes in most archaea. It is likely that over the course of evolution, duplication and divergence have taken place from the single archaeal Mcm. Indeed, comparative genomic studies have demonstrated that the Mcms arose from several gene duplication events before the last common ancestor of the eukaryotes (Liu et al., 2009). This divergence occurs early on during the split of Archaea and Eukarya and is highly conserved because all the eukaryotic genomes examined to date carry each of the *MCM2-7* genes (Liu et al., 2009). Apart from the Mcm proteins, many other replication factors in archaea appear to exist in a simpler form. For example, many archaea only have a single Orc to perform the function of Orc1-6 and Cdc6 in eukaryotes (Lundgren and Bernander, 2005). Similarly, most archaea contains a single GINS protein (Yoshimochi et al., 2008).

Why and how did the single Mcm protein evolve into six distinct copies? The archaea Mcm complex has *in vitro* helicase activity and is required for DNA unwinding. It is likely that the eukaryotic Mcm2-7 complex has diversified from this single copy of archaea Mcm. Because Mcm4 and Mcm7 are required for robust helicase activity and are the most closely related to the archaeal Mcm, they are likely to be the primordial Mcm complex (reviewed in (Bochman and Schwacha, 2009). However, how did Mcm2,3,5 come about? The replication system in archaea is much simpler than the eukarya. As mentioned above, various replication factors exist in a simpler form. Furthermore, archaea also lacks many initiator proteins that eukaryotes have, such as Cdt1, Mcm10, Dpb11, Sld2, and Sld3 (Bryant and Aves, 2011). Therefore, eukaryotes have much higher levels of regulation during DNA replication. It is likely that Mcm2,3,5 and their corresponding functions in S-phase checkpoint and sister chromatid cohesion evolved in order to ensure DNA replication is tightly coupled to these cellular processes during cell cycle progression. Furthermore, the high conservation and no evidence of gene loss over the course of evolution suggests that these functions are essential for the survival of eukaryotes.

APPENDIX

P-VALUES FOR ORIGIN USAGE

The following p-values apply to box-plot shown in Figure 18D. Among each subset of origins, each mutant strain is compared against wild type and the p-values were determined by 1-tailed Wilcoxon rank sum test. A p-value <0.05 indicates that the difference between these strains is statistically significant.

All early origins

WT and *2DENQ*	W = 18903	p-value = 0.53085011337429
WT and mrc1Δ	W = 21619	p-value = 0.994398847050813
WT and *mcm2-1*	W = 16627	p-value = 0.0236748832295089
WT and *chaos3*	W = 16918	p-value = 0.0427432341751403

All late origins

WT and *2DENQ*	W = 2923	p-value = 1.82353136141217e-14
WT and *mrc1*Δ	W = 429	p-value = 1.48217393749816e-35
WT and *mcm2-1*	W = 7040	p-value = 0.647490251736635
WT and *chaos3*	W = 7624	p-value = 0.934029145063178

Late origins that activate in *mrc1*Δ and not *mrc1AQ*

WT and *2DENQ*	W = 10472	p-value = 0.398540204945712
WT and *mrc1*Δ	W = 1065	p-value = 1.21337094014016e-40
WT and *mcm2-1*	W = 17541	p-value = 1
WT and *chaos3*	W = 17435	p-value = 1

BIBLIOGRAPHY

Aggarwal, B.D., and Calvi, B.R. (2004). Chromatin regulates origin activity in Drosophila follicle cells. Nature 430, 372-376.

Alani, E., Thresher, R., Griffith, J., and Kolodner, R.D. (2002). Characterization of DNA-binding and strand-exchange stimulation properties of y-RPA, a yeast single-strand-DNA-binding-protein. J Mol Biol 227, 54-71

Alcasabas, A.A., Osborn, A.J., Bachant, J., Hu, F., Werler, P.J., Bousset, K., Furuya, K., Diffley, J.F., Carr, A.M., and Elledge, S.J. (2001). Mrc1 transduces signals of DNA replication stress to activate Rad53. Nat Cell Biol 3, 958-965.

Allen, J.B., Zhou, Z., Siede, W., Friedberg, E.C., and Elledge, S.J. (1994). The SAD1/RAD53 protein kinase controls multiple checkpoints and DNA damage-induced transcription in yeast. Genes Dev 8, 2401-2415.

Aparicio, O.M., Weinstein, D.M., and Bell, S.P. (1997). Components and dynamics of DNA replication complexes in S. cerevisiae: redistribution of MCM proteins and Cdc45p during S phase. Cell 91, 59-69.

Araki, H. (2011). Initiation of chromosomal DNA replication in eukaryotic cells; contribution of yeast genetics to the elucidation. Genes Genet Syst 86, 141-149.

Arumugam, P., Gruber, S., Tanaka, K., Haering, C.H., Mechtler, K., and Nasmyth, K. (2003). ATP Hydrolysis Is Required for Cohesin's Association with Chromosomes. Curr Biol 13, 1941-1953.

Bae, B., Chen, Y.H., Costa, A., Onesti, S., Brunzelle, J.S., Lin, Y., Cann, I.K., and Nair, S.K. (2009). Insights into the architecture of the replicative helicase from the structure of an archaeal MCM homolog. Structure 17, 211-222.

Bailis, J.M., Luche, D.D., Hunter, T., and Forsburg, S.L. (2008). MCM proteins interact with checkpoint and recombination proteins to promote S phase genome stability. Mol Cell Biol 28, 1724-1738.

Bando, M., Katou, Y., Komata, M., Tanaka, H., Itoh, T., Sutani, T., and Shirahige, K. (2009). Csm3, Tof1, and Mrc1 form a heterotrimeric mediator complex that associates with DNA replication forks. J Biol Chem 284, 34355-34365.

Bell, S.P., and Dutta, A. (2002). DNA replication in eukaryotic cells. Annu Rev Biochem 71, 333-374.

Bell, S.P., Kobayashi, R., and Stillman, B. (1993). Yeast origin recognition complex functions in transcription silencing and DNA replication. Science 262, 1844-1849.

Ben-Shahar, T.R. (2008). Eco1-dependent cohesin acetylation during establishment of sister chromatid cohesion. Science 321, 563-566.

Bhamidipati, A., Denic, V., Quan, E.M., and Weissman, J.S. (2005). Exploration of the Topological Requirements of ERAD Identifies Yos9p as a Lectin Sensor of Misfolded Glycoproteins in the ER Lumen. Mol Cell 19, 741-751.

Blow, J.J., and Gillespie, P.J. (2008). Replication licensing and cancer--a fatal entanglement? Nat Rev Cancer 8, 799-806.

Bochman, M.L., Bell, S.P., and Schwacha, A. (2008). Subunit organization of Mcm2-7 and the unequal role of active sites in ATP hydrolysis and viability. Mol Cell Biol 28, 5865-5873.

Bochman, M.L., and Schwacha, A. (2007). Differences in the single-stranded DNA binding activities of MCM2-7 and MCM467: MCM2 and MCM5 define a slow ATP-dependent step. J Biol Chem 282, 33795-33804.

Bochman, M.L., and Schwacha, A. (2008). The Mcm2-7 Complex Has In Vitro Helicase Activity. Mol Cell 31, 287-293.

Bochman, M.L., and Schwacha, A. (2009). The Mcm Complex: Unwinding the Mechanism of a Replicative Helicase. Microbiol Mol Biol Rev 73, 652-683.

Bochman, M.L., and Schwacha, A. (2010). The Saccharomyces cerevisiae Mcm6/2 and Mcm5/3 ATPase active sites contribute to the function of the putative Mcm2-7 'gate'. Nucleic Acids Res 38, 6078-6088.

Branzei, D., and Foiani, M. (2009). The checkpoint response to replication stress. DNA Repair (Amst) 8, 1038-1046.

Branzei, D., and Foiani, M. (2010). Maintaining genome stability at the replication fork. Nat Rev Mol Cell Biol 11, 208-219.

Brewster, A.S., Wang, G., Yu, X., Greenleaf, W.B., Carazo, J.M.a., Tjajadia, M., Klein, M.G., and Chen, X.S. (2008). Crystal structure of a near-full-length archaeal MCM: Functional insights for an AAA+ hexameric helicase. Proc Natl Acad Sci U S A 105, 20191-20196.

Brill, S.J., and Stillman, B. (1991). Replication factor-A from Saccharomyces cerevisiae is encoded by three essential genes coordinately expressed at S phase. Genes Dev. 5, 1589-1600

Bruck, I., and Kaplan, D.L. (2011). GINS and Sld3 Compete with One Another for Mcm2-7 and Cdc45 Binding. J Biol Chem 286, 14157-14167.

Bryant, J.A., and Aves, S.J. (2011). Initiation of DNA replication: functional and evolutionary aspects. Annals of Botany 107, 1119-1126.

Burke, D., Dawson, D., and Stearns, T. (2000). Methods in Yeast Genetics: A Cold Spring Harbor Laboratory Course Manual (Cold Spring Harbor, N.Y., Cols Spring Harbor Press).

Busse, P.M., Bose, S.K., Jones, R.W., and Tolmach, L.J. (1978). The Action of Caffeine on X-Irradiated HeLa Cells: III. Enhancement of X-Ray-Induced Killing during G2 Arrest. Radiat Res 76, 292-307.

Byun, T.S., Pacek, M., Yee, M.-c., Walter, J.C., and Cimprich, K.A. (2005). Functional uncoupling of MCM helicase and DNA polymerase activities activates the ATR-dependent checkpoint. Genes Dev 19, 1040-1052.

Calzada, A., Hodgson, B., Kanemaki, M., Bueno, A., and Labib, K. (2005). Molecular anatomy and regulation of a stable replisome at a paused eukaryotic DNA replication fork. Genes Dev 19, 1905-1919.

Chen, C., and Kolodner, R.D. (1999). Gross chromosomal rearrangements in Saccharomyces cerevisiae replication and recombination defective mutants. Nat Genet 23, 81-85.

Chen, S., and Bell, S.P. (2011). CDK prevents Mcm2-7 helicase loading by inhibiting Cdt1 interaction with Orc6. Genes Dev 25, 363-372.

Chong, J.P.J., Mahbubani, H.M., Khoo, C.-Y., and Blow, J.J. (1995). Purification of an MCM-containing complex as a component of the DNA replication licensing system. Nature 375, 418-421.

Chong, J.P.J., Th**ö**mmes, P., and Blow, J.J. (1996). The role of MCM/P1 proteins in the licensing of DNA replication. Trends Biochem Sci 21, 102-106.

Ciosk, R., Shirayama, M., Shevchenko, A., Tanaka, T., Toth, A., Shevchenko, A., and Nasmyth, K. (2000). Cohesin's Binding to Chromosomes Depends on a Separate Complex Consisting of Scc2 and Scc4 Proteins. Mol Cell 5, 243-254.

Cortez, D., Glick, G., and Elledge, S.J. (2004). Minichromosome maintenance proteins are direct targets of the ATM and ATR checkpoint kinases. Proc Natl Acad Sci U S A 101, 10078-10083.

Costa, A., Ilves, I., Tamberg, N., Petojevic, T., Nogales, E., Botchan, M.R., and Berger, J.M. (2011). The structural basis for MCM2-7 helicase activation by GINS and Cdc45. Nat Struct Mol Biol 18, 471-477.

Crabbe, L., Thomas, A., Pantesco, V., De Vos, J., Pasero, P., and Lengronne, A. (2010). Analysis of replication profiles reveals key role of RFC-Ctf18 in yeast replication stress response. Nat Struct Mol Biol 17, 1391-1397.

Davey, M.J., Indiani, C., and O'Donnell, M. (2003). Reconstitution of the Mcm2-7p Heterohexamer, Subunit Arrangement, and ATP Site Architecture. J Biol Chem 278, 4491-4499.

De Piccoli, G., Katou, Y., Itoh, T., Nakato, R., Shirahige, K., and Labib, K. (2012). Replisome Stability at Defective DNA Replication Forks Is Independent of S Phase Checkpoint Kinases. Mol Cell 45, 696-704.

Dean, F., Borowiec, J., Eki, T., and Hurwitz, J. (1992). The simian virus 40 T antigen double hexamer assembles around the DNA at the replication origin. J Biol Chem 267, 14129-14137.

Dimitrova, D.S., Todorov, I.T., Melendy, T., and Gilbert, D.M. (1999). Mcm2, but Not Rpa, Is a Component of the Mammalian Early G1-Phase Prereplication Complex. J Cell Biol 146, 709-722.

Dong, F., Weitzel, S.Ä., and von Hippel, P.Ä. (1996). A coupled complex of T4 DNA replication helicase (gp41) and polymerase (gp43) can perform rapid and processive DNA strand-displacement synthesis. Proc Natl Acad Sci 93, 14456-14461.

Eaton, M.L., Galani, K., Kang, S., Bell, S.P., and MacAlpine, D.M. (2010). Conserved nucleosome positioning defines replication origins. Genes Dev 24, 748-753.

Edwards, M.C. (2002). MCM2-7 complexes bind chromatin in a distributed pattern surrounding ORC in Xenopus egg extracts. J Biol Chem 277, 33049-33059.

Edwards, S., Li, C.M., Levy, D.L., Brown, J., Snow, P.M., and Campbell, J.L. (2003). Saccharyomyces cerevisiae DNA Polymerase ε and Polymerase σ Interact Physically and Functionally, Suggesting a Role for Polymerase ε in Sister Chromatid Cohesion. Mol Cell Biol 23, 2733-2748.

Enemark, E.J., and Joshua-Tor, L. (2006). Mechanism of DNA translocation in a replicative hexameric helicase. Nature 442, 270-275.

Feng, W., Collingwood, D., Boeck, M.E., Fox, L.A., Alvino, G.M., Fangman, W.L., Raghuraman, M.K., and Brewer, B.J. (2006). Genomic mapping of single-stranded DNA in hydroxyurea-challenged yeasts identifies origins of replication. Nat Cell Biol 8, 148-155.

Fletcher, R., Bishop, B., Sclafani, R., Ogata, G., and Chen, X. (2003). The structure and function of MCM dodecamer from Archaeal M. thermoautotrophicum. Nature Struct Biol 10, 160-167.

Forsburg, S.L. (2004). Eukaryotic MCM proteins: beyond replication initiation. Microbiol Mol Biol Rev 68, 109-131.

Foss, E.J. (2001). Tof1p regulates DNA damage response during S phase in Saccharomyces cerevisiae. Genetics 157, 567-577.

Fouts, E.T., Yu, X., Egelman, E.H., and Botchan, M.R. (1999). Biochemical and Electron Microscopic Image Analysis of the Hexameric E1 Helicase. J Biol Chem 274, 4447-4458.

Frick, D.N., and Richardson, C.C. (2001). DNA Primases. Annu Rev Biochem 70, 39-80.

Friedman, K.L., Brewer, B.J., and Fangman, W.L. (1997). Replication profile of Saccharomyces cerevisiae chromosome VI. Genes Cells 2, 667-678.

Fu, Y.V., Yardimci, H., Long, D.T., Guainazzi, A., Bermudez, V.P., Hurwitz, J., van Oijen, A., Schärer, O.D., and Walter, J.C. (2011). Selective Bypass of a Lagging Strand Roadblock by the Eukaryotic Replicative DNA Helicase. Cell 146, 931-941.

Gai, D., Zhao, R., Li, D., Finkielstein, C.V., and Chen, X.S. (2004). Mechanisms of Conformational Change for a Replicative Hexameric Helicase of SV40 Large Tumor Antigen. Cell 119, 47-60.

Gambus, A., Jones, R.C., Sanchez-Diaz, A., Kanemaki, M., van Deursen, F., Edmondson, R.D., and Labib, K. (2006). GINS maintains association of Cdc45 with MCM in replisome progression complexes at eukaryotic DNA replication forks. Nat Cell Biol 8, 358-366.

Gambus, A., van Deursen, F., Polychronopoulos, D., Foltman, M., Jones, R.C., Edmondson, R.D., Calzada, A., and Labib, K. (2009). A key role for Ctf4 in coupling the MCM2-7 helicase to DNA polymerase [alpha] within the eukaryotic replisome. EMBO J 28, 2992-3004.

Gandhi, R., Gillespie, P.J., and Hirano, T. (2006). Human Wapl is a cohesin-binding protein that promotes sister-chromatid resolution in mitotic prophase. Curr Biol 16, 2406-2417.

Ge, X.Q., Jackson, D.A., and Blow, J.J. (2007). Dormant origins licensed by excess Mcm2‚Äì7 are required for human cells to survive replicative stress. Genes Dev 21, 3331-3341.

Gentleman, R., Carey, V., Bates, D., Bolstad, B., Dettling, M., Dudoit, S., Ellis, B., Gautier, L., Ge, Y., Gentry, J., et al. (2004). Bioconductor: open software development for computational biology and bioinformatics. Genome Biol 5, R80.

Goffeau, A., Barrell, B.G., Bussey, H., Davis, R.W., Dujon, B., Feldmann, H., Galibert, F., Hoheisel, J.D., Jacq, C., Johnston, M., et al. (1996). Life with 6000 Genes. Science 274, 546-567.

Graham, B.W., Schauer, G.D., Leuba, S.H., and Trakselis, M.A. (2011). Steric exclusion and wrapping of the excluded DNA strand occurs along discrete external binding paths during MCM helicase unwinding. Nucleic Acids Res 39, 6585-6595.

Gruber, S., Haering, C.H., and Nasmyth, K. (2003). Chromosomal Cohesin Forms a Ring. Cell 112, 765-777.

Gueldener, U., Heinisch, J., Koehler, G.J., Voss, D., and Hegemann, J.H. (2002). A second set of loxP marker cassettes for Cre-mediated multiple gene knockouts in budding yeast. Nucleic Acids Res 30, e23

Guillou, E., Ibarra, A., Coulon, V., Casado-Vela, J., Rico, D., Casal, I., Schwob, E., Losada, A., and Méndez, J. (2010). Cohesin organizes chromatin loops at DNA replication factories. Genes Dev 24, 2812-2822.

Haering, C.H., Löwe, J., Hochwagen, A., and Nasmyth, K. (2002). Molecular Architecture of SMC Proteins and the Yeast Cohesin Complex. Mol Cell 9, 773-788.

Hanna, J.S., Kroll, E.S., Lundblad, V., and Spencer, F.A. (2001). Saccharomyces cerevisiae CTF18 and CTF4 Are Required for Sister Chromatid Cohesion. Mol Cell Biol 21, 3144-3158.

Hanson, P.I., and Whiteheart, S.W. (2005). AAA+ proteins: have engine, will work. Nat Rev Mol Cell Biol 6, 519-529.

Hardy, C.F.J., Dryga, O., Seematter, S., Pahl, P.M.B., and Sclafani, R.A. (1997). mcm5/cdc46-bob1 bypasses the requirement for the S phase activator Cdc7p. Proc Natl Acad Sci 94, 3151-3155.

Hartman, T., Stead, K., Koshland, D., and Guacci, V. (2000). Pds5p Is an Essential Chromosomal Protein Required for Both Sister Chromatid Cohesion and Condensation in Saccharomyces cerevisiae. J Cell Biol 151, 613-626.

Haugland, G.T., Sakakibara, N., Pey, A.L., Rollor, C.R., Birkeland, N.-K., and Kelman, Z. (2008). Thermoplasma acidophilum Cdc6 protein stimulates MCM helicase activity by regulating its ATPase activity. Nucleic Acids Res 36, 5602-5609.

Heidinger-Pauli, J.M., Onn, I., and Koshland, D. (2010). Genetic Evidence that the Acetylation of the Smc3p Subunit of Cohesin Modulates Its ATP-Bound State to Promote Cohesion Establishment in Saccharomyces cerevisiae. Genetics 185, 1249-1256.

Hennessy, K.M., Lee, A., Chen, E., and Botstein, D. (1991). A group of interacting yeast DNA replication genes. Genes Dev 5, 958-969.

Hingorani, M.M., and O'Donnell, M. (2000). Sliding clamps: A (tail)ored fit. Curr Biol 10, R25-R29

Hogan, E., and Koshland, D. (1992). Addition of extra origins of replication to a minichromosome suppresses its mitotic loss in cdc6 and cdc14 mutants of Saccharomyces cerevisiae. Proc Natl Acad Sci U S A 89, 3098-3102.

Huang, M., Zhou, Z., and Elledge, S.J. (1998). The DNA Replication and Damage Checkpoint Pathways Induce Transcription by Inhibition of the Crt1 Repressor. Cell 94, 595-605.

Hyrien, O., Maric, C., and Méchali, M. (1995). Transition in Specification of Embryonic Metazoan DNA Replication Origins. Science 270, 994-997.

Ibarra, A., Schwob, E., and Méndez, J. (2008). Excess MCM proteins protect human cells from replicative stress by licensing backup origins of replication. Proc Natl Acad Sci 105, 8956-8961.

Ilves, I., Petojevic, T., Pesavento, J.J., and Botchan, M.R. (2010). Activation of the MCM2-7 helicase by association with Cdc45 and GINS proteins. Mol Cell 37, 247-258.

Ishimi, Y. (1997). A DNA Helicase Activity Is Associated with an MCM4, -6, and -7 Protein Complex. J Biol Chem 272, 24508-24513.

Ivanov, D., Schleiffer, A., Eisenhaber, F., Mechtler, K., Haering, C.H., and Nasmyth, K. (2002). Eco1 Is a Novel Acetyltransferase that Can Acetylate Proteins Involved in Cohesion. Curr Biol 12, 323-328.

Jacob, F., Brenner, S., and Cuzin, F. (1963). On the Regulation of DNA Replication in Bacteria. Cold Spring Harb Symp Quant Biol 28, 329-348.

Kadyk, L.C., and Hartwell, L.H. (1992). Sister Chromatids Are Preferred Over Homologs as Substrates for Recombinational Repair in Saccharomyces cerevisiae. Genetics 132, 387-402.

Kanter, D.M., Bruck, I., and Kaplan, D.L. (2008). Mcm Subunits Can Assemble into Two Different Active Unwinding Complexes. J Biol Chem 283, 31172-31182.

Kaplan, D.L., Davey, M.J., and O'Donnell, M. (2003). Mcm4,6,7 Uses a "Pump in Ring" Mechanism to Unwind DNA by Steric Exclusion and Actively Translocate along a Duplex. J Biol Chem 278, 49171-49182.

Katou, Y., Kanoh, Y., Bando, M., Noguchi, H., Tanaka, H., Ashikari, T., Sugimoto, K., and Shirahige, K. (2003). S-phase checkpoint proteins Tof1 and Mrc1 form a stable replication-pausing complex. Nature 424, 1078-1083.

Kawabata, T., Luebben, S.W., Yamaguchi, S., Ilves, I., Matise, I., Buske, T., Botchan, M.R., and Shima, N. (2011). Stalled fork rescue via dormant replication origins in unchallenged S phase promotes proper chromosome segregation and tumor suppression. Mol Cell 41, 543-553.

Kent, W.J., Sugnet, C.W., Furey, T.S., Roskin, K.M., Pringle, T.H., Zahler, A.M., Haussler, and David (2002). The Human Genome Browser at UCSC. Genome Res 12, 996-1006.

Kim, J.-S., Krasieva, T.B., LaMorte, V., Taylor, A.M.R., and Yokomori, K. (2002). Specific Recruitment of Human Cohesin to Laser-induced DNA Damage. J Biol Chem 277, 45149-45153.

Kim, J.A., Kruhlak, M., Dotiwala, F., Nussenzweig, A., and Haber, J.E. (2007). Heterochromatin is refractory to γ-H2AX modification in yeast and mammals. J Cell Biol 178, 209-218.

Kitagawa, R., Bakkenist, C.J., McKinnon, P.J., and Kastan, M.B. (2004). Phosphorylation of SMC1 is a critical downstream event in the ATM,ÄìNBS1,ÄìBRCA1 pathway. Genes Dev 18, 1423-1438.

Knott, S.R.V., Viggiani, C.J., Tavaré, S., and Aparicio, O.M. (2009). Genome-wide replication profiles indicate an expansive role for Rpd3L in regulating replication initiation timing or efficiency, and reveal genomic loci of Rpd3 function in Saccharomyces cerevisiae. Genes Dev 23, 1077-1090.

Komata, M., Bando, M., Araki, H., and Shirahige, K. (2009). The direct binding of Mrc1, a checkpoint mediator, to Mcm6, a replication helicase, is essential for the replication checkpoint against methyl methanesulfonate-induced stress. Mol Cell Biol 29, 5008-5019.

Koonin, E.V. (1993). A common set of conserved motifs in a vast variety of putative nucleic acid-dependent ATPases including MCM proteins involved in the initiation of eukaryotic DNA replication. Nucleic Acids Res 21, 2541-2547.

Kops, G.J.P.L., Weaver, B.A.A., and Cleveland, D.W. (2005). On the road to cancer: aneuploidy and the mitotic checkpoint. Nat Rev Cancer 5, 773-785.

Krude, T., Musahl, C., Laskey, R.A., and Knippers, R. (1996). Human replication proteins hCdc21, hCdc46 and P1Mcm3 bind chromatin uniformly before S-phase and are displaced locally during DNA replication. J Cell Sci 109, 309-318.

Kubota, T., Hiraga, S.-i., Yamada, K., Lamond, A.I., and Donaldson, A.D. (2011). Quantitative Proteomic Analysis of Chromatin Reveals that Ctf18 Acts in the DNA Replication Checkpoint. Mol Cell Proteomics 10.

Kueng, S., Hegemann, B., Peters, B.H., Lipp, J.J., Schleiffer, A., Mechtler, K., and Peters, J.M. (2006). Wapl controls the dynamic association of cohesin with chromatin. Cell 127, 955-967.

Labib, K. (2010). How do Cdc7 and cyclin-dependent kinases trigger the initiation of chromosome replication in eukaryotic cells? Genes Dev 24, 1208-1219.

Labib, K., Tercero, J.A., and Diffley, J.F. (2000). Uninterrupted MCM2-7 function required for DNA replication fork progression. Science 288, 1643-1647.

Lea, D., and Coulson, C. (1949). The distribution of the numbers of mutants in bacterial populations. J Genetics 49, 264-285.

Lee, J.-K., and Hurwitz, J. (2000). Isolation and Characterization of Various Complexes of the Minichromosome Maintenance Proteins of Schizosaccharomyces pombe. J Biol Chem 275, 18871-18878.

Lee, J.B., Hite, R.K., Hamdan, S.M., Xie, X.S., Richardson, C.C., and van Oijen, A.M. (2006). DNA primase acts as a molecular brake in DNA replication. Nature 439, 621-624.

Lei, M., Kawasaki, Y., and Tye, B. (1996). Physical Interactions among Mcm Proteins and Effects of Mcm Dosage on DNA Replication in Saccharomyces cerevisiae. Mol Cell Biol 16, 5081-5090.

Lengronne, A., McIntyre, J., Katou, Y., Kanoh, Y., Hopfner, K.-P., Shirahige, K., and Uhlmann, F. (2006). Establishment of Sister Chromatid Cohesion at the S. cerevisiae Replication Fork. Mol cell 23, 787-799.

Li, H., Ruan, J., and Durbin, R. (2008). Mapping short DNA sequencing reads and calling variants using mapping quality scores. Genome Res 18, 1851-1858.

Li, X.C., Schimenti, J.C., and Tye, B.K. (2009). Aneuploidy and improved growth are coincident but not causal in a yeast cancer model. PLoS Biol 7, e1000161.

Liku, M.E., Nguyen, V.Q., Rosales, A.W., Irie, K., and Li, J.J. (2005). CDK Phosphorylation of a Novel NLS-NES Module Distributed between Two Subunits of the Mcm2-7 Complex Prevents Chromosomal Rereplication. Mol Biol Cell 16, 5026-5039.

Liu, W., Pucci, B., Rossi, M., Pisani, F.M., and Ladenstein, R. (2008). Structural analysis of the Sulfolobus solfataricus MCM protein N-terminal domain. Nucleic Acids Res 36, 3235-3243.

Liu, Y., Richards, T., and Aves, S. (2009). Ancient diversification of eukaryotic MCM DNA replication proteins. BMC Evol Biol 9, 60.

Lodish, H.B., Arnold, Zipursky, S. Lawrence; Matsudaira, Paul; Baltimore, David; Darnell, James (2000). Molecular Cell Biology, 4th edition. Section 12.11.

Longhese, M.P., Plevani, P., and Lucchini, G. (1994). Replication factor A is required in vivo for DNA replication, repair, and recombination. Mol Cell Biol 14, 7884-7890.

Lopes, M., Cotta-Ramusino, C., Pellicioli, A., Liberi, G., Plevani, P., Muzi-Falconi, M., Newlon, C.S., and Foiani, M. (2001). The DNA replication checkpoint response stabilizes stalled replication forks. Nature 412, 557-561.

Lopez-Mosqueda, J., Maas, N.L., Jonsson, Z.O., Defazio-Eli, L.G., Wohlschlegel, J., and Toczyski, D.P. (2010). Damage-induced phosphorylation of Sld3 is important to block late origin firing. Nature 467, 479-483.

Losada, A., Yokochi, T., and Hirano, T. (2005). Functional contribution of Pds5 to cohesin-mediated cohesion in human cells and Xenopus egg extracts. J Cell Sci 118, 2133-2141.

Lou, H., Komata, M., Katou, Y., Guan, Z., Reis, C.C., Budd, M., Shirahige, K., and Campbell, J.L. (2008). Mrc1 and DNA Polymerase ε Function Together in Linking DNA Replication and the S Phase Checkpoint. Mol Cell 32, 106-117.

Lundgren, M., and Bernander, R. (2005). Archaeal cell cycle progress. Curr Opin Microbiol 8, 662-668.

Lyons, N.A., and Morgan, D.O. (2011). Cdk1-Dependent Destruction of Eco1 Prevents Cohesion Establishment after S Phase. Mol Cell 42, 378-389.

Ma, L., Zhai, Y., Feng, D., Chan, T.-c., Lu, Y., Fu, X., Wang, J., Chen, Y., Li, J., Xu, K., et al. (2010). Identification of novel factors involved in or regulating initiation of DNA replication by a genome-wide phenotypic screen in Saccharomyces cerevisiae. Cell Cycle 9, 4399-4410.

Madeo, F., Fröhlich, E., Ligr, M., Grey, M., Sigrist, S.J., Wolf, D.H., and Fröhlich, K.U. (1999). Oxygen Stress: A Regulator of Apoptosis in Yeast. J Cell Biol 145, 757-767.

Madine, M.A., Khoo, C.-Y., Mills, A.D., Musahl, C., and Laskey, R.A. (1995a). The nuclear envelope prevents reinitiation of replication by regulating the binding of MCM3 to chromatin in Xenopus egg extracts. Curr Biol 5, 1270-1279.

Madine, M.A., Khoo, C.Y., Mills, A.D., and Laskey, R.A. (1995b). MCM3 complex required for cell cycle regulation of DNA replication in vertebrate cells. Nature 375, 421-424.

Mahbubani, H.M., Paull, T., EIder, J.K., and Blow, J.J. (1992). DNA replication initiates at multiple sites on plasmid DNA in Xenopus egg extracts. Nucleic Acids Res 20, 1457-1462.

Maine, G.T., Sinha, P., and Tye, B.-K. (1984). Mutants of S. cerevisiae defective in the maintenance of the minichromosomes. Genetics 106, 365-385.

Majka, J., and Burgers, P.M.J. (2003). Yeast Rad17/Mec3/Ddc1: A sliding clamp for the DNA damage checkpoint. Proc Natl Acad Sci U S A 100, 2249-2254.

Majka, J., Niedziela-Majka, A., and Burgers, P.M.J. (2006). The Checkpoint Clamp Activates Mec1 Kinase during Initiation of the DNA Damage Checkpoint. Mol Cell 24, 891-901.

Marahrens, Y., and Stillman, B. (1992). A yeast chromosomal origin of DNA replication defined by multiple functional elements. Science 255, 817-823.

Masai, H., Matsumoto, S., You, Z., Yoshizawa-Sugata, N., and Oda, M. (2011). Eukaryotic Chromosome DNA Replication: Where, When, and How? Annu Rev Biochem 79, 89-130.

Matsuoka, S., Ballif, B.A., Smogorzewska, A., McDonald, E.R., Hurov, K.E., Luo, J., Bakalarski, C.E., Zhao, Z., Solimini, N., Lerenthal, Y., et al. (2007). ATM and ATR Substrate Analysis Reveals Extensive Protein Networks Responsive to DNA Damage. Science 316, 1160-1166.

Mayer, M.L., Pot, I., Chang, M., Xu, H., Aneliunas, V., Kwok, T., Newitt, R., Aebersold, R., Boone, C., Brown, G.W., et al. (2004). Identification of Protein Complexes Required for Efficient Sister Chromatid Cohesion. Mol Biol Cell 15, 1736-1745.

Megee, P.C., and Koshland, D. (1999). A Functional Assay for Centromere-Associated Sister Chromatid Cohesion. Science 285, 254-257.

Merchant, A.M., Kawasaki, Y., Chen, Y., Lei, M., and Tye, B.K. (1997). A lesion in the DNA replication initiation factor Mcm10 induces pausing of elongation forks through chromosomal replication origins in Saccharomyces cerevisiae. Mol Cell Biol 17, 3261-3271.

Michaelis, C., Ciosk, R., and Nasmyth, K. (1997). Cohesins: Chromosomal Proteins that Prevent Premature Separation of Sister Chromatids. Cell 91, 35-45.

Moir, D., Stewart, S.E., Osmond, B.C., and Botstein, D. (1982). COLD-SENSITIVE CELL-DIVISION-CYCLE MUTANTS OF YEAST: ISOLATION, PROPERTIES, AND PSEUDOREVERSION STUDIES. Genetics 100, 547-563.

Moldovan, G.-L., Pfander, B., and Jentsch, S. (2006). PCNA Controls Establishment of Sister Chromatid Cohesion during S Phase. Mol Cell 23, 723-732.

Morin, I., Ngo, H.-P., Greenall, A., Zubko, M.K., Morrice, N., and Lydall, D. (2008). Checkpoint-dependent phosphorylation of Exo1 modulates the DNA damage response. EMBO J 27, 2400-2410.

Motegi, A., and Myung, K. (2007). Measuring the rate of gross chromosomal rearrangements in Saccharomyces cerevisiae: A practical approach to study genomic rearrangements observed in cancer. Methods 41, 168-176.

Mott, M.L., and Berger, J.M. (2007). DNA replication initiation: mechanisms and regulation in bacteria. Nat Rev Micro 5, 343-354.

Moyer, S.E., Lewis, P.W., and Botchan, M.R. (2006). Isolation of the Cdc45/Mcm2,Äì7/GINS (CMG) complex, a candidate for the eukaryotic DNA replication fork helicase. Proc Natl Acad Sci 103, 10236-10241.

Muramatsu, S., Hirai, K., Tak, Y.-S., Kamimura, Y., and Araki, H. (2010). CDK-dependent complex formation between replication proteins Dpb11, Sld2, Pol ε, and GINS in budding yeast. Genes Dev 24, 602-612.

Naiki, T., Kondo, T., Nakada, D., Matsumoto, K., and Sugimoto, K. (2001). Chl12 (Ctf18) Forms a Novel Replication Factor C-Related Complex and Functions Redundantly with Rad24 in the DNA Replication Checkpoint Pathway. Mol Cell Biol 21, 5838-5845.

Nakamura, A., Olga A Sedelnikova, Christophe Redon, Duane R Pilch, Natasha I Sinogeeva, Robert Shroff, Michael Lichten, William M Bonner (2006). Techniques for gamma-H2AX detection. Methods Enzymol 409, 236-250.

Nasmyth, K., and Haering, C.H. (2009). Cohesin: its roles and mechanisms. Annu Rev Genet 43, 525-558.

Navadgi-Patil, V.M., and Burgers, P.M. (2008). Yeast DNA Replication Protein Dpb11 Activates the Mec1/ATR Checkpoint Kinase. J Biol Chem 283, 35853-35859.

Naylor, M.L., Li, J.-m., Osborn, A.J., and Elledge, S.J. (2009). Mrc1 phosphorylation in response to DNA replication stress is required for Mec1 accumulation at the stalled fork. Proc Natl Acad Sci U S A 106, 12765-12770.

Newlon, C.S., and Theis, J.F. (1993). The structure and function of yeast ARS elements. Curr Opin Genet Dev 3, 752-758.

Nguyen, V.Q., Co, C., Irie, K., and Li, J.J. (2000). Clb/Cdc28 kinases promote nuclear export of the replication initiator proteins Mcm2-7. Curr Biol 10, 195-205.

Nguyen, V.Q., Co, C., and Li, J.J. (2001). Cyclin-dependent kinases prevent DNA re-replication through multiple mechanisms. Nature 411, 1068-1073.

Nieduszynski, C.A., Hiraga, S.-i., Ak, P., Benham, C.J., and Donaldson, A.D. (2007). OriDB: a DNA replication origin database. Nucleic Acids Res 35, D40-D46.

Onn, I., Heidinger-Pauli, J.M., Guacci, V., Unal, E., and Koshland, D.E. (2008). Sister chromatid cohesion: a simple concept with a complex reality. Annu Rev Cell Dev Biol 24, 105-129.

Onn, I., and Koshland, D. (2011). In vitro assembly of physiological cohesin/DNA complexes. Proc Natl Acad Sci U S A 108, 12198-12205.

Osborn, A.J., and Elledge, S.J. (2003). Mrc1 is a replication fork component whose phosphorylation in response to DNA replication stress activates Rad53. Genes Dev 17, 1755-1767.

Pacek, M., and Walter, J.C. (2004). A requirement for MCM7 and Cdc45 in chromosome unwinding during eukaryotic DNA replication. EMBO J 23, 3667-3676.

Padmanabhan, V., Callas, P., Philips, G., Trainer, T.D., and Beatty, B.G. (2004). DNA replication regulation protein Mcm7 as a marker of proliferation in prostate cancer. J Clin Pathol 57, 1057-1062.

Painter, R.B., and Young, B.R. (1980). Radiosensitivity in ataxia-telangiectasia: a new explanation. Proc Natl Acad Sci U S A 77, 7315-7317.

Pandey, M., Syed, S., Donmez, I., Patel, G., Ha, T., and Patel, S.S. (2009). Coordinating DNA replication by means of priming loop and differential synthesis rate. Nature 462, 940-943.

Panizza, S., Tanaka, T., Hochwagen, A., Eisenhaber, F., and Nasmyth, K. (2000). Pds5 cooperates with cohesin in maintaining sister chromatid cohesion. Curr Biol 10, 1557-1564.

Passmore, S., Elble, R., and Tye, B.K. (1989). A protein involved in minichromosome maintenance in yeast binds a transcriptional enhancer conserved in eukaryotes. Genes Dev 3, 921-935.

Patel, P.K., Arcangioli, B., Baker, S.P., Bensimon, A., and Rhind, N. (2006). DNA Replication Origins Fire Stochastically in Fission Yeast. Mol Biol Cell 17, 308-316.

Patel, S.S., and Picha, K.M. (2000). STRUCTURE AND FUNCTION OF HEXAMERIC HELICASES1. AnnuRev Biochem 69, 651-697.

Paulovich, A.G., and Hartwell, L.H. (1995). A checkpoint regulates the rate of progression through S phase in S. cerevisiae in Response to DNA damage. Cell 82, 841-847.

Perkins, G., Drury, L.S., and Diffley, J.F.X. (2001). Separate SCFCDC4 recognition elements target Cdc6 for proteolysis in S phase and mitosis. EMBO J 20, 4836-4845.

Petronczki, M., Chwalla, B., Siomos, M.F., Yokobayashi, S., Helmhart, W., Deutschbauer, A.M., Davis, R.W., Watanabe, Y., and Nasmyth, K. (2004). Sister-chromatid cohesion mediated by the alternative RF-CCtf18/Dcc1/Ctf8, the helicase Chl1 and the polymerase-Œ±-associated protein Ctf4 is essential for chromatid disjunction during meiosis II. J Cell Sci 117, 3547-3559.

Poli, J., Tsaponina, O., Crabbe, L., Keszthelyi, A., Pantesco, V., Chabes, A., Lengronne, A., and Pasero, P. (2012). dNTP pools determine fork progression and origin usage under replication stress. EMBO J 31, 883-894

Pucci, B., De Felice, M., Rocco, M., Esposito, F., De Falco, M., Esposito, L., Rossi, M., and Pisani, F.M. (2007). Modular organization of the Sulfolobus solfataricus mini-chromosome maintenance protein. J Biol Chem 282, 12574-12582.

Putnam, C.D., Hayes, T.K., and Kolodner, R.D. (2009). Specific pathways prevent duplication-mediated genome rearrangements. Nature 460, 984-989.

Raghuraman, M.K., and Brewer, B.J. (2010). Molecular analysis of the replication program in unicellular model organisms. Chromosome Res 18, 19-34.

Randell, J.C.W., Bowers, J.L., RodrÌguez, H.K., and Bell, S.P. (2006). Sequential ATP Hydrolysis by Cdc6 and ORC Directs Loading of the Mcm2-7 Helicase. Mol Cell 21, 29-39.

Randell, J.C.W., Fan, A., Chan, C., Francis, L.I., Heller, R.C., Galani, K., and Bell, S.P. (2010). Mec1 Is One of Multiple Kinases that Prime the Mcm2-7 Helicase for Phosphorylation by Cdc7. Mol Cell 40, 353-363.

RDevelopmentCoreTeam (2010). R: A Language and Environment for Statistical Computing. Vienna Austria R Foundation for Statistical Computing 1, ISBN 3-900051-07-0. Available at: http://www.r-project.org.

Remus, D., and Diffley, J.F. (2009). Eukaryotic DNA replication control: lock and load, then fire. Curr Opin Cell Biol 21, 771-777.

Rowland, B.D. (2009). Building sister chromatid cohesion: Smc3 acetylation counteracts an antiestablishment activity. Mol Cell 33, 763-774.

Ryba, T., Battaglia, D., Pope, B.D., Hiratani, I., and Gilbert, D.M. (2011). Genome-scale analysis of replication timing: from bench to bioinformatics. Nat Protoc 6, 870-895.

Samuels, M., Gulati, G., Shin, J.-H., Opara, R., McSweeney, E., Sekedat, M., Long, S., Kelman, Z., and Jeruzalmi, D. (2009). A biochemically active MCM-like helicase in Bacillus cereus. Nucleic Acids Res 37, 4441-4452.

Sanchez, Y., Desany, B.A., Jones, W.J., Liu, Q., Wang, B., and Elledge, S.J. (1996). Regulation of RAD53 by the ATM-like kinases MEC1 and TEL1 in yeast cell cycle checkpoint pathways. Science 271, 357-360.

Santocanale, C., and Diffley, J.F. (1998). A Mec1- and Rad53-dependent checkpoint controls late-firing origins of DNA replication. Nature 395, 615-618.

Savitsky, K., Bar-Shira, A., Gilad, S., Rotman, G., Ziv, Y., Vanagaite, L., Tagle, D., Smith, S., Uziel, T., Sfez, S., et al. (1995). A single ataxia telangiectasia gene with a product similar to PI-3 kinase. Science 268, 1749-1753.

Scheffzek, K., and Ahmadian, M.R. (2005). GTPase activating proteins: structural and functional insights 18 years after discovery. Cell Mol Life Sci 62, 3014-3038.

Schwacha, A., and Bell, S.P. (2001). Interactions between Two Catalytically Distinct MCM Subgroups Are Essential for Coordinated ATP Hydrolysis and DNA Replication. Mol Cell 8, 1093-1104.

Schweitzer, B., and Philippsen, P. (1991). CDC15, an essential cell cycle gene in Saccharomyces cerevisiae, encodes a protein kinased domain. Yeast 7, 265-273.

Segurado, M., and Diffley, J.F.X. (2008). Separate roles for the DNA damage checkpoint protein kinases in stabilizing DNA replication forks. Genes Dev 22, 1816-1827.

Shen, Z. (2011). Genomic instability and cancer: an introduction. J Mol Cell Biol 3, 1-3.

Sheu, Y.-J., and Stillman, B. (2006). Cdc7-Dbf4 Phosphorylates MCM Proteins via a Docking Site-Mediated Mechanism to Promote S Phase Progression. Mol Cell 24, 101-113

Sheu, Y.-J., and Stillman, B. (2010). The Dbf4-Cdc7 kinase promotes S phase by alleviating an inhibitory activity in Mcm4. Nature 463, 113-117.

Shima, N., Alcaraz, A., Liachko, I., Buske, T.R., Andrews, C.A., Munroe, R.J., Hartford, S.A., Tye, B.K., and Schimenti, J.C. (2007). A viable allele of Mcm4 causes chromosome instability and mammary adenocarcinomas in mice. Nat Genet 39, 93-98.

Shimada, K., Pasero, P., and Gasser, S.M. (2002). ORC and the intra-S phase checkpoint: a threshold regulates Rad53p activation in S phase. Genes Dev 16, 3236-3252.

Shimada, K., and Gasser, S.M. (2007). The Origin Recognition Complex Functions in Sister-Chromatid Cohesion in Saccharomyces cerevisiae. Cell 128, 85-99.

Shinomiya, T., and Ina, S. (1991). Analysis of chromosomal replicons in early embryos of Drosophila melanogaster by two-dimensional gel electrophoresis. Nucleic Acids Res 19, 3935-3941.

Silva, P., Barbosa, J., Nascimento, A.V., Faria, J., Reis, R., Bousbaa, H. (2011). Monitoring the fidelity of mitotic chromosome segregation by the spindle assembly checkpoint. Cell Prolif 44, 391-400.

Singleton, M.R., Dillingham, M.S., Gaudier, M., Kowalczykowski, S.C., and Wigley, D.B. (2004). Crystal structure of RecBCD enzyme reveals a machine for processing DNA breaks. Nature 432, 187-193.

Sinha, P., Chang, V., and Tye, B.-K. (1986). A mutant that affects the function of autonomously replicating sequences in yeast. J Mol Biol 192, 805-814.

Sjögren, C., and Ström, L. (2010). S-phase and DNA damage activated establishment of Sister chromatid cohesion--importance for DNA repair. Exp Cell Res 316, 1445-1453.

Skibbens, R.V., Corson, L.B., Koshland, D., and Hieter, P. (1999). Ctf7p is essential for sister chromatid cohesion and links mitotic chromosome structure to the DNA replication machinery. Genes Dev 13, 307-319.

Sogo, J.M., Lopes, M., and Foiani, M. (2002). Fork Reversal and ssDNA Accumulation at Stalled Replication Forks Owing to Checkpoint Defects. Science 297, 599-602.

Stano, N.M., Jeong, Y.-J., Donmez, I., Tummalapalli, P., Levin, M.K., and Patel, S.S. (2005). DNA synthesis provides the driving force to accelerate DNA unwinding by a helicase. Nature 435, 370-373.

Stead, B.E., Sorbara, C.D., Brandl, C.J., and Davey, M.J. (2009). ATP Binding and Hydrolysis by Mcm2 Regulate DNA Binding by Mcm Complexes. J Mol Biol 391, 301-313.

Straight, A.F., Belmont, A.S., Robinett, C.C., and Murray, A.W. (1996). GFP tagging of budding yeast chromosomes reveals that protein protein interactions can mediate sister chromatid cohesion. Curr Biol 6, 1599-1608.

Ström, L., Karlsson, C., Lindroos, H.B., Wedahl, S., Katou, Y., Shirahige, K., and Sjögren, C. (2007). Postreplicative Formation of Cohesion Is Required for Repair and Induced by a Single DNA Break. Science 317, 242-245.

Ström, L., Lindroos, H.B., Shirahige, K., and Sjögren, C. (2004). Postreplicative Recruitment of Cohesin to Double-Strand Breaks Is Required for DNA Repair. Mol Cell 16, 1003-1015.

Sutani, T., Kawaguchi, T., Kanno, R., Itoh, T., and Shirahige, K. (2009). Budding Yeast Wpl1(Rad61)-Pds5 Complex Counteracts Sister Chromatid Cohesion-Establishing Reaction. Curr Biol 19, 492-497.

Suter, B., Tong, A., Chang, M., Yu, L., Brown, G.W., Boone, C., and Rine J. (2004). The Origin Recognition Complex Links Replication, Sister Chromatid Cohesion and Transcriptional Silencing in Saccharomyces cerevisiae. Genetics 167, 579-591.

Szyjka, S.J., Viggiani, C.J., and Aparicio, O.M. (2005). Mrc1 Is Required for Normal Progression of Replication Forks throughout Chromatin in S. cerevisiae. Mol Cell 19, 691-697.

Takahashi, K., Yamada, H., and Yanagida, M. (1994). Fission yeast minichromosome loss mutants mis cause lethal aneuploidy and replication abnormality. Mol Biol Cell 5, 1145-1158.

Takahashi, T.S., Basu, A., Bermudez, V., Hurwitz, J., and Walter, J.C. (2008). Cdc7-Drf1 kinase links chromosome cohesion to the initiation of DNA replication in Xenopus egg extracts. Genes Dev 22, 1894-1905.

Takahashi, T.S., Wigley, D.B., and Walter, J.C. (2005). Pumps, paradoxes and ploughshares: mechanism of the MCM2,Äì7 DNA helicase. Trends Biochem Sci 30, 437-444.

Takahashi, T.S., Yiu, P., Chou, M.F., Gygi, S., and Walter, J.C. (2004). Recruitment of Xenopus Scc2 and cohesin to chromatin requires the pre-replication complex. Nat Cell Biol 6, 991-996.

Takara, T.J., and Bell, S.P. (2011). Multiple Cdt1 molecules act at each origin to load replication-competent Mcm2-7 helicases. EMBO J 30, 4885-4896.

Tanaka, S., and Diffley, J.F.X. (2002). Interdependent nuclear accumulation of budding yeast Cdt1 and Mcm2-7 during G1 phase. Nat Cell Biol 4, 198-207.

Tercero, J.A., and Diffley, J.F.X. (2001). Regulation of DNA replication fork progression through damaged DNA by the Mec1/Rad53 checkpoint. Nature 412, 553-557.

Terret, M.-E., Sherwood, R., Rahman, S., Qin, J., and Jallepalli, P.V. (2009). Cohesin acetylation speeds the replication fork. Nature 462, 231-234.

Thomas, B.J., and Rothstein, R. (1989). Elevated recombination rates in transcriptionally active DNA. Cell 56, 619-630.

Tonkin, E.T., Wang, T.-J., Lisgo, S., Bamshad, M.J., and Strachan, T. (2004). NIPBL, encoding a homolog of fungal Scc2-type sister chromatid cohesion proteins and fly Nipped-B, is mutated in Cornelia de Lange syndrome. Nat Genet 36, 636-641.

Tóth, A., Ciosk, R., Uhlmann, F., Galova, M., Schleiffer, A., and Nasmyth, K. (1999). Yeast Cohesin complex requires a conserved protein, Eco1p(Ctf7), to establish cohesion between sister chromatids during DNA replication. Genes Dev 13, 320-333.

Toyokawa, G., Masuda, K., Daigo, Y., Cho, H.-S., Yoshimatsu, M., Takawa, M., Hayami, S., Maejima, K., Chino, M., Field, H., et al. (2011). Minichromosome Maintenance Protein 7 is a potential therapeutic target in human cancer and a novel prognostic marker of non-small cell lung cancer. Molecular Cancer 10, 65.

Uhlmann, F., and Nasmyth, K. (1998). Cohesion between sister chromatids must be established during DNA replication. Curr Biol 8, 1095-1102.

Ünal, E., Arbel-Eden, A., Sattler, U., Shroff, R., Lichten, M., Haber, J.E., and Koshland, D. (2004). DNA Damage Response Pathway Uses Histone Modification to Assemble a Double-Strand Break-Specific Cohesin Domain. Mol Cell 16, 991-1002.

Ünal, E., Heidinger-Pauli, J.M., Kim, W., Guacci, V., Onn, I., Gygi, S.P., and Koshland, D.E. (2008). A Molecular Determinant for the Establishment of Sister Chromatid Cohesion. Science 321, 566-569.

Ünal, E., Heidinger-Pauli, J.M., and Koshland, D. (2007). DNA Double-Strand Breaks Trigger Genome-Wide Sister-Chromatid Cohesion Through Eco1 (Ctf7). Science 317, 245-248.

Vernis, L., Piskur, J., and Diffley, J.F.X. (2003). Reconstitution of an efficient thymidine salvage pathway in Saccharomyces cerevisiae. Nucleic Acids Res 31, e120.

Vialard, J.E., Gilbert, C.S., Green, C.M., and Lowndes, N.F. (1998). The budding yeast Rad9 checkpoint protein is subjected to Mec1/Tel1-dependent hyperphosphorylation and interacts with Rad53 after DNA damage. EMBO J 17, 5679-5688.

Vogelauer, M., Rubbi, L., Lucas, I., Brewer, B.J., and Grunstein, M. (2002). Histone Acetylation Regulates the Time of Replication Origin Firing. Mol Cell 10, 1223-1233.

Wang, Z., Castaño, I.B., De Las Peñas, A., Adams, C., and Christman, M.F. (2000) Pol κ: A DNA Polymerase Required for Sister Chromatid Cohesion. Science 289, 774-779.

Warren, C.D., Eckley, D.M., Lee, M.S., Hanna, J.S., Hughes, A., Peyser, B., Jie, C., Irizarry, R., and Spencer, F.A. (2004). S-Phase Checkpoint Genes Safeguard High-Fidelity Sister Chromatid Cohesion. Mol Biol Cell 15, 1724-1735.

Watrin, E., Schleiffer, A., Tanaka, K., Eisenhaber, F., Nasmyth, K., and Peters, J.-M. (2006). Human Scc4 Is Required for Cohesin Binding to Chromatin, Sister-Chromatid Cohesion, and Mitotic Progression. Curr Biol 16, 863-874.

Weinert, T.A., and Hartwell, L.H. (1988). The RAD9 gene controls the cell cycle response to DNA damage in Saccharomyces cerevisiae. Science 241, 317-322.

Weinreich, M., and Stillman, B. (1999). Cdc7p-Dbf4p kinase binds to chromatin during S phase and is regulated by both the APC and the RAD53 checkpoint pathway. EMBO J 18, 5334–5346.

Weitzer, S., Lehane, C., and Uhlmann, F. (2003). A Model for ATP Hydrolysis-Dependent Binding of Cohesin to DNA. Curr Biol 13, 1930-1940.

Wilmes, G.M., Archambault, V., Austin, R.J., Jacobson, M.D., Bell, S.P., and Cross, F.R. (2004). Interaction of the S-phase cyclin Clb5 with an 'RXL' docking sequence in the initiator protein Orc6 provides an origin-localized replication control switch. Genes Dev 18, 981-991.

Wright, A.P., Bruns, M., and Hartley, B.S. (1989). Extraction and rapid inactivation of proteins from Saccharomyces cerevisiae by trichloroacetic acid precipitation. Yeast 5, 51-53.

Wyrick, J.J., Aparicio, J.G., Chen, T., Barnett, J.D., Jennings, E.G., Young, R.A., Bell, S.P., and Aparicio, O.M. (2001). Genome-Wide Distribution of ORC and MCM Proteins in S. cerevisiae: High-Resolution Mapping of Replication Origins. Science 294, 2357-2360.

Xu, H., Boone, C., and Brown, G.W. (2007). Genetic Dissection of Parallel Sister-Chromatid Cohesion Pathways. Genetics 176, 1417-1429.

Xu, H., Boone, C., and Klein, H.L. (2004). Mrc1 Is Required for Sister Chromatid Cohesion To Aid in Recombination Repair of Spontaneous Damage. Mol Cell Biol 24, 7082-7090.

Yamashita, M., Hori, Y., Shinomiya, T., Obuse, C., Tsurimoto, T., Yoshikawa, H., and Shirahige, K. (1997). The efficiency and timing of initiation of replication of multiple replicons of Saccharomyces cerevisiae chromosome VI. Genes Cells 2, 655-665.

Yardimci, H., Loveland, A.B., Habuchi, S., van Oijen, A.M., and Walter, J.C. (2010). Uncoupling of Sister Replisomes during Eukaryotic DNA Replication. Mol Cell 40, 834-840.

Yoshimochi, T., Fujikane, R., Kawanami, M., Matsunaga, F., and Ishino, Y. (2008). The GINS Complex from Pyrococcus furiosus Stimulates the MCM Helicase Activity. J Biol Chem 283, 1601-1609.

You, Z., Ishimi, Y., Masai, H., and Hanaoka, F. (2002). Roles of Mcm7 and Mcm4 Subunits in the DNA Helicase Activity of the Mouse Mcm4/6/7 Complex. J Biol Chem 277, 42471-42479.

Yu, Z., Feng, D., and Liang, C. (2004). Pairwise Interactions of the Six Human MCM Protein Subunits. J Mol Cell 340, 1197-1206.

Zegerman, P., and Diffley, J.F. (2010). Checkpoint-dependent inhibition of DNA replication initiation by Sld3 and Dbf4 phosphorylation. Nature 467, 474-478.

Zegerman, P., and Diffley, J.F.X. (2009). DNA replication as a target of the DNA damage checkpoint. DNA Repair 8, 1077-1088.

Zhang, J. (2008). Acetylation of Smc3 by Eco1 is required for S phase sister chromatid cohesion in both human and yeast. Mol Cell 31, 143-151.

Zhao, X., and Rothstein, R. (2002). The Dun1 checkpoint kinase phosphorylates and regulates the ribonucleotide reductase inhibitor Sml1. Proc Natl Acad Sci U S A 99, 3746-3751.

Zink, D. (2006). The temporal program of DNA replication: new insights into old questions. Chromosoma 115, 273-287.

Zou, L., and Elledge, S.J. (2003). Sensing DNA damage through ATRIP recognition of RPA-ssDNA complexes. Science 300, 1542-1548